Characterisation of Aardvark, a *Dictyostelium* β-catenin

Jonathan Peter Reynolds

MRC Laboratory for Molecular Cell Biology
&
Department of Biology
University College London

A thesis submitted to the
University of London for the degree of
Doctor of Philosophy (Ph.D.)

December 2002

Abstract

Wnt signalling is active both in development and the progression of certain disease processes, most notably cancer. Glycogen Synthase Kinase-3 (GSK-3) and β-catenin both define the canonical Wnt pathway, where GSK-3 negatively regulates β-catenin, which, in turn, regulates gene expression. Mutations to β-catenin that prevent GSK-3 phosphorylation are associated with the progression of many different tumour types. In addition to its signalling function, β-catenin is required structurally at adherens junctions, linking cadherin molecules to the actin cytoskeleton via its interaction with α-catenin. Loss of β-catenin from adherens junctions is associated with the increased invasiveness and metastasis of tumour cells.

Homologues of GSK-3 (GskA) and β-catenin (Aardvark) have been cloned in the cellular slime mould *Dictyostelium discoideum*. Aardvark is required for both the expression of the pre-sprore marker gene *pspA* and the formation of adherens junctions in *Dictyostelium*. This thesis describes the characterisation of Aardvark, with particular regard to its function and interaction with GskA.

This work shows that distinct regions of Aar are required for its signalling and adhesion functions and suggests that two distinct proteins may bind to it to mediate the formation of adherens junctions. A novel protein kinase has been identified that may phosphorylate the N-terminus of Aar to regulate the expression of the pre-spore marker gene *pspA*. Full-length Aar is unstable and a 'destabilisation' region has been identified within the core of the protein. A novel derepression mechanism is used to explain GskA and Aar function in the expression of *pspA*. The characterisation of non-canonical Wnt signalling will enhance the understanding of the evolution and function of the core components of the pathway, giving greater insight into their roles in both development and disease processes.

This thesis is dedicated to my late grandfather

John 'Jack' Saxton, who died of cancer

23 September 1998

Acknowledgements

Firstly I would like to thank The Wellcome Trust who funded my work through a Wellcome Prize Studentship. I want to thank my supervisor Adrian Harwood for the tremendous support he has given me during my three years in the lab and also whilst writing this thesis. The unwavering encouragement to keep working throughout the highs and the lows was vital.

I would also like to thank the other members of the Harwood lab, past and present: Emma for her technical support and excellent running of the lab and Robin and Jonny, the gurus of molecular biology and biochemistry, respectively. Thanks should also go to Juliet for many useful comments and Hazel and Melanie for reading parts of my thesis. Thanks also to the Nurrish lab, especially Paul for many useful pieces of advice, work related or otherwise, and many other friends and colleagues at the LMCB.

I would also like to give a special thanks to my parents. Without their encouragement (and financial support towards the end), this thesis would never been completed.

Lastly, I would like to thank the friends I live with for coping with my stress so well and always keeping the fridge well stocked with beer. The importance of this last contribution should not be underestimated.

Table of contents

Table of figures

List of tables

Chapter 1

Introduction

1.1 Introduction

1.1.1 Genes, development and disease

The human genome contains 30,000-40,000 protein-coding genes (Lander et al., 2001). It is the differential expression of these genes that underlies the differences in cell types seen in an adult human. Gene expression controls both growth and development to produce a new-born baby from a fertilised egg. This growth and differentiation also needs to be coupled with morphogenesis; that is, the movement of cells into the required pattern to determine the correct final body plan. During morphogenesis, cells must communicate with one another (cell signalling) and also stick to one another (cell-cell adhesion). It is this coupling of growth and differentiation with morphogenesis that defines 'development'. Defects in development can often lead to the onset of disease process; cancer being a common example. Both cell signalling and cell adhesion processes are active in cancer. These cells continuously perceive the signal to grow and divide, with the reduced adhesion of cells leading to the metastasis of tumours.

1.1.2 The Wnt Pathway

One of the major pathways contributing to both development and cancer is the Wnt pathway. Genetic experiments in the fruit fly, *Drosophila melanogaster*, gave the first glimpse of the pathway. The Wingless protein (Wg) controls cell fate; for example, instructing cells of the wing that they should be posterior cells. Later, Int-1 was shown to be the human homologue of Wg, and the amalgamation of the two names produced the name 'Wnt'. The pathway has since been shown to control many developmental processes – including cell fate specification, embryonic axis formation, and cell proliferation - across a wide spectrum of vertebrate and invertebrate organisms (Cadigan and Nusse, 1997; Moon et al., 1997). Mutations to many of the genes of this pathway have been shown to be coincidental with a large number of tumour types (Polakis, 2000).

Signals mediated by Wnt ligands have been shown to branch into four intracellular pathways: (1) a canonical Wnt pathway, which signals through TCF/LEF-1 transcription factors via GSK-3 and β-catenin (see Cadigan and Nusse, 1997); (2) a planar cell polarity pathway, which utilises Rho-kinase and JNK to cause cytoskeletal rearrangements (see Sokol, 2000); (3) a Wnt/Ca^{2+} pathway that controls PKC and CamKII to regulate cell adhesion and motility (see Kuhl et al., 2000); and (4) a novel pathway that regulates spindle orientation and asymmetric cell division, through GSK-3 and APC (see Huelsken and Birchmeier, 2001). Whilst Wnt is common to all of these pathways, many of the other components differ greatly. Dishevelled is a protein that may act as the switch between the different pathways (figure 1.1).

Wnt signalling via the canonical pathway requires the accumulation of β-catenin within the cell. β-catenin complexes with HMG-box transcription factors of the TCF/LEF-1 family to induce expression of downstream genes (Huber et al., 1996b). However, β-catenin is normally targeted for breakdown via the proteasome, following phosphorylation by a complex containing Axin, APC, GSK-3 and Casein Kinase 1. The Wnt signal inhibits GSK-3, via a process that is known to require Dishevelled.

1.1.3 β-catenin and GSK-3: central components of the Canonical Wnt Pathway

Canonical Wnt signalling in cancer is typified by tumorigenesis in the epithelial lining of the colon. Wnt regulates cell proliferation. A critical balance exists between the rate of proliferation and the rate of death of cells due to attrition. Mutations to single components of the pathway can tip the balance in the favour of proliferation, with unregulated division leading to the onset of carcinogenesis.

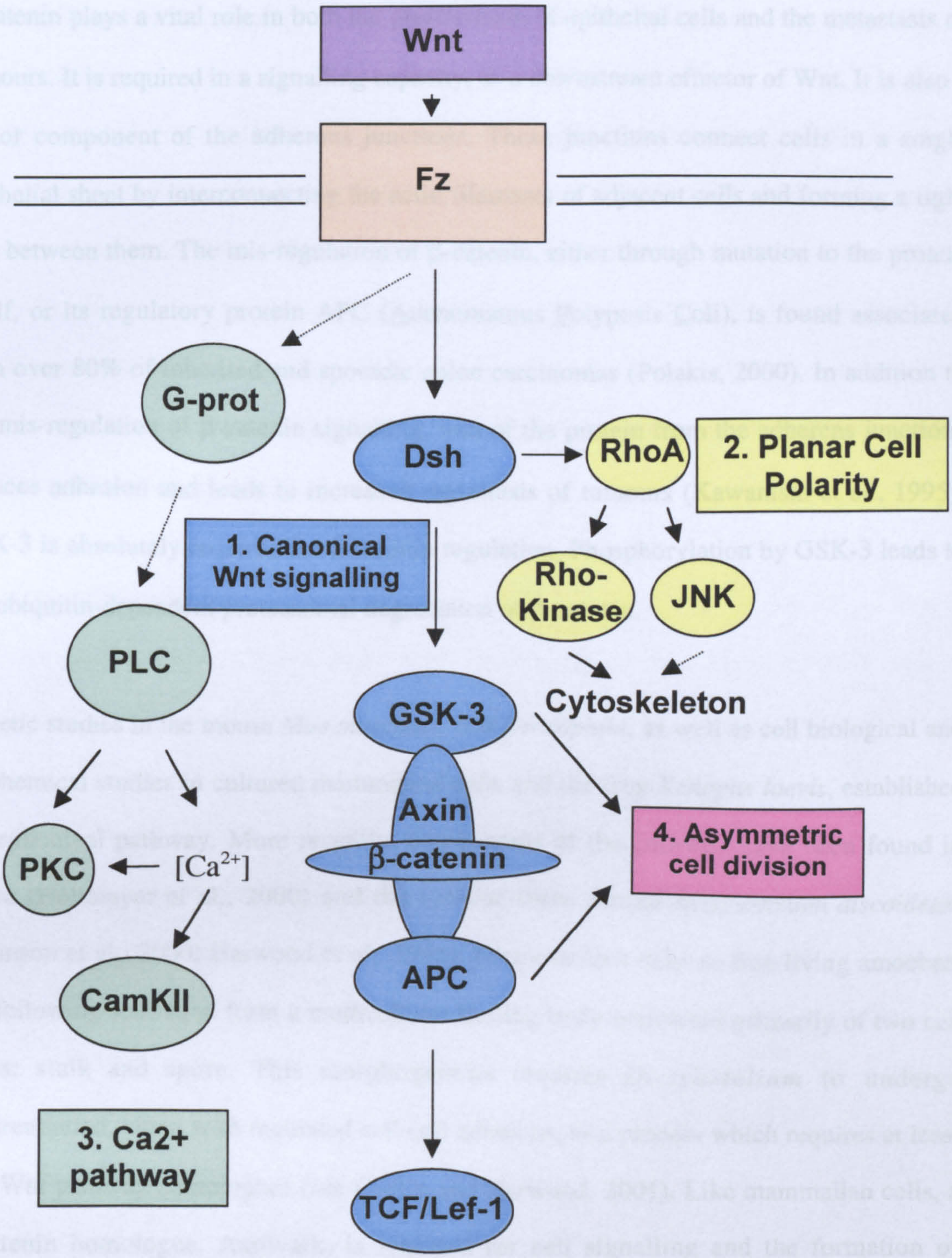

Figure 1.1 Wnt signalling diversifies into at least 4 branches

Wnt signalling via Dishevelled has been shown to regulate both canonical Wnt signalling and planar cell polarity. Recent evidence suggests that PLC activation by Wnt signalling in the Ca^{2+} pathway may involve G-proteins, whilst a pathway utilising GSK-3 and APC has been shown to regulate asymmetric cell division in *C. elegans*. Figure adapted from Polakis, 2001.

β-catenin plays a vital role in both the proliferation of epithelial cells and the metastasis of tumours. It is required in a signalling capacity, as a downstream effector of Wnt. It is also a major component of the adherens junctions. These junctions connect cells in a single epithelial sheet by interconnecting the actin filaments of adjacent cells and forming a tight belt between them. The mis-regulation of β-catenin, either through mutation to the protein itself, or its regulatory protein APC (Adenomatous Polyposis Coli), is found associated with over 80% of inherited and sporadic colon carcinomas (Polakis, 2000). In addition to the mis-regulation of β-catenin signalling, loss of the protein from the adherens junctions reduces adhesion and leads to increased metastasis of tumours (Kawanishi et al., 1995). GSK-3 is absolutely required for β-catenin regulation. Phosphorylation by GSK-3 leads to the ubiquitin-dependent proteasomal degradation of β-catenin.

Genetic studies in the mouse *Mus musculus*, and *Drosophila*, as well as cell biological and biochemical studies in cultured mammalian cells and the frog *Xenopus laevis*, established the canonical pathway. More recently, components of the pathway have been found in hydra (Hobmayer et al., 2000) and the cellular slime mould *Dictyostelium discoideum* (Grimson et al., 2000; Harwood et al., 1995). *Dictyostelium* exist as free-living amoebae, but following starvation form a multicellular fruiting body composed primarily of two cell types: stalk and spore. This morphogenesis requires *Dictyostelium* to undergo differentiation, along with regulated cell-cell adhesion, in a process which requires at least two Wnt pathway homologues (see Coates and Harwood, 2001). Like mammalian cells, a β-catenin homologue, Aardvark, is required for cell signalling and the formation of adherens junctions in *Dictyostelium* (Grimson et al., 2000). The further characterisation of Aar is described in this thesis.

1.2 Wnt ligands and receptors

1.2.1 Wnts

In 1982, Roel Nusse and Harold Varmus discovered that *int*-1 (later renamed Wnt-1 due to its homology with the *Drosophila* protein Wingless) was responsible for the majority of tumours in mice infected with the mouse mammary tumour virus (Nusse and Varmus, 1982). To date, 18 human and four *Drosophila* Wnt genes have been identified (Huelsken and Birchmeier, 2001). Wnts are cysteine-rich secreted proteins that act as intercellular signalling molecules. Purification is made difficult by the high level of hydrophobicity and the formation of aggregates by secreted Wnts.

1.2.2 Frizzleds and LRPs

For many years the inability to purify Wnt proteins made identification of their cognate receptors difficult. More recently, genetic, cell biological and biochemical approaches have suggested that the frizzled (Fz) cell-surface receptors act as receptors for Wnt proteins.

Fzs are seven-pass transmembrane proteins. They contain a putative N-terminal signal sequence, and C-terminal to this is a sequence of 120 amino acids, which contains 10 highly conserved cysteine residues. A highly divergent region of 40-100 amino acids are predicted to form a flexible linker and seven transmembrane segments are separated by short extracellular and cytoplasmic loops before the protein ends with a C-terminal cytoplasmic tail (Wang et al., 1996).

The overall structure of Fzs resembles that of G-protein coupled receptors (GPCRs), but whether Wnt signalling proceeds via G-proteins remains controversial. Little evidence exists, but one group has recently tried to answer this question using a chimaeric receptor with the ligand-binding and transmembrane segments from the β_2-adrenergic receptor

(β_2AR) and the cytoplasmic domains from rat Frizzled-1 (Rfz1) (Liu et al., 2001b). They show that treatment with the β-adrenergic agonist isoproterenol leads to the stabilisation of β-catenin in mouse cells transformed with the chimaeric receptor. Furthermore, G-protein inactivation or depletion of Gαq and Gαo blocked the response.

Ten human and four *Drosophila* Fzs have been identified to date. The first mutation in a *fz* (*fz1*) was discovered by genetic screens in *Drosophila* and exhibits a tissue polarity defect (Vinson and Adler, 1987). The epithelial cells that make up the wing blade are usually aligned such that the single hairs on each cell all point in a distal direction (Adler, 1992). In *fz1* mutants, hairs point in every direction. In addition, *fz1* mutants display a mis-orientation of the ommatidia comprising the compound eye (Zheng et al., 1995), something which is also seen with mutants of Dsh, a protein which is required for transduction of the Wg signal – see section 1.3 (Theisen et al., 1994). The endogenous ligand of Fz1 has not been established, however the role of Dsh suggested that the Fz family may transduce Wnt signals.

Subsequent analysis showed that the *fz*-related gene in *Drosophila*, *Dfz*2 is a Wg receptor. Stable transfection of *Dfz*2 into cell lines in which it would not normally be expressed, turn them from Wg non-responsive to Wg-responsive (Bhanot et al., 1996). Wg protein, however, does not bind uniquely to *Dfz*2, and in fact will also bind the original Fz. Some redundancy appears to exist between the Fz receptors, but the identification of a Wnt co-receptor has shed more light onto the subject.

LRP5 and LRP6 (*arrow* in *Drosophila*), members of the low-density lipoprotein-related proteins (LRPs), are coreceptors of Wnt. Arrow is essential for the transduction of Wingless in *Drosophila* (Wehrli et al., 2000), whilst LRP6 is essential for Wnt transduction

in *Xenopus*, and the extracellular domain of LRP6 has been shown to interact with Frizzled in a Wnt-dependent manner (Tamai et al., 2000). The intracellular domain of LRP5 binds Axin, and this is enhanced by the addition of Wnt (Mao et al., 2001). In addition, binding to LRP5 induces degradation of Axin, which can trigger LEF-1-mediated gene transcription.

1.2.3 Wnt antagonists

Several classes of protein have been discovered that will block Wnt signalling at the cell surface. They do this by directly binding Wnt proteins, or by competing for binding with either the Fz receptors, or the LRP receptors.

Wnt-inhibitory factor-1 (WIF-1) is a secretory protein that binds Wnts and inhibits their function; presumably by preventing them from binding to the Fz receptors (Hsieh et al., 1999). Highly conserved orthologues are found in mice, *Xenopus* and zebrafish.

Cerberus encodes a secreted protein that is expressed in the anterior endomesoderm of *Xenopus* (Bouwmeester et al., 1996). Cerberus has been shown to directly bind XWnt8, with microinjection of cerberus mRNA into *Xenopus* embryos inducing ectopic heads. Independent of Wnt binding, Cerberus also possesses two further sites required for nodal-related and bone morphogenic protein (BMP) signalling – two pathways required for head formation in *Xenopus*. A murine homologue, mCer-1, has also been isolated (Biben et al., 1998).

sFRPs (secreted frizzled-related proteins) are a family of secreted proteins, all approximately 30kDa in size, which contain a cysteine-rich domain (CRD) similar to that of Fzs. C-terminal to the CRD is a stretch of charged residues with homology to nectrins; a family of secreted proteins involved in axon guidance (Finch et al., 1997; Rattner et al.,

1997). The first sFRP to be cloned, Frizzled in bone, Fzb (also known as sFRP-3) was discovered in rats, where it is required for skeletal development (Hoang et al., 1996). sFRPs have been shown to bind Wg and inhibit downstream signalling, with the CRD both necessary and sufficient for this (Wang et al., 1997; Xu et al., 1998). More recently, evidence of an activating role for sFRP-1 in Wg signalling has been shown (Uren et al., 2000), raising the possibility that these proteins may act as inhibitors or activators of Wg signalling, depending on their cellular context.

Dikkopf-1 (Dkk-1), the first Dkk to be discovered (four have been found to date), was isolated as a secreted protein that induces the Spemann's organiser (an embryonic region with potent head-inducing activity) in *Xenopus* (Glinka et al., 1998). Injection of mRNA showed that Dkk-1 is both necessary and sufficient to cause head induction in *Xenopus*. Dkks are composed of two CRDs separated by a spacer region of variable length. The domains are well conserved across all four Dkk family members (Krupnik et al., 1999). Both Dkk-1 and Dkk-2 have been shown to interact with the Fz co-receptor LRP6/Arrow to antagonise Wg signalling (Bafico et al., 2001; Glinka et al., 1998; Li et al., 2002); presumably, by competing for binding with Wg. This interaction occurs in a Dsh-independent manner. Dkk-4 is also a Wg antagonist, but there is no evidence that Dkk-3 modulates Wnt signalling.

The individual domains of Dkk-1 and Dkk-2 possess distinct functional activities. Both Dkks inhibit Wnt8 and cooperate in the induction of head structures, but only Dkk-2 synergises with the Wnt co-receptor LRP6 to activate β-catenin signalling (Brott and Sokol, 2002). These differences have been attributed to variations in the N-terminal domains of the proteins.

1.3 Dishevelled

1.3.1 Dishevelled and the Canonical Wnt Pathway

The dishevelled gene (*dsh*) of *Drosophila* encodes a cytoplasmic phosphoprotein with no known biochemical function. Genetic epistasis experiments placed Dsh downstream of Wg and upstream of Zw-3 (figure 1.1).

Dsh becomes hyperphosphorylated following Wg stimulation and this form of the protein is found enriched at the plasma membrane (Yanagawa et al., 1995). This suggests that Wg signalling recruits Dsh to the membrane. Casein Kinase 2 (CK2) has been implicated as the kinase which phosphorylates Dsh, following the discovery that Dsh is found in a complex with CK2 and CK2 will phosphorylate Dsh at high levels *in vitro* (Willert et al., 1997). The CK2 inhibitor apigenin blocks proliferation in *Wnt-1* transfected cell lines, abolishes β-catenin phosphorylation, and reduces β-catenin and Dvl (the mammalian homologue of Dsh) protein levels (Song et al., 2000). This implies that both Dsh and CK2 are part of the Wg signalling pathway and both are positive regulators of the signal. However, over-expression of one of the Wg receptors, *Dfz*2, leads to phosphorylation of Dsh, but not accumulation of the β-catenin homologue Armadillo (Arm) (Willert et al., 1997). Therefore Dsh phosphorylation is insufficient for the transduction of the Wg signal to Arm.

Dsh has highly conserved homologues in *Xenopus* and mice. Over-expression of Dsh in *Drosophila* and *Xenopus* can mimic Wnt signalling, (Rothbacher et al., 1995; Yanagawa et al., 1995), but a knockout of the *dsh* homologue *dvl1* in mice fails to display any of the drastic Wnt phenotypes (Lijam et al., 1997). However, this may reflect a redundancy amongst the 3 mice homologues of Dsh (Dvl1/2/3).

At least three conserved domains have been identified in Dsh, the N-terminal DIX (dishevelled, axin interaction) domain, a central PDZ (postsynaptic density 95, discs large, zonula occludens-1) domain and a C-terminal DEP (dishevelled, egl-10, pleckstrin homology) domain (Boutros and Mlodzik, 1999). The DIX domain binds to the C-terminus of Axin, which also possesses a DIX domain, whilst the PDZ domain appears to bind Frat1 (frequently rearranged in advanced T-cell lymphomas 1), one of the two human homologues of GBP (GSK-3 binding protein) (Li et al., 1999). The DEP domain is required for planar cell polarity (see below), but not Wg signalling (Axelrod et al., 1998). This supports the idea that Dsh may act as the switch between Fz-mediated cell fate and Fz-mediated planar cell polarity.

1.3.2 Dishevelled and planar cell polarity

Epithelial cells are polarised in two ways. Apical-basal polarity distinguishes the top and bottom surfaces of the epithelial sheet, and planar polarity allows cells to determine directions in the plane of the sheet. Wnt signalling regulates planar cell polarity (or PCP). Each of the hexagonal cells that comprise the *Drosophila* wing secrete a single hair, an actin-rich plasma membrane projection. Each and every one of the hairs points distally from the distal cell vertex. Mutations, which disrupt PCP, orientate the polymerised actin in random locations, and hence the hairs point in all directions.

A non-canonical Wnt pathway appears to control PCP (Boutros and Mlodzik, 1999). Genetic epistasis experiments have suggested the involvement of the small GTPase RhoA and c-Jun NH_2-terminal kinase (JNK) downstream of Fz in the PCP pathway. Dsh can activate JNK (Boutros et al., 1998), suggesting that Dsh may act at the branch point between Wnt-mediated cell fate and Wnt-mediated PCP. In addition, Axin has been shown to interact with MEKK1, dimerising to activate JNK signalling (Zhang et al., 1999). The

involvement of both Dsh and Axin raises the possibility that an interaction between the two may be required for Dsh-mediated control of PCP.

1.3.3 Dishevelled and Notch

Mutations in presenilin (PS) genes are associated with Alzheimer's disease (see De Ferrari and Inestrosa, 2000). PS proteins mediate cleavage of the C-terminal domain of Notch. Notch subsequently enters the nucleus to regulate transcription. Genetic epistasis experiments have suggested that Dsh interacts antagonistically with Notch and Dsh has been shown to bind the cytoplasmic tail of Notch in a yeast two-hybrid system (Axelrod et al., 1996).

1.4 β-catenin and TCF/LEF-1

Along with GSK-3, these two proteins define the canonical Wnt pathway. It is the interaction of β-catenin with HMG-box transcription factors of the TCF/LEF-1 family that leads to the activation of Wnt target genes such as cyclin D and c-*myc* (Huber et al., 1996b). Co-expression of β-catenin and these transcription factors leads to the accumulation of β-catenin in the nucleus. Mutations to Pangolin (Pan) – the *Drosophila* LEF homologue – that block binding to Armadillo, reduce Wg signalling *in vivo* (Brunner et al., 1997). In *Xenopus*, injection of RNA encoding a mutant form of XTcf-3 (the LEF-1 homologue) that cannot bind β-catenin acts as a dominant negative (Molenaar et al., 1996). This, along with the finding that β-catenin accumulates in the nucleus upon Wnt stimulation, led to the idea that Wnts induce the accumulation of a β-catenin/TCF complex in the nucleus (Huber et al., 1996a). Further extrapolation of these findings led to the hypothesis that the β-catenin/TCF complex acts as a composite transcription factor, where TCF provides the site-specific DNA binding and β-catenin activates the transcription of target genes bound by the complex (van de Wetering et al., 1997).

In addition to β-catenin, a second protein, Pygopus (Pygo), that is required for TCF-mediated transcription has recently been discovered in *Drosophila*; and possesses two homologues in humans and one in *Xenopus* (Belenkaya et al., 2002; Kramps et al., 2002; Parker et al., 2002; Thompson et al., 2002). Mutations to Pygo carry the Wg phenotype, and the protein is required for TCF-mediated transcription but not the stabilisation of β-catenin. Pygo is a nuclear protein that is found complexed with the β-catenin homologue Armadillo, in *Drosophila*. The amino acid sequence identifies a PHD domain, suggesting a function in chromatin remodelling. In addition, the *Drosophila* BCL9 homologue Legless (Lgs) appears to be required for the recruitment of Pygo to the β-catenin-TCF complex (Kramps et al., 2002). An alternative hypothesis to the widely-accepted β-catenin/TCF transcription factor model has recently emerged (Chan and Struhl, 2002). This new model suggests that β-catenin may transduce Wnt signals by exporting TCF from the nucleus or by activating it in the cytoplasm.

In the absence of a Wnt signal, β-catenin is phosphorylated in a complex with Axin, GSK-3, CK1α and APC. Mutations at four Ser and Thr residues in the N-terminus of β-catenin, are prevalent in several types of human carcinoma (Korinek et al., 1997; Morin et al., 1997; Rubinfeld et al., 1997). It is the phosphorylation of Ser-33 and Ser-37 by GSK-3 that targets β-catenin for ubiquitination, facilitating the binding of the F-box protein βTrcp, and leading to proteosome-mediated degradation (Orford et al., 1997; Aberle et al., 1997; Liu et al., 1999).

The *Dropsohila* gene *slimb*, which contains and F-box and WD-40 repeats, negatively regulates Wg signalling (Jiang and Struhl, 1998). Proteins containing F-boxes are thought to serve as adaptor molecules, with the F-box binding to the E3 ubiquitin ligase. Studies in *Xenopus* revealed that the F-box/WD40-repeat protein β-Trcp bridges phosphorylated β-

catenin and the E3 ubiquitin ligase Skp1, targeting it for breakdown via the proteasome (Liu et al., 1999).

More recently, Siah-1, the human homologue of *Drosophila seven in absentia* has been shown to mediate a novel β-catenin degradation pathway (Liu et al., 2001a). Siah proteins have a short half-life and are normally kept at a low level within the cell (Hu and Fearon, 1999). Activation of the tumour suppressor protein p53 is thought to stabilise Siah-1. Breakdown of β-catenin following p53 activation has previously been reported (Sadot et al., 2001). Siah-1 binds the C-terminus of APC and a second protein SIP which, like βTrcp, is able to bind Skp1, along with the F-box protein Ebi (Matsuzawa and Reed, 2001). Ebi is able to bind to β-catenin, in a non phosphorylation-dependent manner and APC binds to both Siah-1 and β-catenin, bridging the two (Matsuzawa and Reed, 2001). Figure 1.2 highlights these two β-catenin degradation pathways.

This proposes a two-tiered mechanism for the destruction of β-catenin. In the canonical Wnt Pathway, β-catenin is targeted for breakdown following phosphorylation within the N-terminus and the binding of the F-box protein β-Trcp. Mutations to the phosphate-accepting residues in the N-terminus of β-catenin are only associated with a small number of incidences of colon cancer. This low incidence could be explained by the discovery of this second, p53-mediated, β-catenin degradation pathway. Forms of β-catenin which have escaped recognition by βTrcp become bound by the F-box protein Ebi, again at the N-terminus, in a non-phosphorylation-dependent manner (for a review of both βTrcp and Ebi-mediated β-catenin degradation, see Polakis, 2001).

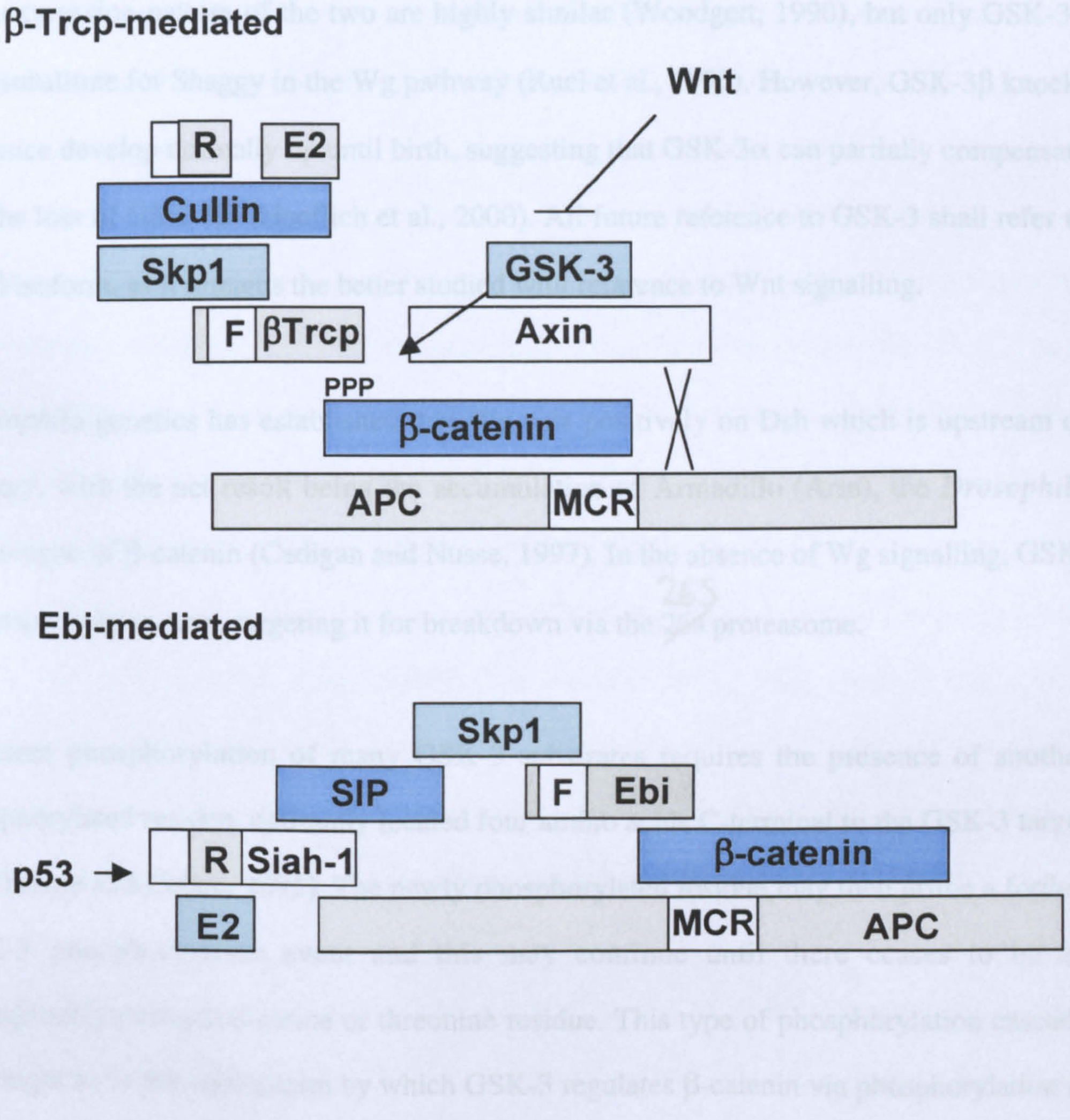

Figure 1.2 Protein interactions in the degradation of β-catenin
R = ring domain, F = F-box, MCR = mutation cluster region. See text for details.

1.5 GSK-3

The Zeste-White-3/Shaggy (Zw3/Shg) serine/threonine protein kinase of *Drosophila* possesses two highly homologous mammalian paralogues, glycogen synthase kinase 3-α (GSK-3α) and glycogen synthase kinase 3-β (GSK-3β). The two kinases were named due to their ability to phosphorylate and inactivate glycogen synthase, although roles in many other signalling pathways have now been shown (Grimes and Jope, 2001; Harwood, 2001).

The expression pattern of the two are highly similar (Woodgett, 1990), but only GSK-3β will substitute for Shaggy in the Wg pathway (Ruel et al., 1993). However, GSK-3β knock-out mice develop normally up until birth, suggesting that GSK-3α can partially compensate for the loss of GSK-3β. (Hoeflich et al., 2000). All future reference to GSK-3 shall refer to the β isoform, as it remains the better studied with reference to Wnt signalling.

Drosophila genetics has established that Wg acts positively on Dsh which is upstream of Shaggy, with the net result being the accumulation of Armadillo (Arm), the *Drosophila* homologue of β-catenin (Cadigan and Nusse, 1997). In the absence of Wg signalling, GSK-3 phosphorylates Arm, targeting it for breakdown via the ~~26~~ 26S proteasome.

Efficient phosphorylation of many GSK-3 substrates requires the presence of another phosphorylated residue, optimally located four amino acids C-terminal to the GSK-3 target site (Frame and Cohen, 2001). The newly phosphorylated residue may then prime a further GSK-3 phosphorylation event and this may continue until there ceases to be an appropriately positioned serine or threonine residue. This type of phosphorylation cascade is thought to be the mechanism by which GSK-3 regulates β-catenin via phosphorylation at its N-terminus. In addition to phosphorylating β-catenin, GSK-3 also phosphorylates and stabilises Axin and also phosphorylates APC, which promotes its binding with β-catenin (Rubinfeld et al., 1996; Yamamoto et al., 1999).

A >50% reduction in activity is seen in GSK-3 purified from cells treated with Wg-conditioned medium (Cook et al., 1996), but the exact mechanism of GSK-3 inhibition in the Wnt pathway is not entirely clear. Several mechanisms of GSK-3 regulation have been demonstrated. Phosphorylation at Tyr-216 is thought to be essential for GSK-3β function,

and so the action of a phosphatase would reduce GSK-3 activity. However, there is no evidence to suggest that a phosphatase inactivates GSK-3 in the Wnt pathway.

GSK-3 is also inactivated via phosphorylation at Ser-9 and several kinases have been shown to phosphorylate GSK-3 at this position. These include; cAMP-dependent protein kinase (PKA); PKB/Akt, protein kinase C (PKC); and p70 S6 kinase and p90Rsk (Cross et al., 1995; Eldar-Finkelman et al., 1995; Fang et al., 2000; Goode et al., 1992; Sutherland et al., 1993). GSK-3 is central to the insulin signalling pathway, where it is inactivated following phosphorylation at Ser-9 by PKB/Akt (Cross et al., 1995). However, PKB activity is insufficient to significantly increase TCF-dependent transcription (Ding et al., 2000). Wg-induced inactivation of GSK-3 is sensitive to the PKC inhibitor Ro31-8220 (Cook et al., 1996). This could, of course, be via phosphorylation of a second protein; for example, Dvl, although the *in vitro* data supports a more direct interaction. Dvl does however, have a putative PKC binding site in its DEP domain. (Mudher et al., 2001).

It may be that a change in the subcellular localisation of GSK-3 is responsible for the loss of β-catenin phosphorylation following Wnt signalling, or maybe it is a combination of this and direct inactivation. It has already been established that Dvl binds both Axin and Frat1. Axin and Frat1 also bind GSK-3 (Li et al., 1999; Yost et al., 1996). Dvl, Axin and GSK-3 can form a ternary complex, where Axin acts as a bridge for the other two proteins. Frat1 can be recruited to the complex, probably by Dvl. The finding that the Dvl binding domain of either Frat1 or Axin will inhibit Wnt induction of downstream target genes suggests that their interactions with GSK-3 may be an important step in the pathway (Li et al., 1999). Exactly how Frat1, Axin and Dvl bring about Wg-induced inactivation of GSK-3 remains unclear. The Dvl binding site of Axin overlaps with the β-catenin binding site (Julius et al., 2000), which suggests a mechanism whereby Dvl competes with β-catenin for binding to

Axin following Wnt stimulation. GSK-3 would become separated from β-catenin, allowing levels of the latter to rise.

In addition to Dishevelled and Axin, GBP (GSK-3 Binding Protein)/Frat (frequently rearranged in advanced T-cell lymphomas) also binds GSK-3. A role for GBP/Frat in the Wnt pathway was proposed following the discovery that in addition to binding GSK-3, the protein also interacts with Dishevelled (Li et al., 1999). A role for GBP/Frat in the nuclear export of GSK-3 has recently been proposed, following the finding that Frat-binding mutants of GSK-3 accumulate in the nucleus and a peptide of Frat that competes for binding with GSK-3 causes endogenous GSK-3 to accumulate in the nucleus (Franca-Koh et al., 2002).

The current model for Frat action proposes that Dishevelled recruits Frat to the Axin complex following Wnt stimulation. Frat then titrates GSK-3 from Axin, inhibiting GSK-3 dependent phosphorylation of β-catenin, allowing levels of the latter to rise (Li et al., 1999; Salic et al., 2000). To date, no change in the localisation of Frat or GSK-3 has been observed following stimulation of cells with either Wnt or insulin.

1.6 Protein Phosphatase 2A (PP2A)

The association of PP2A with the Wnt pathway arose from the observation that it will bind the C-terminus of Axin *in vitro* (Hsu et al., 1999). This suggested that PP2A may interact with the Axin/APC/GSK-3/β-catenin complex to modulate the effect of GSK-3 phosphorylation of β-catenin and/or other proteins.

The PR61 subunit of PP2A has been shown to inhibit β-catenin-dependent TCF activation and *Xenopus* axis duplication, without dephosphorylation of Axin or β-catenin degradation (Yamamoto et al., 2001). The exact target of PP2A in the Wnt pathway remains unclear.

1.7 Casein Kinase 1

Two Casein Kinase 1 family members appear to be active in the Wnt pathway. Casein Kinase 1ε (CK1ε) is a positive regulator of Wnt signalling. Overexpression of CK1ε mimics Wnt signalling, inducing a secondary axis in *Xenopus*, stabilising β-catenin and stimulating gene expression (Sakanaka et al., 1999). Both kinase-dead CK1ε and anti-sense CK1ε inhibit Wnt signalling. Furthermore, CK1ε has been found in a complex with Axin and Dishevelled (Sakanaka et al., 1999). The kinase is brought into the complex by the ankyrin repeat protein Diversin (Schwarz-Romond et al., 2002).

Phosphorylation of Ser-33 and Ser-37 of β-catenin is dependent on prior phosphorylation of residues Thr-41 and Ser-45 (van Noort et al., 2002). Despite Ser-45 being the most frequent tumour mutation spot (Polakis, 2000), GSK-3 is unable to phosphorylate this residue *in vitro* (Hagen and Vidal-Puig, 2002). CK1α can phosphorylate β-catenin *in vitro* at Ser-45, in an Axin-dependent manner (Liu et al., 2002; Amit et al., 2002). CK1α phosphorylation of Ser-45 is both necessary and sufficient to prime the GSK-3-mediated phosphorylation of Thr-41. Furthermore, CK1α phosphorylation of β-catenin has been shown to be inhibited by Wnt. This suggests a mechanism where in the absence of Wnt stimulation, Axin facilitates CK1α phosphorylation of β-catenin at Ser-45, initiating a GSK-3 phosphorylation cascade ending at Ser-33. βTrcp is then able to bind ubiquitinated β-catenin, targeting it for breakdown via the proteosome.

1.8 Axin and APC

Axin is the product of the *fused* locus. Mutations have pleiotropic effects on development, including the formation of axial duplications in homozygous vertebrate embryos (Zeng et al., 1997). Axin shows similarity to RGS (regulators of G-protein signalling) proteins and to the N-teminus of Dsh proteins. Injection of Axin mRNA inhibits dorsal axis formation in *Xenopus* embryos by interfering with Wnt signalling (Zeng et al., 1997). Ectopic expression in dorsal blastomeres of *Xenopus* embryos causes ventralisation, indicating an inhibitory function in normal axis formation. Conversely, ventral injection of RNA encoding a mutant Axin lacking the RGS domain leads to axis duplication, suggesting that this mutant is a dominant-negative. Co-injection of Axin RNA with the RNA of Wnt pathway components reveals that it acts downsteam of Wnt, Dsh, and GSK-3 but upstream of β-catenin (Fagotto et al., 1999).

What is the mechanism by which Axin inhibits axis duplication? The Axin protein contains binding sites for both GSK-3 and β-catenin, with all three forming a ternary complex when co-expressed in COS cells (Ikeda et al., 1998). GSK-3 does not significantly phosphorylate β-catenin *in vitro* (Rubinfeld et al., 1996). However, the addition of Axin significantly increases GSK-3 phosphorylation of β-catenin *in vitro* (Ikeda et al., 1998), suggesting that at least one of the roles of Axin is to enhance GSK-3 phosphorylation of β-catenin. This could be through bringing GSK-3, CK1α and β-catenin together.

Conductin is a paralogue of Axin, sharing 45% amino acid identity (Behrens et al., 1998). Biochemically it behaves like Axin, promoting the degradation of β-catenin. Unlike Axin though, Conductin is selectively expressed in the mouse embryo (Behrens et al., 1998). Conductin is upregulated in colonic and hepatocellular carcinomas (Lustig et al., 2002). Furthermore, Conductin expression in colorectal tumour cells can be blocked through the

expression of dominant-negative TCF, and is upregulated following Wnt-1 stimulation of cultured cells or in Min mice (mice null for APC) (Lustig et al., 2002). The evidence to date therefore suggests that Conductin itself is a target of Wnt signalling, acting in a negative feedback loop. In a normal cell, Conductin can scaffold β-catenin into the degradation complex containing GSK-3, promoting β-catenin breakdown. Wnt-1 stimulation stabilises β-catenin, allowing it to complex with TCF and activate target genes, one of which is Conductin, a negative regulator of β-catenin.

Mutations in the APC (adenomatous polyposis coli) gene are responsible for up to 80% of both inherited and sporadic forms of colon cancer (Miyoshi et al., 1992). The APC gene encodes a large (approximately 310kDa) protein with several distinct motifs; namely, an N-terminal oligomerisation domain, seven armadillo repeats, three repeats of 15 amino acids, seven repeats of 20 amino acids, and a basic domain (see Polakis, 1999). The first three of the 20 amino acid repeats of APC encompass what has been termed the mutation cluster region (MCR) and contains the majority of somatic APC mutations seen in colon cancer (Miyoshi et al., 1992). The oligomerisation domain is required for the homodimerisation of APC molecules, whilst the C-terminal basic domain binds microtubules. It is the 15 amino acid and 20 amino acid repeats that are of greatest relevance to cancer. The three 15 amino acids repeats each bind β-catenin independently, whilst the seven 20 amino acid repeats each bind β-catenin in a phosphorylation-dependent manner. It is the deletion of four or five of the 20 amino acid repeats that is most commonly associated with incidents of colon cancer (Polakis, 1997). Experimental deletions to APC, showed that loss of β-catenin regulation occurred as the 3' boundary of the MCR was crossed. However, these deletions also represent a loss of 2 of the 3 binding sites for Axin (Behrens et al., 1998), suggesting another route to β-catenin mis-regulation.

The over-expression of Axin in *APC*-mutant cancer cells is sufficient to downregulate β-catenin (Hart et al., 1998). So what is the precise role that APC plays in the downregulation of β-catenin? Several theories exist and one attractive idea has resulted from the *in vitro* reconstruction of Axin-mediated β-catenin degradation (Salic et al., 2000). APC may be required to sequester β-catenin throughout the cytoplasm, or may bind nuclear β-catenin and transport it to the Axin complex (Bienz, 1999). Two pieces of evidence support this theory. Firstly, the finding that APC contains nuclear export sequences (Rosin-Arbesfeld et al., 2000) and, secondly, APC has been shown to move along microtubules and concentrate at their growing ends in epithelial cells (Mimori-Kiyosue et al., 2000).

1.9 Wnt signalling in *Caenorhabditis elegans*

Three highly divergent β-catenin homologues with different functions have been identified in *C. elegans*: WRM-1, BAR-1 and HMP-2. (Korswagen et al., 2000). BAR-1 is the only one that interacts with the TCF-like transcription factor POP-1 to activate expression of Wnt target genes. WRM-1 activates the kinase LIT-1/Nemo-like kinase, which participates in MAP kinase signalling and opposes signalling by POP-1. HMP-2 interacts with the *C. elegans* cadherin, HMR-1 to regulate adhesion.

A non-canonical Wnt pathway in *C. elegans* is required for the control of asymmetric cell divisions (for a review, see Thorpe et al., 2000). The Wnt homologue MOM-2 (more mesoderm–2) binds to the Fz homologue MOM-5, to activate a signalling cascade which is required for the induction of endoderm in the early embryo (Rocheleau et al., 1997; Thorpe et al., 1997), and the specification of several asymmetric cell divisions during larval development (Herman and Horvitz, 1994; Herman et al., 1995).

A mitogen-activated protein kinase (MAPK) pathway, consisting of MOM-4/TAK1 and LIT-1/NLK, acts in parallel to the MOM-2/Wnt pathway to downregulate POP-1 levels (Kaletta et al., 1997; Meneghini et al., 1999; Rocheleau et al., 1999). The reduction in POP-1 levels leads to derepression of *end*-1 and the induction of endoderm development (Lin et al., 1995). Therefore, instead of turning POP-1/TCF into a transcritional activator, the MOM-2/Wnt/MAPK pathway blocks the repressive function of POP-1. Figure 1.3 illustrates this non-canonical Wnt pathway.

BAR-1 has been shown to bind PRY-1, the *C. elegans* Axin homologue, and regulate a second and more canonical Wnt pathway (Korswagen et al., 2002). This suggests that two parallel pathways, one canonical and one non-canonical, transduce Wnt signals in worms (see Korswagen, 2002).

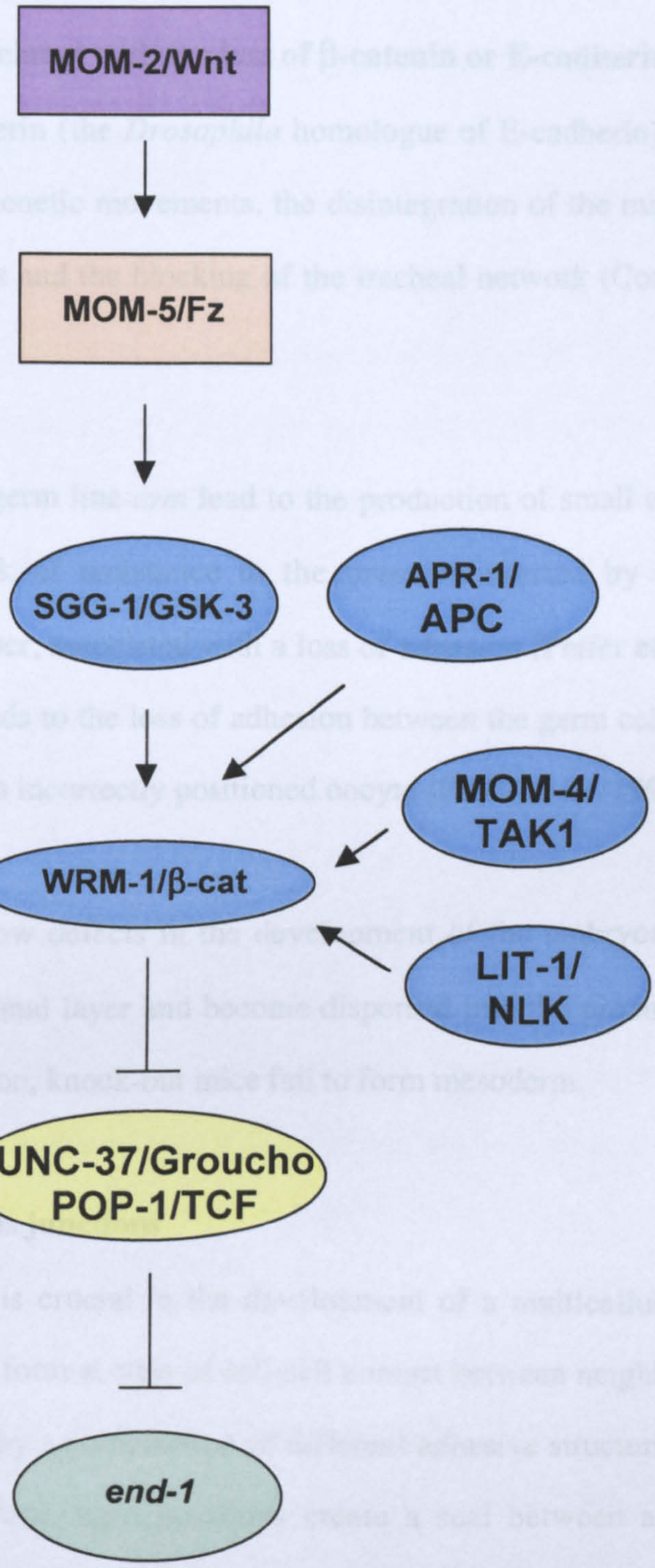

Figure 1.3 Non-canonical Wnt signalling in *C. elegans*

MOM-2/Wnt signalling, in combination with a MAPK pathway, leads to depression of *end-1*. WRM-1 and LIT-1/NLK form a complex that is activated by MOM-4/TAK1 to phosphorylate and inactivate POP-1. Both the GSK-3 homologue SGG-1 and the APC related protein APR-1 appear to function as positive regulators of the pathway.

1.10 β-catenin and cell-cell adhesion

1.10.1 Adhesion defects associated with the loss of β-catenin or E-cadherin

The loss of zygotic *D*E-cadherin (the *Drosophila* homologue of E-cadherin) is associated with the reduction of morhogenetic movements, the disintegration of the malpighian tube into small spherical structures and the blocking of the tracheal network (Cox et al., 1996; Uemura et al., 1996).

In *Drosophila,* mutations to germ line *arm* lead to the production of small eggs, which is presumed to be from a lack of resistance to the pressure exerted by the muscular contractions of the egg chamber, associated with a loss of adhesion (Peifer et al., 1993). In addition, mutations to *arm* leads to the loss of adhesion between the germ cells, but not the follicle cells, which leads to an incorrectly positioned oocyte (Peifer et al., 1993).

β-catenin knock-out mice show defects in the development of the embryonic ectoderm. Cells detach from the ectodermal layer and become dispersed into the proamniotic cavity (Haegel et al., 1995). In addition, knock-out mice fail to form mesoderm.

1.10.2 β-catenin and adherens junctions

Regulated cell-cell adhesion is crucial in the development of a multicellular organism. Intercellular junctions usually form at sites of cell-cell contact between neighbouring cells; epithelial cells are connected by a combination of different adhesive structures (see figure 1.4). Near to the apical surface, tight junctions create a seal between adjacent cells restricting the movement of molecules between them. Below the tight junctions are the adherens junctions, which join the actin cytoskeleton of adjacent cells, forming an adhesion belt, also known as the *zonula adherens*. Nearer to the basal surface are the desmosomes and the gap junctions. The desmosomes join the intermediate filaments of adjacent cells,

whilst the gap junctions contain channels that allow small molecules and ions to pass from one cell to another, rather like the plasmodesmata of plants. The hemidesmosomes anchor the intermediate filaments inside the cell to the basal lamina.

Cadherin molecules play essential roles in development, cell polarity and tissue morphology (Takeichi, 1991). E-cadherin has an extracellular domain of five cadherin-type repeats. It is these repeats that interact in a calcium-dependent fashion with the cadherin molecules on opposing cell surfaces to regulate cell adhesion (Nagar et al., 1996). The cytoplasmic domain of E-cadherin was found to associate with α-, β- and γ-catenin (Ozawa et al., 1989).

The binding of β-catenin to the cytoplasmic tail of E-cadherin introduces α-catenin to the adherens junction complex (for a review, see Nagafuchi, 2001). α-catenin, in turn, links with the actin cytoskeleton. γ-catenin, or plakoglobin, is a paralogue of β-catenin, sharing high sequence similarity (Cowin et al, 1986). Plakoglobin is mainly found localised at desmosomes, where it binds the desmosomal cadherin proteins, desmogleins and desmocollins. Plakoglobin is also able to bind to E-cadherin, but with weaker affinity than β-catenin (Knudsen and Wheelok, 1992; Peifer et al, 1992).

The importance of β-catenin localisation at the adherens junctions is two-fold; (1) It is required for maintaining the integrity of the adherens junctions: loss of β-catenin from adherens junctions leads to reduced adhesion and thus increased invasiveness and metastasis of tumour cells (Birchmeier et al., 1993); (2) When not bound to E-cadherin, β-catenin can move to the nucleus and activate target genes of the Wnt pathway, another possible factor in the progression of certain types of tumour.

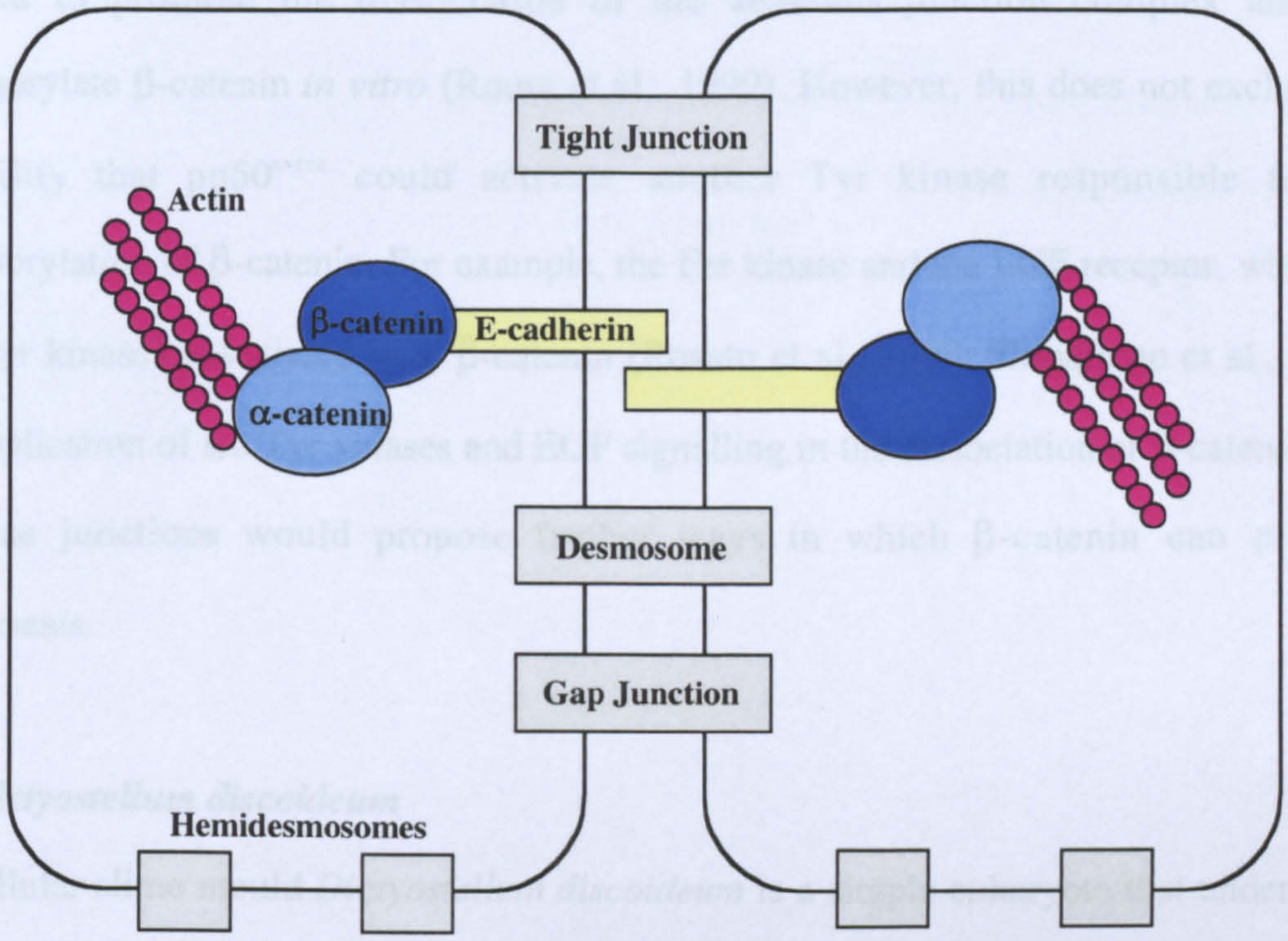

Figure 1.4 Schematic of epithelial cell junctions, highlighting the major protein components

E-cadherin cell adhesion molecules bind homophilically to one another, to connect adjacent cells. β-catenin links the cadherin molecules with the actin cytoskeleton via α-catenin, to provide a continuous belt of actin across the epithelium.

1.10.3 Tyrosine phosphorylation of β-catenin

There is no evidence that phosphorylation of β-catenin by GSK-3 plays a role in its binding at adherens junctions. However, tyrosine phosphorylation (at Tyr-654) has been shown to decrease the interaction of β-catenin with E-cadherin *in vivo* (Kinch and Burridge, 1995; Roura et al., 1999). Elucidation of the crystal structure of the β-catenin/E-cadherin complex demonstrated that Tyr-654 is a key residue in this interaction (Huber and Weis, 2001).

p120-catenin is a further catenin molecule often found associated with the adherens junctions, and was originally identified as a substrate for the pp60src Tyr kinase (Kanner et

al., 1991). In addition, $pp60^{c\text{-}src}$ Tyr kinase, or its viral homologue $pp60^{v\text{-}src}$, has been reported to promote the dissociation of the adherens junction complex and will phosphorylate β-catenin *in vitro* (Roura et al., 1999). However, this does not exclude the possibility that $pp60^{c\text{-}src}$ could activate another Tyr kinase responsible for the phosphorylation of β-catenin. For example, the Fer kinase and the EGF receptor, which are both Tyr kinases associated with β-catenin (Rosato et al., 1998; Shibamoto et al., 1994). The implication of src Tyr kinases and EGF signalling in the dissociation of β-catenin from adherens junctions would propose further ways in which β-catenin can promote oncogenesis.

1.11 *Dictyostelium discoideum*

The cellular slime mould *Dictyostelium discoideum* is a simple eukaryote that undergoes a programme of multicellular development with similarities to that of animal development. Cells grow as unicellular amoebae and divide with a short generation time, making it simple to obtain large numbers for use in biochemical assays. A 34Mb haploid genome makes *Dictyostelium* genetically tractable and a cDNA sequencing project has, to date, yielded 6,400 independent sequences, which represents 70-80% of all of the expected genes (Urushihara, 2002).

1.11.1 *Dictyostelium* development

It is the starvation of *Dictyostelium* that initiates the developmental programme, leading to multicellularity. Hemispherical mounds of approximately 100,000 amoebae form following cAMP-induced chemotaxis. From the mound, a small tip appears which extends until a finger-like structure, the slug, is produced. The slug then falls over and, guided by photo- and thermotaxis, migrates to the soil surface in order to produce a fruiting body. See figure 1.5 for the timing of events.

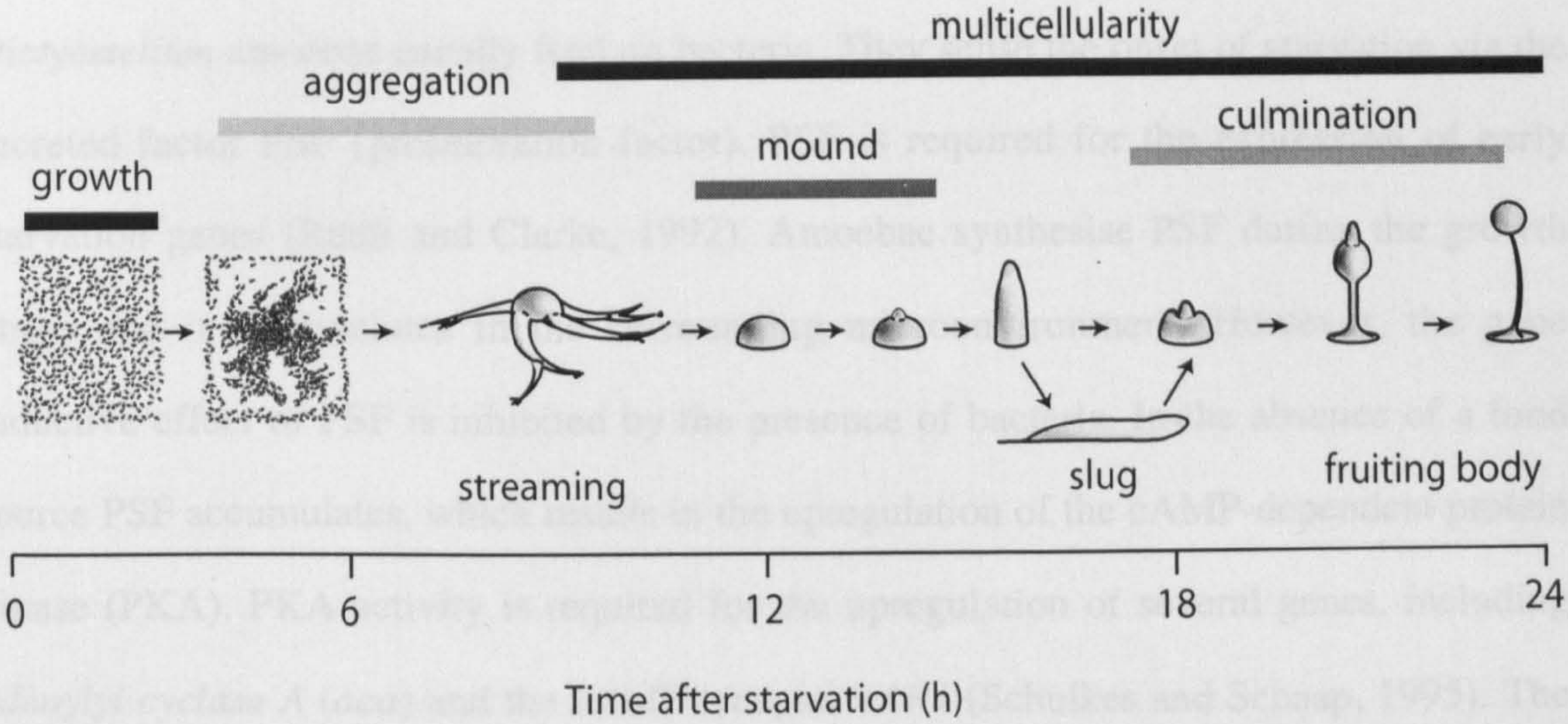

Figure 1.5 *Dictyostelium* development
In the presence of a plentiful food source, amoebae grow and divide. Upon starvation, cells coalesce into adherent cell 'streams' which tighten to form the mound. The 'tip' then develops from the mound and extends to make a slug, which will either culminate, or migrate until conditions are more favourable for making a fruiting body. (Figure reproduced with permission from A. J. Harwood).

The natural habitat of *Dictyostelium discoideum* is the forest floor; they were first isolated from decaying leaves in North America by Kenneth Raper in 1935 (Raper, 1935). *Dictyostelium* amoebae usually feed on bacteria. They sense the onset of starvation via the secreted factor PSF (prestarvation factor). PSF is required for the expression of early starvation genes (Rathi and Clarke, 1992). Amoebae synthesise PSF during the growth phase and it accumulates in the surrounding microenvironment. However, the gene inductive effect of PSF is inhibited by the presence of bacteria. In the absence of a food source PSF accumulates, which results in the upregulation of the cAMP-dependent protein kinase (PKA). PKA activity is required for the upregulation of several genes, including *adenylyl cyclase A* (*aca*) and the cAMP receptor *cAR1* (Schulkes and Schaap, 1995). The activation of adenylyl cyclase leads to the secretion of cAMP in the nanomolar range. ACA becomes activated via cAR1, which becomes adapted following exposure to cAMP. Consequently, ACA becomes inactive until extracellular cAMP is removed by phosphodiesterase (PDE) (see Kimmel and Firtel, 1991). This leads to the relay of cAMP pulses across the field of aggregating cells (Van Haastert, 1995). In addition to emitting cAMP pulses, cells respond to cAMP by chemotaxing towards the source, hence the field of developing cells move towards the aggregation centre.

In addition to the cAMP relay, cells also need to sense the accumulation of a secreted factor called CMF (conditioned medium factor). When the number of starving cells within a 10mm proximity reaches the required density, the concentration of CMF will reach a level that induces cells to aggregate. Once an aggregate is formed, micromolar levels of cAMP, in combination with CMF, induce the expression of prespore and prestalk genes (Gomer et al., 1991; Mehdy and Firtel, 1985). Within the slug, the posterior two thirds are composed of prespore cells, whilst the anterior third is composed of prestalk cells. These two cell types will subsequently give rise to the spore and stalk cells, respectively, of the mature

fruiting body (MacWilliams and Bonner, 1979). Once the slug begins to culminate, prestalk cells in the tip move down through the developing prespore mass and embed into the basal disc (see Dormann et al., 1996). As the stalk develops, it becomes enclosed in a protein- and cellulose-containing tube (Grimson et al., 1996). As the prestalk cells enter the tube, they become terminally differentiated, forming vacuolated stalk cells. The stalk grows by elongation, via the addition of stalk cells to its top, which raises the spore head up to the top of the stalk.

Conditions have been established whereby, in the absence of multicellularity, spore and stalk cells can be formed in monolayers (Berks and Kay, 1988; Town et al., 1976). This approach has led to the discovery of further factors required for cell differentiation in *Dictyostelium*. Differentiation-inducing factor-1 (DIF-1) is a small chlorinated alkyl phenone required for the determination of pre-stalk cell fate (Kopachik et al., 1983; Morris et al., 1987). DIF-1 promotes the differentiation of pre-stalk cells, whilst repressing the differentiation of pre-spore cells (Early and Williams, 1988).

SDF-1 and SDF-2 (spore differentiation factor 1 & 2) are peptides that promote terminal spore differentiation under submerged conditions (Anjard et al., 1997). The two SDF peptides appear to regulate independent pathways, but both may require phosphorylation by PKA (Anjard et al., 1997). SDF-1 and SDF-2 are produced and secreted at different times in development and are released in single bursts, which may represent an irreversible step in cell differentiation (Anjard et al., 1998).

Ammonia and adenosine both affect ~~differentiaton~~ differentiation. Ammonia accumulates as cells develop, and if sufficient levels do not evaporate, aggregation is delayed and slugs will migrate (Anjard et al., 1997). The addition of well-buffered substrates leads to the immediate

production of a fruiting body, thought to be due to the neutralisation of ammonia. Adenosine is thought to bind cells on the cAR1 receptor (Newell, 1982). Binding of adenosine inhibits the cAMP relay and blocks adaptation in perfusion experiments (Theibert and Devreotes, 1984). Some evidence also exists for a role in later development (Schaap and Wang, 1986).

1.11.2 GSK-3 signalling in *Dictyostelium*

The *Dictyostelium* GSK-3 homologue, GskA, has been shown to be crucial for the early prespore/prestalk cell patterning event, although not essential for cell differentiation (Harwood et al., 1995). In the *gskA* null mutant, the prestalk cell population is grossly expanded at the expense of the prespore cell population and cAMP repression of both *ecmB* expression (a marker of pre-stalk cells) and stalk formation is lost in monolayer culture (Harwood et al., 1995). A rise in GskA activity is seen at the onset of multicellular development, when *ecmB* and *pspA* (a marker of pre-spore cells) are first expressed. This increase in activity is mediated by the cAMP receptor cAR3; *cAR3* null mutants have many features common to the loss of *gskA* (Plyte et al., 1999). The *Dictyostelium* tyrosine kinase Zak-1 has been shown to increase GSK-3 activity *in vitro* and is required for the increase in GskA activity seen in development (Kim et al., 1999). It is regulated by cAMP via cAR3 and mutants also have effects similar to loss of *gskA*. Conversely, loss of the lower-affinity cAMP receptor, cAR4, leads to greater activity of GskA and prolonged tyrosine phosphorylation when treated with cAMP (Ginsburg and Kimmel, 1997; Kim et al., 2002). This suggests that a tyrosine phosphatase may be downstream of cAR4. Figure 1.6 illustrates this dual regulation of GskA by cAMP.

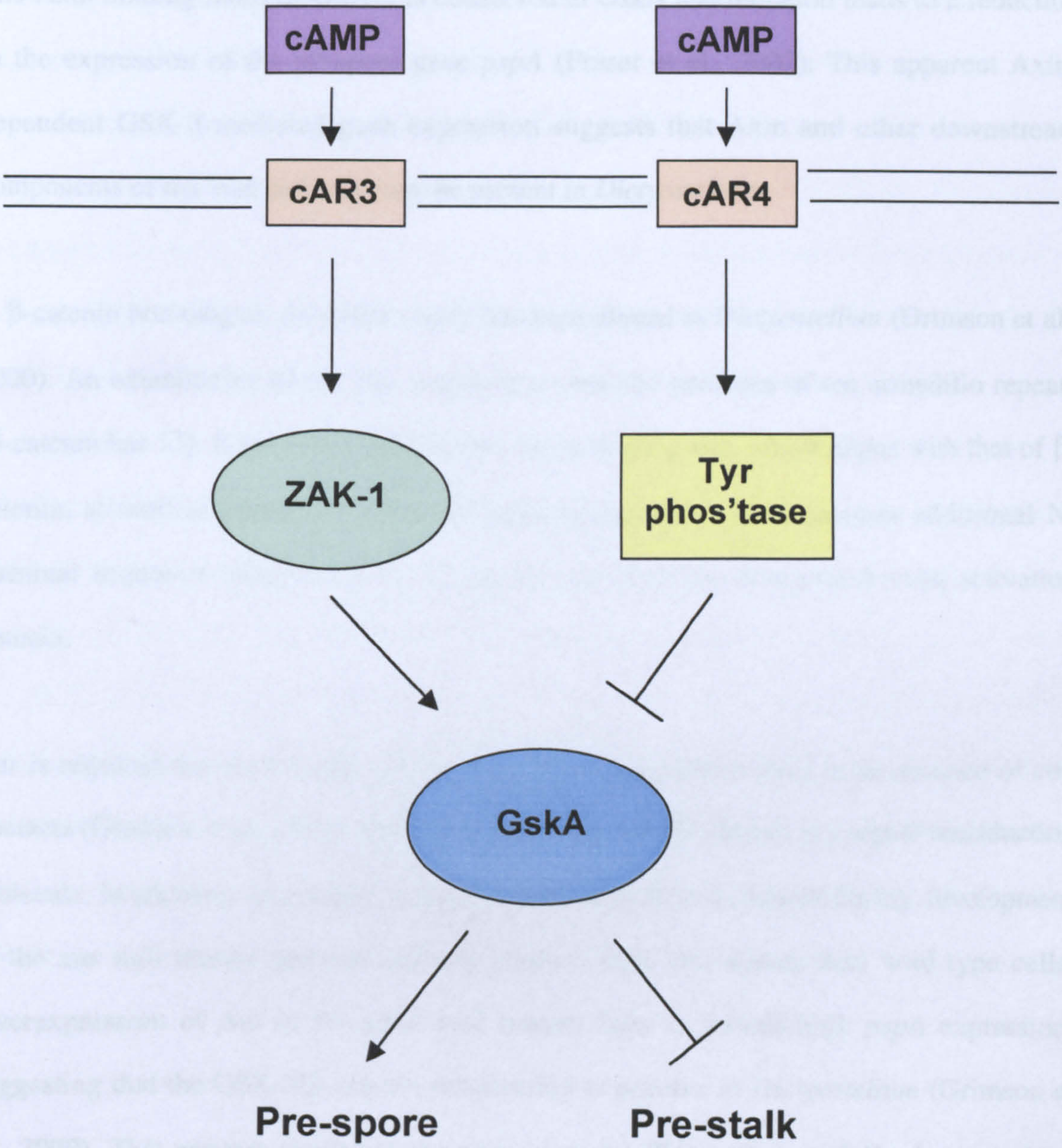

Figure 1.6 cAMP regulation of GskA

cAMP binding at the cAR3 receptor activates GskA via the tyrosine kinase ZAK-1. GskA induces pre-spore gene expression whilst at the same time inhibiting pre-stalk gene expression. cAMP binding at the cAR4 receptor inhibits GskA via a tyrosine phosphatase.

The Axin binding motif of GSK-3 is conserved in GskA and mutation leads to a reduction in the expression of the prespore gene *pspA* (Fraser et al., 2002). This apparent Axin-dependent GSK-3-mediated gene expression suggests that Axin and other downstream components of the Wnt pathway may be present in *Dictyostelium*.

A β-catenin homologue, Aardvark (Aar), has been cloned in *Dictyostelium* (Grimson et al., 2000). An examination of the Aar sequence reveals the presence of ten armadillo repeats (β-catenin has 12). It also has a putative α-catenin binding site, which aligns with that of β-catenin, as well as potential GSK-3 phosphorylation sites. Aar possesses additional N-terminal sequence compared with β-catenin and lacks the C-terminal trans-activation domain.

Aar is required for *pspA* expression in cell suspension, where there is an absence of cell contacts (Grimson et al., 2000). This shows that Aar, like β-catenin, is a signal transduction molecule. In addition, expression of *pspA* is both delayed and reduced during development in the *aar* null mutant and *aar* mutants produce 50% less spores than wild type cells. Overexpression of Aar in the *gskA* null mutant fails to restore high *pspA* expression, suggesting that the GSK-3/β-catenin relationship is positive in *Dictyostelium* (Grimson et al., 2000). This appears similar to the non-canonical Wnt pathway of *C. elegans* where GSK-3 acts positively on WRM-1, the β-catenin homologue, for endoderm induction (Korswagen, 2002).

1.11.3 Aar and cell adhesion

As with β-catenin, in addition to a cell signalling function, Aar also has a structural function (Grimson et al., 2000). Aar localises to cell-cell contacts, which have the morphology of adherens junctions. *aar* mutants develop, but fruiting bodies are

mechanically weak, and the majority collapse onto the substratum. Transmission electron microscopy of longitudinal sections of the stalk tube reveal a loss of actin from the adherens junctions in *aar* mutant fruiting bodies, further supporting a role for Aar in the formation of *Dictyostelium* adherens junctions (Grimson et al., 2000). Conversely, overexpression of *aar* in wild type cells leads to the mis-localisation of large amounts of actin at the adherens junctions, causing the membrane to buckle. This results in the instability of fruiting bodies, but the phenotype is not as severe as the *aar* mutant.

The fruiting body of wild type *Dictyostelium* contains just one single stalk, positioned in the centre of the stalk tube. Stalk cells only normally differentiate inside the stalk tube, but in *aar* mutant fruiting bodies stalk cells can differentiate outside of the stalk tube (Coates et al., 2002). This can lead to the formation of additional stalks. The exact mechanism behind ectopic stalk formation is unclear. One possibility is that the loss of adherens junctions associated with the *aar* mutant disrupts the integrity of the stalk tube. This would allow the stalk-inducing factor to escape, giving rise to the formation of ectopic stalks. This illustrates how changes in structure can lead to effects on signalling.

1.12 Aims of thesis

The observation that the GskA-Aar interaction appears to mimic that of the GSK-3-WRM-1 interaction in *C. elegans* was an interesting one. Further analysis of the *Dictyostelium*, and other, non-canonical Wnt-like signalling pathways may reveal important findings about both the evolution and function of these pathways in mammalian development.

Whilst the structure of Aar has been examined at the sequence level, no physiological relevance has been attributed to features such as the putative α-catenin binding and GSK-3

phosphorylation sites. At the outset of this project, the following questions were to be addressed:

- Does GskA directly phosphorylate Aar?
- What physiological roles can be assigned to the various features of the Aar sequence?
- What does the subcellular localisation of Aar reveal about Aar protein function?

Chapter 2

Materials and Methods

2.1 List of abbreviations used

aar, Aar, *aar*$^-$	Aardvark gene, protein product and knock-out
AEBSF	4-(2-Aminoethyl)benzenesulphonyl Fluoride
Ala	Alanine
amp^R	Ampicillin resistant
APS	Ammonium persulphate
Arg	Arginine
bp	base pairs
BSA	Bovine serum albumin (Fraction V)
°C	degrees Celsius
cAMP	Adenosine 3':5'-cyclic monophosphate
cDNA	complementary DNA
Ci	Curie
Cys	Cysteine
dATP	2'-Deoxyadenosine 5'-triphosphate
dCTP	2'-Deoxycytosine 5'-triphoshate
ddH_2O	Double distilled water (Millipore)
DEAE	Diethylaminoethanol
DEPC	Diethyl pyrocarbonate
dGTP	2'-Deoxyguanosine 5'-triphosphate
DIF	Differentiation Inducing Factor
DMSO	Dimethyl sulphoxide
DNA	Deoxyribonucleic acid
DTT	DL-Dithiothreitol
dTTP	Thymidine 5'-triphosphate
ECL	Enhanced chemiluminescence

EDTA	Disodium Ethylenediaminetetra-acetic acid
EGTA	Ethylene Glycol-bis(ß-aminoethylether)-N,N,N'N'-tetraacetic acid
g	gram
Glu	Glutamic acid
Gly	Glycine
His	Histidine
His-tag	6x histidine epitope tag
hrp	Horseradish peroxidase
IgG	Immunoglobulin
kb	kilobase
kDa	kiloDalton
l	litre
Leu	Leucine
M	molar
MBq	Mega bequerels
m	metre
m (prefix)	milli (10^{-3})
μ	micro (10^{-6})
Met	Methionine
min	minutes
mol	moles
MOPS	3-(N-Morpholino)propanesulphonid acid
mRNA	Messenger RNA
n	nano (10^{-9})
OD_x	Optical density at x nm
p	pico (10^{-12})

^{32}P	Radioactive phosphorous
PBS	Phosphate-buffered saline
PBST	PBS/0.1% Tween-20
pfu	Plaque-forming units
Phe	Phenylalanine
Pro	Proline
RNA	Ribonucleic acid
rpm	Revolutions per minute
s	seconds
SDS	Sodium dodecyl sulphate
SDS-PAGE	SDS-polyacrylamide gel electrophoresis
Ser	Serine
SSC	Standard sodium citrate
TBE	Tris/Borate/EDTA
TE	Tris/EDTA
TEM	Transmission electron microscopy
TEMED	N'N'N'N'Tetramethylethylenediamine
Thr	Threonine
Tris	Tris (hydroxymethyl) methylamine
TRITC	Tetramethylrhodamine B Isothiocyanate
Tyr	Tyrosine
UV	Ultraviolet
V	Volt
Val	Valine
v/v	volume for volume
w/v	weight for volume

2.2 *Dictyostelium* culture and transformation

2.2.1 Cell culture

Vegetative cells were grown at 22°C, either on lawns of *Klebsiella aerogenes* plated on Sussman's medium, or in shaking culture in axenic medium containing 0.1mg/ml streptomycin (and 20µg/ml G418 or 10µg/ml if selecting for overexpressors or knock-outs, respectively). Ax2 was used as the wild type strain throughout this thesis.

For long term storage, 10^7 cells or more were resuspended in 1ml horse serum containing 5% DMSO in a 2ml cryovial (Nunc) and slowly frozen at –80°C, before being transferred to liquid nitrogen stores.

2.2.2 Transformation of *Dictyostelium* by electroporation

10^7 log phase (1-2x 10^6/ml) cells were spun out of axenic medium at 700g for 4min and washed once in sterile electroporation buffer (50mM sucrose in KK_2) before resuspension in 800µl of the same buffer. The cell suspension was then incubated on ice for 10 min and electroporated in 50x4mm electroporation cuvettes using a BioRad Gene Pulser (at 1.6KV with a capacitance of 3µF). Cells were then incubated on ice for 10 min, before the addition of 8µl of 1mM $MgCl_2$/1mM $CaCl_2$ and further incubation for 15 min at room temperature (RT). The contents of each cuvette were split between two axenic plates. Media containing 20µg/ml streptomycin was added. After 24 hours, the media was replaced with media containing 20µg/ml strep, 20µg/ml G418 and 1% (v/v) heat-killed *E. coli* (strain B/R).

2.3 Molecular biology

2.3.1 Agarose gel electrophoresis of DNA

Agarose gels were prepared in 0.5xTBE (see section 2.6 for recipe) as described previously (Sambrook, 1989). The percentage of the gel was determined by the size of DNA fragments

to be resolved. Ethidium bromide (0.5μg/ml) was included in gels for visualisation of DNA under UV light. DNA was loaded in 10% (v/v) DNA loading buffer. 1μg of size markers was also loaded (1kb λ digest, Gibco).

2.3.2 Amplification of DNA by Polymerase Chain Reaction (PCR)

50μl reactions were set up in thin-walled 200μl tubes (Radleys) or multiwell plates (Perkin Elmer), as follows:

- 0.1μg *aar* plasmid DNA (or ddH_2O control)
- 0.2µl of 100pmol/µl 5' primer (or ddH_2O control)
- 0.2µl of 100pmol/µl 3' primer (or ddH_2O control)
- 5µl of dNTPs (200μM dATP, dCTP, dTTP and dGTP - Amersham Pharmacia Biotech),
- 5µl 1x Pfu buffer (Stratagene)
- 2.5 units of *Taq* polymerase and 2.5 units of recombinant *Pfu* polymerase (Stratagene)

Volume made up to 50µl using ddH_2O

For a standard amplification of *aar* DNA up to 2.5Kb in length, the DNA was denatured at 95°C for 30s then subjected to 28 cycles of 95°C for 30s, 55°C for 30s, 65°C for 5 min followed by a final extension step at 65°C for 10 min before storage at 4°C. For amplification of larger PCR products, extension times of 10 min were used in the cycles.

2.3.3 TOPO Cloning reactions

All PCR products were cloned into the pCRII-TOPO vector (Invitrogen) and subsequently transformed into TOP10 chemically competent *E. coli* (see below). The TOPO cloning reaction utilises the 3' deoxyadenosine overhang of *Taq* amplified PCR products. The linearised pCR-II vector contains overhanging 3' deoxythymidine. These overhangs ligate efficiently with the PCR products due to the activity of topoisomerase which is covalently

bound to the vector. Resulting colonies were analysed by miniprep and digest analysis (see sections 2.3.6 and 2.3.7).

2.3.4 Bacterial permanents

Glycerol stocks of positive colonies were made by the addition of 0.5ml 50:50 (v/v) L-broth/glycerol to 0.5ml of the overnight culture; stocks were stored at –80°C. The pCRII vector contains the M13 and T7 promoter sites, facilitating the sequencing of the PCR insert.

2.3.5 Plasmid DNA preparations - maxiprep

For large-scale plasmid DNA preps, QIAGEN Plasmid Maxi kits (Qiagen Ltd) were used, which employ a variation on the alkaline lysis method of DNA preparation. These kits utilise columns containing anion-exchange resin to covalently bind plasmid DNA to immobilised diethylaminoethanol (DEAE) groups over a wide range of salt conditions.

In brief, plasmid-containing *E. coli* cells were grown overnight in a 250ml L-broth culture, supplemented with 100µg/ml ampicillin. Cells were lysed with SDS and the lysate passed through the columns by gravity flow. Protein, carbohydrates and small metabolites were washed from the column with low-salt buffers, while the plasmid DNA remained tightly bound. Plasmid DNA was then eluted with a high-salt buffer. Up to 500µg plasmid DNA per column may be isolated by this method. (Glycerol stocks were made as per section 2.3.4 and stored at –80°C).

2.3.6 Plasmid DNA preparations - miniprep

For smaller scale plasmid preps, requiring sequencing quality DNA, spin miniprep kits (MoBio Laboratories Inc.) were used. These utilise the same principle as the QIAGEN

Plasmid Maxi kits to purify plasmid DNA. A typical yield from an individual prep is 5-10μg plasmid DNA from a 1.5ml bacterial culture.

Small-scale DNA plasmid preps for all applications other than sequencing were carried out via the rapid boiling method (Harwood, 1996). 1.5ml of plasmid-containing *E. coli* were spun out of medium by centrifugation for 1min at 12,000*g* in a benchtop centrifuge. Pellets were resuspended in 100μl of 1mg/ml lysozyme/STET mix (see section 2.6 for STET recipe), and vortexed to break up the pellet. Samples were boiled for 45s and centrifuged for 10 min at 12,000*g*. The resulting pellet containing the cell debris (including the bacterial chromosome) was removed and the plasmid DNA was precipitated by the addition of 200μl of isopropanol and centrifugation for 5 min at 12,000*g*. The pellet was then washed in 70% ethanol, air-dried for 10 min and resuspended in 100μl TE buffer. Typical yields of 1-5μg plasmid DNA are obtained via this method.

2.3.7 Restriction enzyme digestion analysis of plasmid DNA

0.1-1μg of DNA was usually digested with 1μl of appropriate restriction enzyme, according to the manufacturers instructions. All restriction enzymes were obtained commercially from New England Biolabs and digests were performed in a 20μl volume of 1x appropriate manufacturer's enzyme buffer for 1h at 37°C. For analysis, half the digest was added to 1μl 10x DNA loading buffer and DNA fragments separated on TBE agarose gels.

2.3.8 Gel purification of DNA fragments

DNA fragments were separated on 0.8% TBE/agarose gels and the relevant bands excised. DNA was purified from the gel bands using the QIAquick Gel Extraction Kit (Qiagen Ltd). In brief, gel slices were melted in a buffer containing guanidine thiocyanate. This chelates

the water, forcing the DNA to bind to a silica resin contained in a gravity-flow column. Columns were then ethanol washed before elution with TE buffer.

2.3.9 Ligations – oligonucleotide insertion

For the creation of double stranded oligonucleotides, 0.1µg of each strand of the oligonucleotides were annealed at 60°C for 1h in a volume of 20µl of 1x T4 DNA ligase buffer (New England Biolabs).

For the insertion of the double-stranded oligonucleotide into the vector, the following ligation reactions were set up:

Vector (V)	Oligo (O)	10x ligase buffer	ddH_2O	Molar Ratio (O:V)
1.5µl	-	1µl	6.8µl	-
1.5µl	3µl	1µl	3.5µl	approx. 50:1
1.5µl	6µl	1µl	0.5µl	approx. 100:1

0.2µl of T4 DNA ligase (New England Biolabs) was added to each ligation reaction, and incubated at room temperature for 2h.

2.3.10 Ligations - standard reaction

For ligation of larger fragments of DNA into vectors, 20 µl reactions were set up as for oligonucleotide insertion, but with molar ratios of 2:1 and 10:1 (insert:vector) used instead.

2.3.11 Transformation of bacteria

TOP10™ chemically competent *Escherichia coli* (Invitrogen) were transformed as per the manufacturer's instructions. 50µl of transformed cells were spread onto LB agar plates

containing the appropriate selective antibiotic (100μg/ml ampicillin unless stated otherwise). Single transformed colonies were picked using a sterile loop and inoculated into L-Broth with appropriate selection. Cultures were shaken at 37°C, 250rpm, in a tube or flask at least 4 times the volume of the culture to ensure good aeration.

2.3.12 Sequencing and analysis of DNA

PCR fragments were purified away from the PCR reaction using spin columns (S400, Amersham Pharmacia Biotech), according to the manufacturer's instructions. 1µg plasmid DNA or 5µg PCR product was sent to MWG Biotech Ltd for sequencing. The resulting sequencing data was analysed using Lasergene software (DNAStar™).

2.3.13 Oligonucleotides

The following oligonucleotides were used in this thesis:

Oligo Name	Use	Sequence (5'-3')
XhoI 5' GFP	Primer for the amplification of GFP from pDNeoGFP, adds a 5' XhoI site for insertion into pDXA-3C-aar	GGA CGG AGA AGA TGC TCG AGC TTG CAT GCC CAT GAG
XbaI 3' GFP	Primer for the amplification of GFP from pDNeoGFP, adds a 3' XbaI site for insertion into pDXA-3C-aar	CGA GCT CGA GAT CTA GAT ATC GAT GAA TTC GAG
aar 5' KpnI ΔN201	5' primer for the creation of Aar ΔN201, used with 'aar 3' XhoI'. Adds 5' KpnI site for insertion into pDXA-3C.	GGT ACC TTA GAA GGT ATA GAA GAT CAA AAC G
aar 5' ATG KpnI ΔN258	5' primer for the creation of Aar ΔN258, used with 'aar 3' XhoI'. Adds 5' KpnI site, (followed by ATG) for insertion into pDXA-3C.	GGG TAC CAA AAA TGG GTA GCA CTA ATA ACC ACA ACA AC
aar 5' ATG KpnI ΔN371	5' primer for the creation of Aar ΔN371, used with 'aar 3' XhoI'. Adds 5' KpnI site, (followed by ATG) for insertion into pDXA-3C.	GGG TAC CAA AAA TGT CAA GAT GGT CAA ATC CAA C
aar 5' ATG KpnI ΔN587	5' primer for the creation of Aar ΔN587, used with 'aar 3' XhoI'. Adds 5' KpnI site, (followed by ATG) for insertion into pDXA-3C.	GGG TAC CAA AAA TGA GTG CAA AAG AAG GTG
aar 3' XhoI	3' primer used with 5' Aar ΔN primers. Adds 3' XhoI site for insertion into pDXA-3C-aar	ATA ACT CGA GTT CCA TCT TCT AAT GCT ACT TG

Oligo Name	Use	Sequence
aar 5' KpnI	5' primer used with 3' Aar ΔC primers. Adds 5' KpnI site for insertion into pDXA-3C-aar	GTC CTA ATG GTA CCT ACC ACA CCA CAC ACC C
aar 3' XhoI ΔC210	3' primer for the creation of Aar ΔC210, used with 'aar 5' KpnI'. Adds 3' XhoI site, for insertion into pDXA-3C.	CTG ACT CGA GCA TCG TTT TGA TCT TCT ATA CCT TC
aar 3' XhoI ΔC288	3' primer for the creation of Aar ΔC288, used with 'aar 5' KpnI'. Adds 3' XhoI site, for insertion into pDXA-3C.	GAT TCT CGA GCA TTA TTA CTA CTT TCA ATT AAA TTA C
aar ΔC623 up	Upper strand oligo of a pair. Annealed with 'aar ΔC623 down' to make a double-stranded oligonucleotide, used to replace the sequence between the EcoRI and XhoI sites of pDXA-3C-aar to create Aar ΔC623.	AAT TCA AAC ACA AGG TTG TGG TGC CCT AAG AAA TTT AGG TTG TAG
aar ΔC623 down	See 'aar ΔC623 up'.	TCG ACT ACA ACC TAA ATT TCT TAG GGC ACC ACA ACC TTG TGT TTG
aar V5His up	Upper strand oligo of a pair. Annealed with 'aar V5His down' to make a double-stranded oligonucleotide with a 5' XhoI site and a 3' XbaI site. Inserted into pDXA-3C-aar to create pDXA-aar-V5-his.	TCG AGA TGC ATT AGG TAA ACC AAT TCC AAA TCC ACT TCT TGG TCT TGA TTC AAC TCA TCA TCA TCA TCA TCA TCA TTA AT
aar V5His down	See 'aar V5His up'.	CTA GAT TAA TGA TGA TGA TGA TGA TGA TGA GTT GAA TCA AGA CCA AGA AGT GGA TTT GGA ATT GGT TTA CCT AAT GCA TC

2.3.14 RNA hybridisation – northern analysis

2-5x10^7 *Dictyostelium* cells were placed on dry ice. They were lysed immediately by adding 500μl of RNA buffer containing 1% SDS (v/v) and 500μl of phenol and then vortexing. In addition, the lysate was shaken for 15 min at room temperature. The mixture was cooled on ice before spinning at 20,000g, 15 min, 4°C to separate aqueous and phenol layers. 350μl of the aqueous layer was removed and transferred to 500μl chloroform, the mixture was vortexed, spun as above and the upper aqueous layer transferred to 1ml ethanol. RNA was precipitated for 1 hour at -20°C before spinning at 20,000g for 10 min, 4°C. The pellet was washed in 70% ethanol, left to air dry on ice, and dissolved in 20µl sterile ddH_2O. RNA concentration was determined by measuring the OD at A_{260} on a spectrophotometer. RNA was prepared for electrophoresis in 1x MOPS buffer, 0.2M formaldehyde, 50% (v/v) formamide and 10% (v/v) sterile RNA loading dye, denatured at 60°C for 15 min and cooled on ice. 5μg RNA per lane was loaded on a 1% (w/v) agarose gel containing 1x MOPS buffer, 0.65M formaldehyde and ethidium bromide to a final concentration of 0.25µg/ml.

The gel was run in 1x MOPS buffer at 120V for 3.5 hours. After electrophoresis, RNA was visualised under UV light and photographed before equilibrating in 10xSSC (see section 2.6 for recipe) and blotting onto Hybond N nylon membrane (Amersham Pharmacia Biotech) by capillary transfer in 10xSSC. The RNA was UV-crosslinked to the membrane (Stratalinker, Stratagene).

Filters were prehybridised at 42°C for 5 hours in RNA hybridisation buffer and then hybridised in denatured probe. Aar, D19, or Ig7 PCR products, were labelled with [α-^{32}P] dATP using the Megaprime DNA labelling kit (Amersham Pharmacia Biotech). Unicorporated nucleotides were removed by purifying the probe on MicroSpin™ S-400 HR

columns (Amersham Pharmacia Biotech). The purified probes were denatured by boiling for 5 mins, before being added to RNA hybridisation buffer, and incubated with filters overnight at 42°C. Unbound probe was removed with 2xSSC/0.1%SDS washes (2x 15 minutes), followed by 0.5xSSC/0.1%SDS (2x 15 minutes). Filters were sealed in plastic and exposed against a phosphorimaging screen (K-Screen, Kodak), before imaging in BioRad phosphorimager. Band intensities were quantified, where desired, using the Quantity One™ software (BioRad).

2.4 Biochemistry

2.4.1 Protein separation and western blotting of whole cell extracts

Approximately 1x 10^7 logarithmically growing cells were pelleted at 2,000g for 2 min. Sodium dodecyl sulphate-polyacrylamide gel electrophersis (SDS-PAGE) was used to separate proteins for western blotting. Cells were lysed by boiling for 5 min in Laemmli buffer and debris pelleted at 20,000g for 5 min before loading on a polyacrylamide gel. Between 10^5 and 10^6 cell equivalents per lane were loaded on to a discontinuous gel composed of a 4% polyacrylamide stacking gel, on top of either a 8.0% or 10% polyacrylamide resolving gel (Protogel, National Diagnostics Corporation), according to the range of size separation required.

Electrophoresis was at 150V for 1.5 hours, and coloured molecular weight standards (Rainbow markers, Amersham Pharmacia Biotech) were run alongside samples for size determination. After electrophoresis, some gels were stained with Coomassie Blue overnight and destained over several hours with 4-5 changes of destain to visualise total protein. All other gels were equilibrated in western transfer buffer for 10 minutes.

Protein was electrophoretically transferred from gels to Hybond C-extra nitrocellulose membrane (Amersham Pharmacia Biotech) by semi-dry blotting in a BioRad transfer cell according to the manufacturer's instructions. The membrane was rinsed in phosphate buffered saline (PBS) and proteins were visualised using 2% PonceauS (w/v) in 1% acetic acid (v/v) to ensure even transfer and loading. Membranes were blocked for 1 hour at room temperature or overnight at 4°C in 5% dried skimmed milk (w/v), 0.1% Tween-20 (v/v) in PBS. After five 5 minute washes in PBS/0.1% Tween-20 (v/v) (PBST) membranes were incubated in primary antibody diluted in PBST for 1-2 hours at room temperature. (Anti-V5 was HRP tagged. All other antibodies required incubation with an HRP-conjugated secondary antibody.) After incubation with primary antibody, filters were washed extensively in a large volume of PBST and incubated in secondary antibody diluted in PBST for a further hour. After further washes, the secondary antibody was detected using enhanced chemoiluminescence reagent (ECL, Pierce) according to the manufacturer's instructions. Protein bands were detected in a BioRad FluorSMax fluorimager.

2.4.2 Antisera : The following antibodies were used during the course of this work:

Primary

- **Aar:** Rabbit polyclonal IgG, raised to a synthetic Aar peptide representing the final 5 armadillo repeats of the protein. Used at 1:1,000 for immunofluorescent cell staining, following testing of both the preimmune and immune sera at 1:50, 1:100, 1:500 and 1:1,000 (the titration of the antisera was performed previously by Juliet Coates, in the lab – see also Coates, 1999).
- **GFP:** Rabbit polyclonal IgG which recognises the epitope corresponding to amino acids 1-238 of green fluorescent protein (GFP) of *Aequorea victoria*. Used at 1:1,000 for western blotting. (Santa Cruz).
- **V5:** Mouse monoclonal IgG, which recognises the V5 epitope (GKPIPNPLLGLDST). Used at 1:5,000 for western blotting. (Invitrogen).

- **Ubiquitin:** Rabbit polyclonal IgG. Used at 1:100 for western blotting. (Sigma-Aldrich).

Secondary

- **Anti-Rabbit IgG (H+L).** Horseradish peroxidase-conjugated antibody, raised in goats. Used at 1:10,000 for western blottting. Vector Laboratories.

2.4.3 Fast Protein Liquid Chromatography – FPLC

An Amersham Pharmacia Biotech FPLC system was used for the size separation of protein samples. 0.25-0.5ml of sample was loaded onto a Superose™ 12 column (Amersham Pharmacia Biotech) and washed with a solution of 50mM Tris/100mM NaCl (pH8.0). Samples were eluted with a flow rate of 0.25ml/min, and collected into 50µl of kinase protection buffer (see section 2.6). The apparent molecular weight of the proteins contained in each fraction was established from the standard curve previously generated in our laboratory by W. J. Ryves.

2.4.4 Purification of peptides

All peptides were synthesised commercially by Zinser Analytic and purified as follows. C18 Sep-Pak Cartridges® (Waters) were washed with 5ml of acetonitrile, followed by 5ml ddH_2O. Peptides were resuspended in 5ml ddH_2O before loading on the cartridges. Cartridges were then washed with 5ml ddH_2O, before elution of peptide in 5ml 60% MeOH (v/v). Peptides were then dried down in a speed vac and re-suspended in the desired volume of ddH_2O.

2.4.5 *In Vitro* kinase assays

In vitro kinase assays were performed as described before (Ryves et al., 1998). 5mUnits of recombinant GSK-3β (Upstate), 40 units of recombinant casein kinase 1δ (New England Biolabs), or FPLC-purified Aark (as stated in the text) were added to each assay. In

addition, where indicated, lithium chloride was used at 50mM, and the casein kinase 1 inhibitor CKI-7 (Seikagaku Corporation) was used at 10μM.

Each assay was initiated by the addition of an ATP/Mg^{2+} mix (100μM final concentration), containing 4.625MBq/ml [γ-^{32}P] ATP. After 10 minutes had elapsed, the peptide was immobilised on P81 cellulose phosphate paper (Whatman), by spotting 20μl of each assay onto squares of the paper. The P81 squares were then washed 3 times in 100mM phosphoric acid to remove the unincorporated radioactive phosphate. The papers were washed for a total of 1hour, and the activity of each square counted in a beta counter (Tri-Carb 1900 TR, Packard). In addition to counting the activity of each individual assay, an equivalent quantity of ATP/Mg^{2+}/[γ-^{32}P] ATP as was used in the assay was also counted to enable the determination of the amount of phosphate transferred as a ratio of the amount added.

2.5 Cell biology

2.5.1 Development of Dictyostelium

Cells were spun down from logarithmically growing culture (1-2x10^6 cells/ml) and washed four times in KK_2. Cells were resuspended in 300μl of KK_2 and spread evenly across black, nitrocellulose filters (4.7cm diameter, 0.45μm pore size, Millipore) on a KK_2 –soaked pre-filter. Filters were incubated at 22°C in a humid atmosphere for the required length of time.

2.5.2 Immunofluorescent cell staining

Vegetative cells were allowed to settle on glass coverslips (BDH). To fix cells, the media was removed and replaced with 200μl 0.1% paraformaldehyde (w/v) in picric acid (pH6.5) for 30 minutes. Cells were then washed in the following sequence: 10mM PIPES, PBS/glycin (twice), 70% ethanol, and 100mM PBS/glycin (three times). Cells were

blocked against non-specific binding in PBG (see section 2.6 for recipe), for 15 minutes. Antibodies were diluted as above, in blocking reagent. After incubation with primary antibody for 2-3hours at room temperature, cells were washed 7 times in blocking solution, before incubation with secondary antibody for 1-2 hours at room temperature. Cells were then washed in the following sequence PBG, 100mM PBS/glycin (three times), and finally once in ddH_2O before mounting with mowial mountant. Slides were viewed on a Bio-Rad MRC1024 confocal microscope.

2.5.3 Live cell imaging of GFP transformants

'Hanging drop' slides were made as follows: a rubber 'O' ring, approximately 2cm in diameter, was greased and placed on a glass coverslip. 0.5ml of log phase culture was spun out of media and washed once in KK_2 buffer, before resuspension in 50µl of KK_2 +/- inhibitor: 10mM LiCL, or 10µM of the specific IMPase inhibitor L-690,330 (Tocris Cookson). Cells were then pippetted into the middle of the 'O' ring and allowed to settle before 25µl of the liquid was removed. A glass slide was placed on top of the 'O' ring with sufficient pressure as to create a seal between the coverslip, 'O' ring and slide. The slide was then inverted, thus producing a 'hanging drop', ready for viewing on a Bio-Rad MRC1024 confocal microscope.

2.6 Inhibitors

The following inhibitors were used during the course of this work:

- **CKI-7 (casein kinase 1 inhibitor):** purchased from Seikagaku Corporation; 10mM stock solution (in DMSO); added as 1/4 part to *in vitro* kinase assays (see section 2.4.5) at 10μM final concentration (the manufacturers quote an IC_{50} value of 9.5μM).
- **L-690,330 (IMPase inhibitor):** purchased from Tocris Cookson; 100mM stock solution (in ddH_20); used at 10μM. L-690,330 has an IC_{50} value of 1μM (Klein and Melton, 1996). L-690,330 was used at 10μM (following titration experiments performed previously by R. Williams in the lab). The inhibitor was added to the KK_2 cell suspension during live cell imaging of GFP transformants.
- **SB-415286 (GSK-3 inhibitor):** a kind gift from GlaxoSmithkline; 2mM stock solution (in DMSO); added as 1/4 part to *in vitro* kinase assays (see section 2.4.5) at 1μM final concentration. The inhibitor has a K_i value of 31nM, but was titrated into a standard assay to determine the optimum concentration for the level of ATP used in these assays, since it is a direct competitor of ATP (this was previously performed by W. J. Ryves).

2.6 Recipes and reagents

Standard laboratory chemicals were from BDH. Other chemicals were from Sigma Chemical Company unless otherwise stated. All chemicals were reagent grade or better.

Media

Axenic medium

- 1.43% peptone (w/v) (Oxoid, L34)
- 0.72% yeast extract (w/v) (Oxoid L21)
- 3.6mM Na_2HPO_4, 3mM KH_2PO_4
- 30% glucose (w/v)
- 0.5mg/ml vitamin B12, 1mg/ml folic acid pH9.0

Final pH 6.4 (sterile)

KK_2

- 15.5mM KH_2PO_4
- 3.8mM K_2HPO_4
- Final pH 6.2

L-Broth

- 1% bactotryptone (w/v) (Difco)
- 0.5% bacto-yeast extract (w/v) (Difco)
- 17mM NaCl

Final pH 7.0 (sterile)

LB agar

- L-broth
- 1.5% Bactoagar (w/v) (Difco)

SM (Sussman's medium)

- 1% glucose (w/v)
- 1% peptone (w/v) (Oxoid L34)
- 0.1% yeast extract (w/v) (Oxoid L21)
- 2% agar (w/v) (Difco)
- 4mM $MgSO_4$, 4mM KH_2PO_4, 6mM K_2HPO_4

Molecular Biology

50x Denhardt's solution

- 1% BSA (w/v) (FractionV)
- 1% Ficoll (w/v)
- 1% Polyvinylpyrollidine (w/v)

DNA loading buffer

- 0.25% bromophenol blue (w/v)
- 0.5% xylene cyanol (w/v)
- 15% Ficoll-400 (w/v)

MOPS buffer

- 20mM MOPS pH7.0
- 5mM Na Acetate
- 1mM EDTA

RNA buffer

- 100mM Tris-HCl, pH 7.4
- 200mM NaCl,
- 20mM EDTA

RNA hybridisation buffer

- 43% formamide (v/v)
- 5x SSC
- 10x Denhardt's solution
- 10mM Na_2HPO_4/NaH_2PO_4 pH 6.8
- 200mg/ml denatured, sheared salmon testis DNA
- 0.1% SDS (v/v)

RNA loading dye

- 50% glycerol (v/v)
- 1mM EDTA
- 0.4% bromophenol blue (w/v)
- 0.4% xylene cyanol (w/v)

SSC

- 150mM NaCl
- 15mM Na_3citrate

STET

- 50mM Tris-HCl pH8
- 50mM EDTA
- 8% sucrose (w/v)
- 5% Triton-X 100 (v/v)

0.5x TBE

- 45mM Tris-HCl
- 45mM Boric acid
- 1mM EDTA

TE

- 10mM Tris-HCl pH 7.4
- 1mM EDTA

Biochemistry

Coomassie destain

1 25% methanol (v/v)

2 16% acetic acid (v/v)

Coomassie stain

- 0.25% Coomassie Brilliant Blue (v/v)
- 10% acetic acid (v/v)
- 45% methanol (v/v)

6x Kinase Protection Buffer

- 50mM Tris (pH7.4)
- 100μM EGTA
- 50mM NaCl
- 50% glycerol (v/v)
- 1mM AEBSF
- 1mM benzamidine
- 10mM DTT

Laemmli buffer

- 10% glycerol (v/v)
- 100mM DTT
- 2% SDS (v/v)
- 50mM Tris-HCl pH6.8
- 0.1% bromophenol blue (w/v)

PBS

- 137mM NaCl
- 2.68mM KCl
- 7.98mM Na_2HPO_4
- 1.47mM KH_2PO_4

Final pH 7.2

Tris Kinase Buffer (TKB)

- 20mM Tris
- 2mM DTT
- pH 7.5

- Western transfer buffer
- 48mM Tris
- 39mM glycine
- 20% methanol

Mowial mountant

- 2.4g MOWIAL
- 6g glycerol

Add 6ml ddH_2O and stir for several h at RT.

Add 12ml 0.2M Tris, pH8.5 and heat to 50°C

Add 2.5% DABCO (w/v)

PBG

In 1L PBS:

- 5g BSA
- 1g fish gelatin

Sterile filter.

PBS/Glycin

- 500ml PBS
- 3.75g glycin

Sterile filter.

Picric acid

- 0.4g paraformaldehyde
- 5ml ddH_2O
- 3 drops 1M NaOH, heat to 40°C and make up to 7ml before adding:
- 10ml 20mM PIPES
- 3ml saturated picric acid solution

Final pH 6.5

Chapter 3

Phosphorylation of Aardvark

3.1 Introduction

Aardvark (Aar) possesses signalling functions known to be dependent on the activity of the *Dictyostelium* GSK-3 homologue, GskA (Grimson et al., 2000; Fraser et al., 2002). GSK-3 phosphorylation of β-catenin targets the protein for breakdown following the binding of the F-box protein βTrcp. In *C. elegans* however, the relationship between GSK-3 and the β-catenin homologue WRM-1 appears to be a positive one (Korswagen et al., 2000). This also appears to be the case in *Dictyostelium* (Grimson et al., 2000), but it has yet to be established whether the interaction between GskA and Aar is a direct one. Therefore, one of the aims at the outset of this project was to determine whether GskA phosphorylates Aar.

3.2 Establishing an *in vitro* kinase assay for GSK-3 phosphorylation of β-catenin peptides

The study of β-catenin phosphorylation *in vivo* is complex: it requires either the over-expression of a dominant negative form of βTrcp, or the addition of proteosome inhibitors (Amit et al., 2002). GSK-3 will only phosphorylate β-catenin at low levels *in vitro* (Yost et al., 1996). Both priming phosphorylation by Casein Kinase 1α (CK1α) and the addition of other protein factors such as Axin, are required (Hagen and Vidal-Puig, 2002; Amit et al., 2002; Liu et al., 2002).

In vitro GSK-3 kinase assays utilising peptide substrates have previously been reported (Wang et al., 1994; Ryves et al., 1998; Ginger et al., 2000). To establish whether this approach would work for a known GSK-3/β-catenin interaction, peptides based upon the N-terminal GSK-3 target sites of β-catenin, encompassing Ser-33, Ser-37, Thr-41 and Ser-45, were commercially synthesised. Two peptides were made, corresponding to amino acids 24 to 49 of β-catenin. One peptide was synthesised with the priming phosphate on Ser-45. Both peptides (and all future peptides) had the addition of two N-terminal and three

C-terminal Arg residues. This was to facilitate the binding of the peptides to P81 cation exchange cellulose phosphate paper, in the *in vitro* kinase assays (see section 2.4.5). Figure 3.1 outlines the sequence of the two peptides and also shows the site at the N-terminus of the protein from where the peptides were derived.

(a)

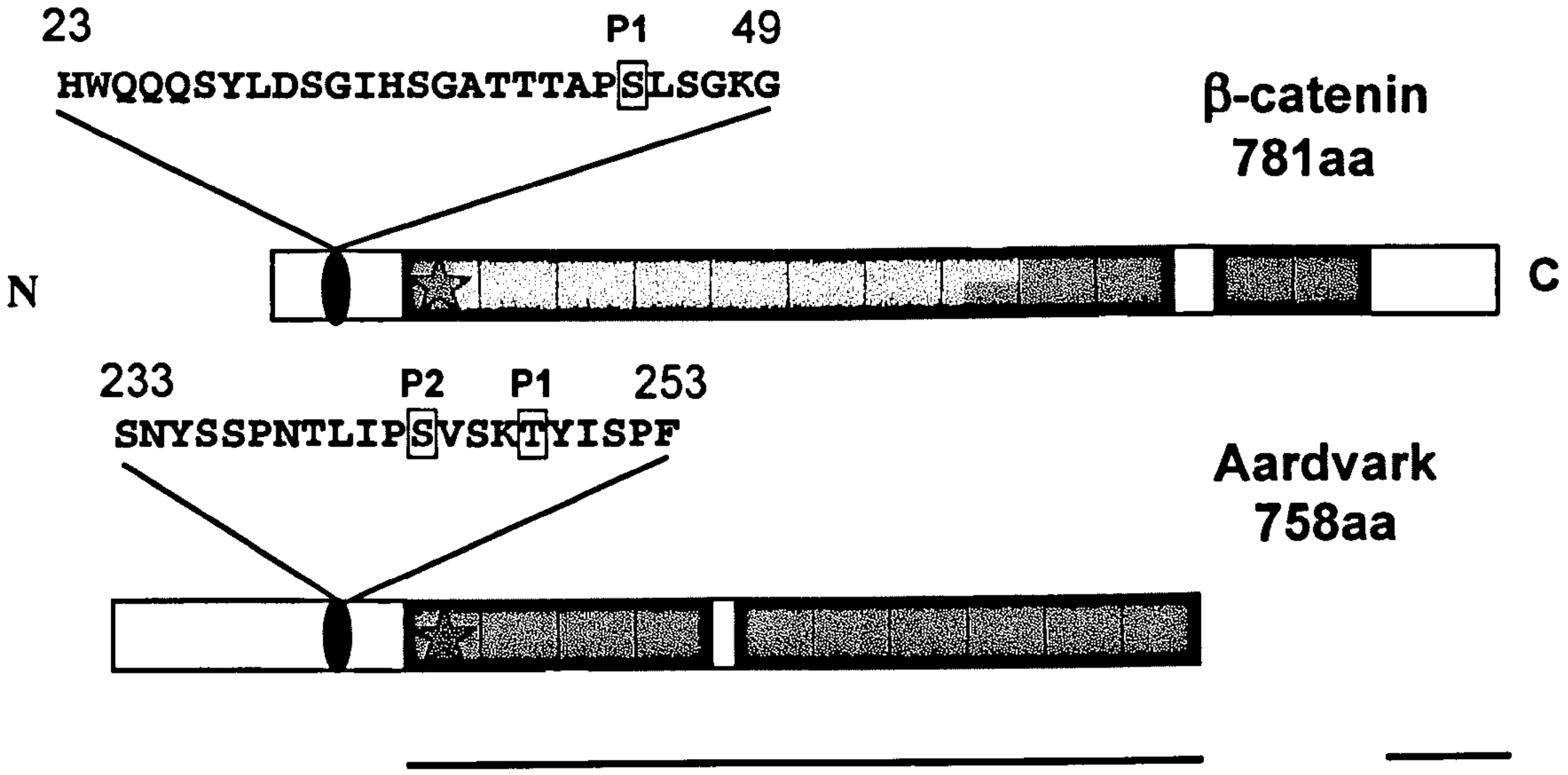

(b)

Peptide name	Sequence
β-UP	RRHWQQQSYLDSGIHSGATTTAPSLSGKRRR
β-P1	RRHWQQQSYLDSGIHSGATTTAP[S]LSGKRRR
Aar-UP	RRSNYSSPNTLIPSVSKTYISPFRRR
Aar-P1	RRSNYSSPNTLIPSVSK[T]YISPFRRR
Aar-P2	CRRSNYSSPNTLIP[S]VSKTYISPFRRR

Figure 3.1 Comparison of β-catenin and Aar proteins and peptide substrates

(a) Alignment of β-catenin and Aardvark proteins, based upon the shared homology of their Arm domains, GSK-3 phosphorylation sites (black oval) and α-catenin binding sites (red star). The GSK-3 sites and α-catenin binding site of Aardvark are putative. Residues in red represent the known/putative phosphate-accepting residues and the priming sites are boxed and marked P1 or P2.

(b) Sequences of Aardvark and β-catenin peptides. All peptides possess two N-terminal and three C-terminal Arg residues to facilitate binding to the cellulose phosphate paper in the *in vitro* kinase assay. Red residues represent the Ser/Thr residues to receive the phosphate. UP = unprimed; P1 = primed, position 1; P2 = primed, position 2.

3.3 GSK-3β phosphorylates a phosphate-primed β-catenin peptide *in vitro*

Recombinant GSK-3β was unable to phosphorylate the un-primed β-catenin peptide (β-UP) in the *in vitro* kinase assay (see section 2.4.5). However, the addition of the priming phosphate at Ser-45 (producing β-P1) created a GSK-3 substrate (figure 3.2). Furthermore, the addition of 50mM lithium chloride (LiCl), to inhibit the kinase activity of GSK-3β, reduced activity towards the peptide by almost 90%.

The Michaelis constant, K_m, of an enzyme is calculated by measuring the activity from a range of substrate concentrations, and creating a double reciprocal plot of velocity versus substrate concentration, known as the Lineweaver-Burke plot. The intercept on the horizontal axis represents $-1/K_m$.

To calculate the K_m value for the interaction between GSK-3β and β-P1, an *in vitro* kinase assay was performed with GSK-3β and serial dilutions of 200μM β-P1. Figure 3.3 (a) and (b) show the activity of GSK-3β towards each dilution of β-P1, and the resultant Lineweaver-Burk plot is shown in (c). The K_m value was calculated from the plot, using Excel software (Microsoft), to be 85μM. This value falls within the range of K_m values for known GSK-3β peptide substrates, for example CREB, 200μM (Wang et al., 1994); the modified glycogen synthase peptide GSM, 75μM (Ryves et al., 1998); and DdSTATa, 25μM (Ginger et al., 2000).

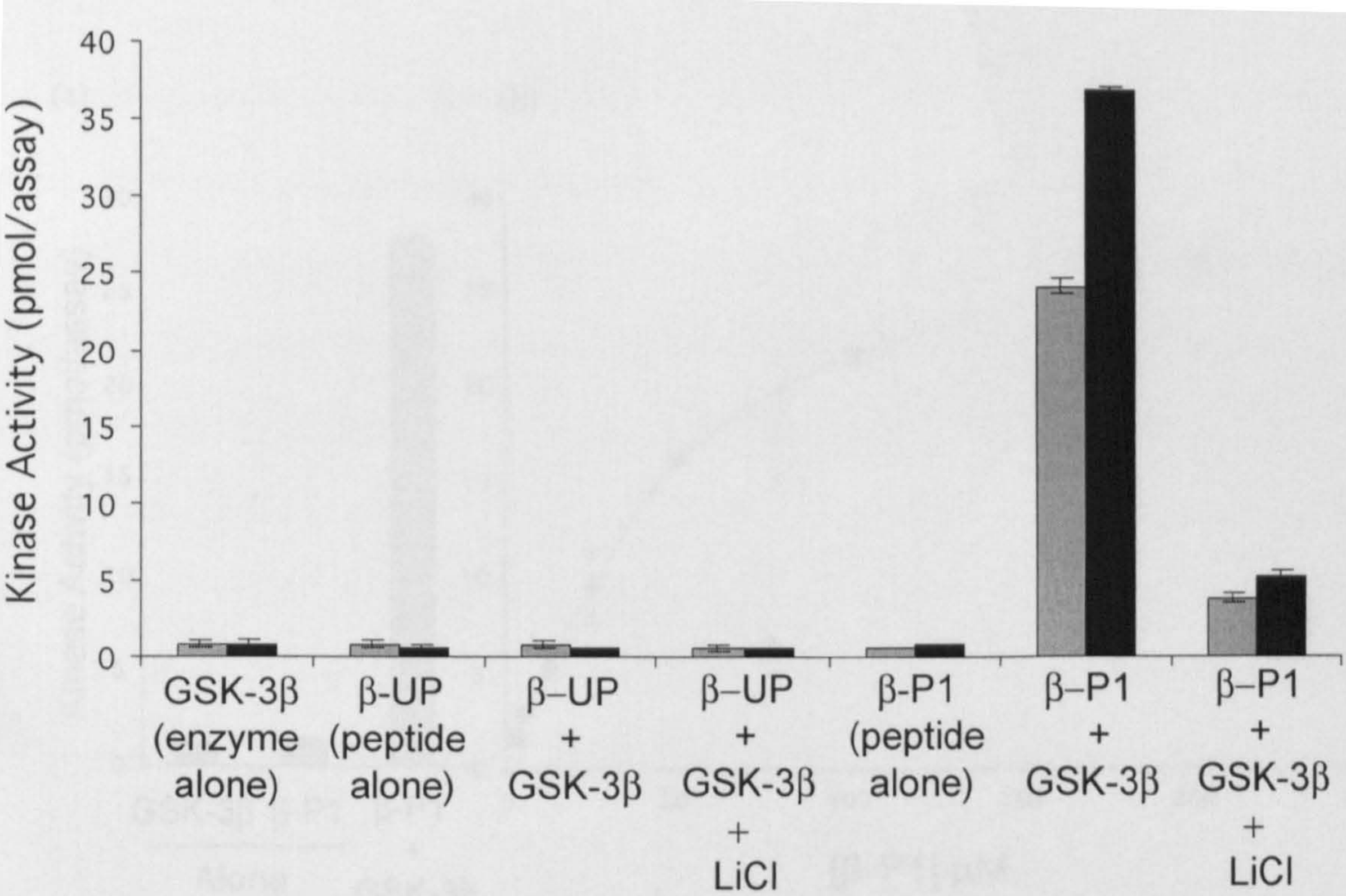

Figure 3.2 GSK-3β phosphorylation of β-catenin peptides

Activity of recombinant GSK-3β towards β–catenin-UP (β-UP), and β–catenin-P1 (β-P1) peptides in an *in vitro* kinase assay. Lithium chloride was added to the assay, as indicated, at 50mM to inhibit the kinase activity of GSK-3β. The 1st columns (grey) represent peptides at 400μM; the 2nd columns (black) represent peptides at 800μM. The assay was performed in triplicate, and the results are shown +/- SEM.

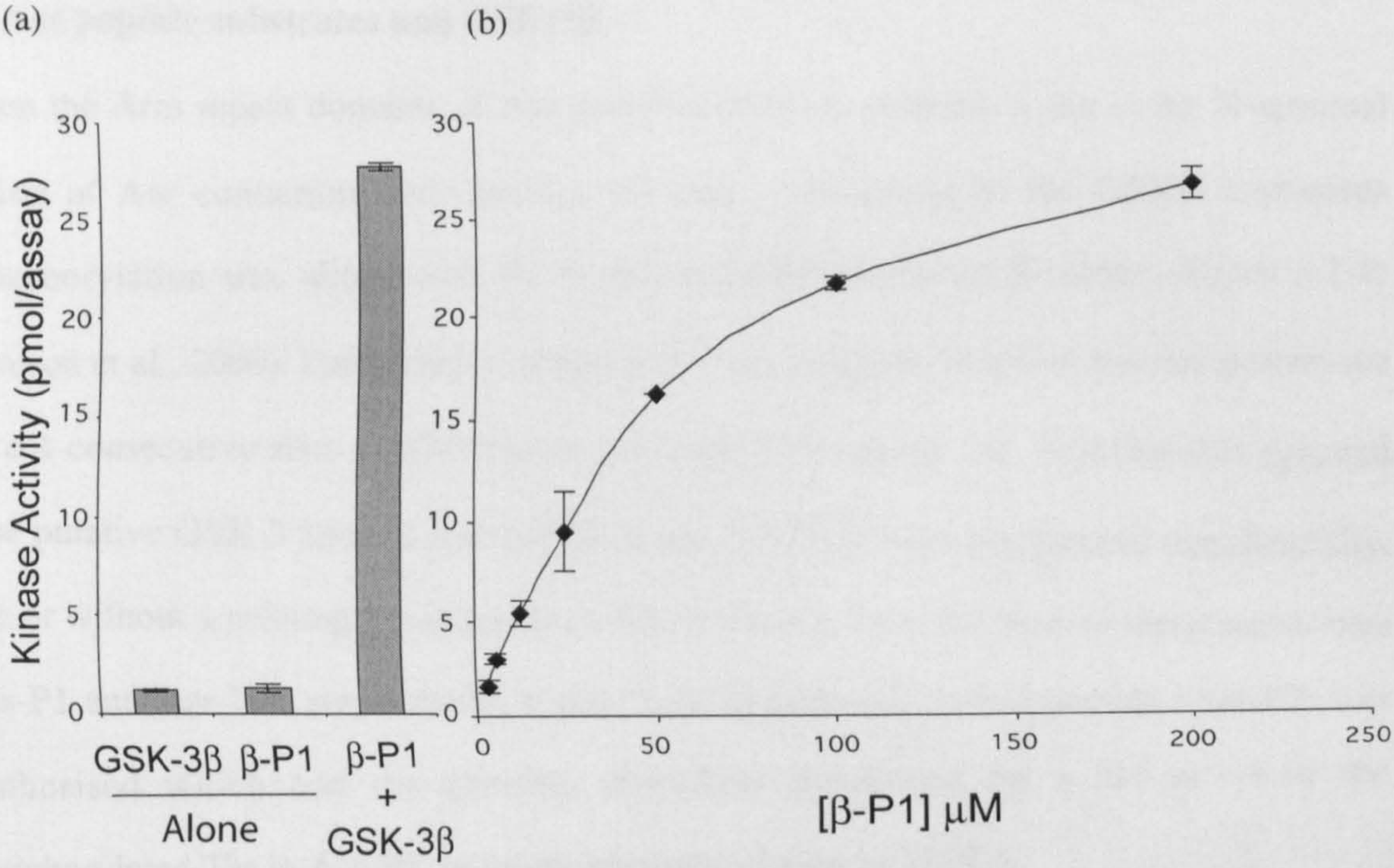

(c)

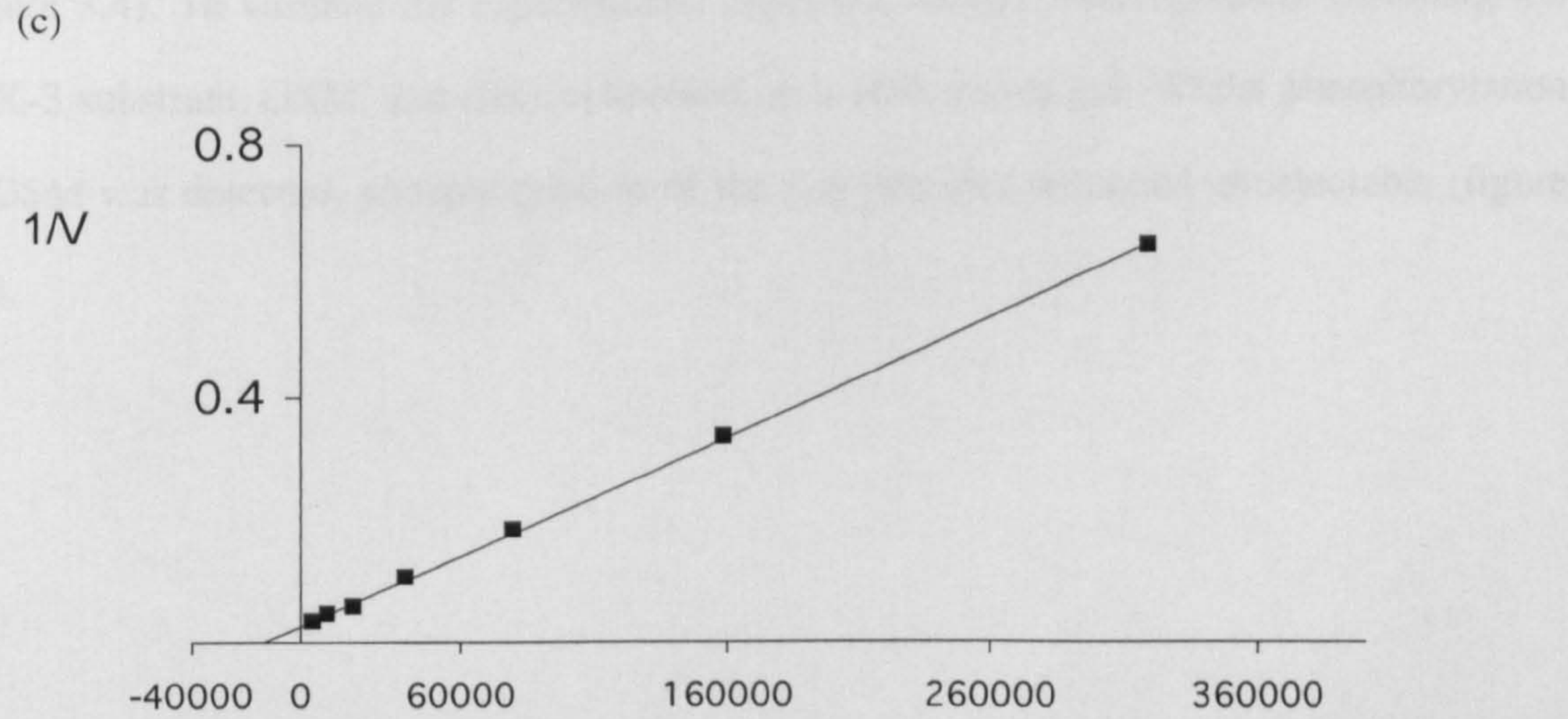

Figure 3.3 Calculating the *K*m value for GSK-3β phosphorylation of β-P1

a) Phosphorylation of 200μM β-P1 by GSK-3β

b) Serial dilutions of β-P1 from 200μM to 3.125μM

c) Double-reciprocal plot of GSK-3β activity against β-P1. *K*m value = 85μM
■ = BP —— = linear BP. The assay was performed in triplicate. Results are shown +/- SEM.

3.4 Aar peptide substrates and GSK-3β

When the Arm repeat domains of Aar and β-catenin are aligned, a site in the N-terminal region of Aar containing four Ser/Thr residues, conforming to the GSK-3 consensus phosphorylation site, aligns with the N-terminal GSK-3 sites of β-catenin (figure 3.1 & Grimson et al., 2000). Furthermore, at no other point along the length of the Aar protein are there 4 consecutive sites conforming to the GSK-3 consensus site. Peptides that spanned these putative GSK-3 sites of Aar (amino acids 233-253) were synthesised commercially, with or without a priming phosphate on a Thr residue at +4 to the start of the putative sites (Aar-P1 and Aar-UP, respectively; figure 3.1). In addition, a third peptide (Aar-P2) was synthesised which had the priming phosphate positioned on a Ser at –4 to the phosphorylated Thr in Aar-P1, to mimic phosphorylation by GSK-3.

Recombinant GSK-3β did not phosphorylate any of the three Aardvark peptides *in vitro* (figure 3.4). To validate the experimental approach, assays were repeated, including the GSK-3 substrate, GSM, and electrophoresed on a 16% tricine gel. Whilst phosphorylation of GSM was detected, phosphorylation of the Aar peptides remained undetectable (figure 3.4).

(a)

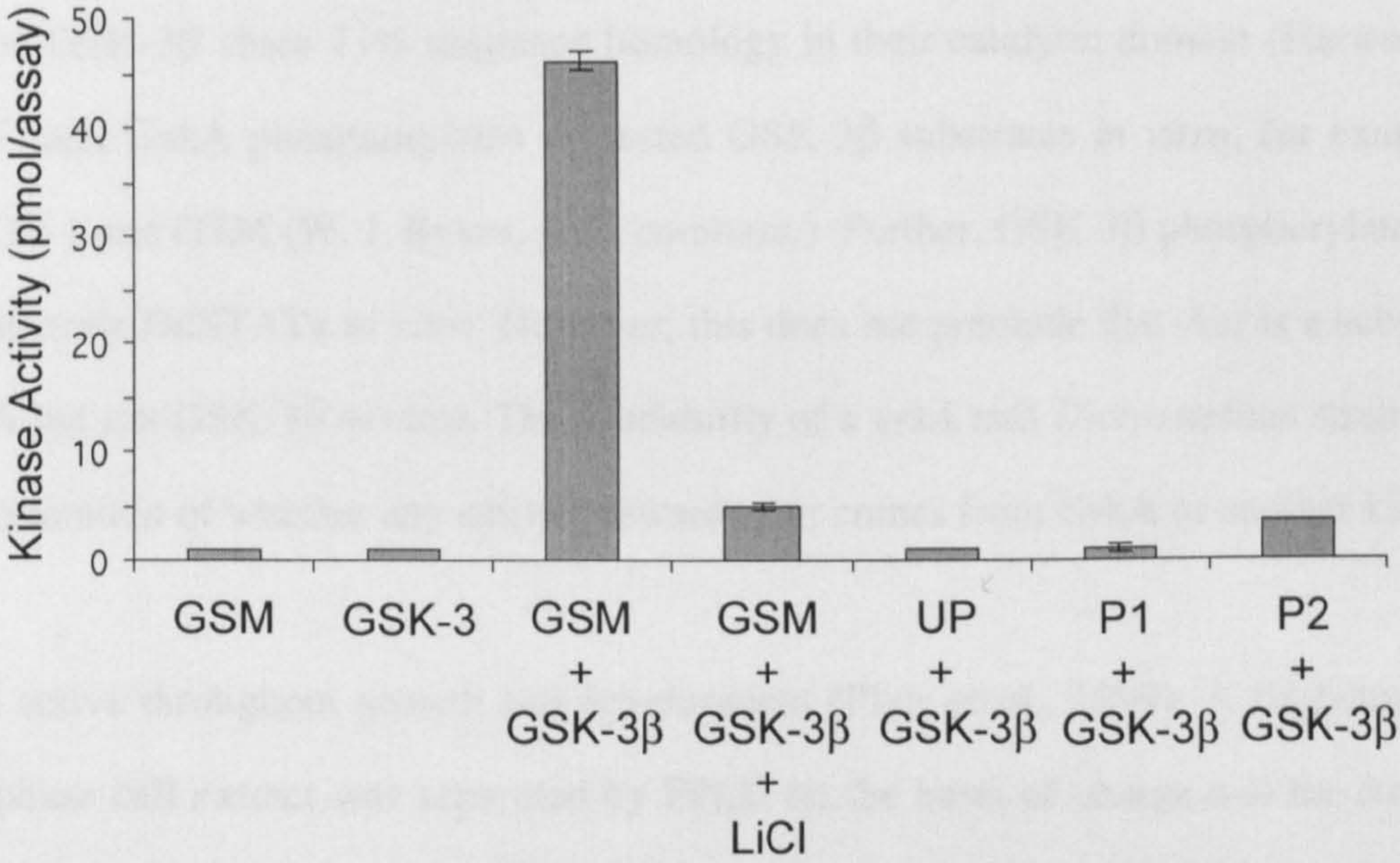

(b)

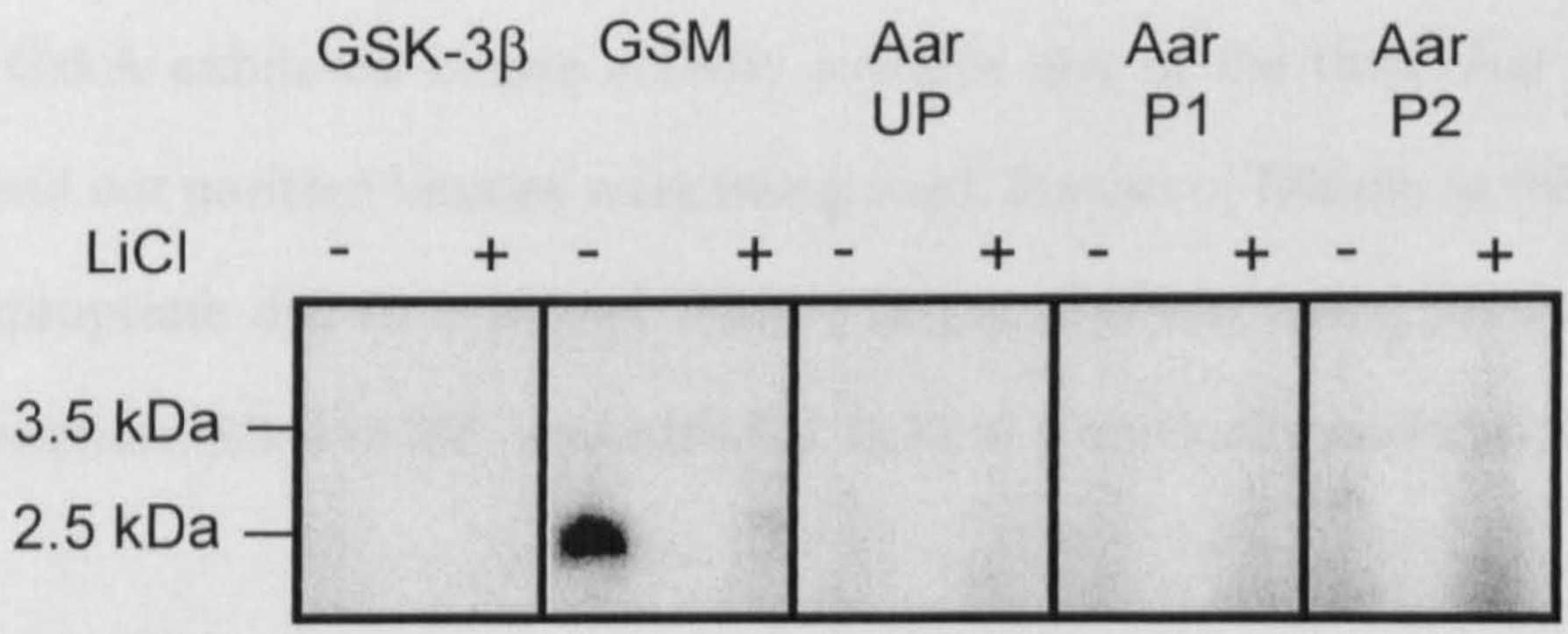

Figure 3.4 GSK-3β kinase activity towards Aar peptides

(A) Recombinant GSK-3β was tested for activity towards the modified GSK-3 peptide substrate, GSM, and towards all three Aar peptides in an *in vitro* kinase assay. No phosphorylation of the unprimed Aar peptide (Aar-UP) or the two primed peptides (Aar-P1 and Aar-P2) was detectable. GSK-3β activity was inhibited with 50mM LiCl. The results of one triplicate assay are shown +/- SEM.

(B) The assays in (a) were repeated, but stopped by the addition of SDS before separation of samples on a 16% tricine gel. Phosphorylation was detected by phosphorimaging. Whilst phosphorylation of GSM could be detected, there was no detectable phosphorylation of any of the Aar peptides. GSK-3β activity was inhibited with 50mM lithium chloride. The assay was repeated and the same results obtained.

3.5 Phosphorylation of Aar peptides by FPLC-purified *Dictyostelium* cell extracts

GskA and GSK-3β share 71% sequence homology in their catalytic domain (Harwood et al., 1995) and GskA phosphorylates all tested GSK-3β substrates *in vitro*; for example, CREB, GS-1 and GSM (W. J. Ryves, pers. commun.). Further, GSK-3β phosphorylates the GskA substrate DdSTATa *in vitro*. However, this does not preclude that Aar is a substrate for GskA but not GSK-3β *in vitro*. The availability of a *gskA* null *Dictyostelium* strain aids the determination of whether any activity towards Aar comes from GskA or another kinase.

GskA is active throughout growth and development (Plyte et al., 1999). A *Dictyostelium* growth phase cell extract was separated by FPLC on the basis of charge and the fraction exhibiting peak GskA activity was determined by its activity towards GSM (this work was previously performed by W. J. Ryves in the lab). This peak fraction was used to determine whether GskA exhibited kinase activity towards any of the three Aar peptides. As cell extracts and not purified kinases were being used, the use of lithium to inhibit GSK activity was inappropriate due to a second lithium target, IMPase, being present. Therefore, the GSK-3 inhibitor, SB-415286, was added at 1μM to specifically inhibit GskA activity.

Figure 3.5 shows the levels of GskA phosphorylation of the three Aar peptides. Partly-purified GskA phosphorylated Aar-P1 to a level four-fold higher than with the unprimed peptide, which itself was higher than the Aar-P2 phosphorylation. This phosphorylation of Aar is therefore dependent on priming and, in addition, the positioning of the priming phosphate is critical. However, the addition of SB-415286 reduced the observed activity towards Aar-P1 by 20%, whereas it reduced phosphorylation of GSM by 59%. This suggested that a kinase other than GskA (later termed Aark for 'Aar kinase') was responsible for phosphorylation of Aar-P1. Further investigation of the biochemical characteristics and identity of Aark were subsequently initiated.

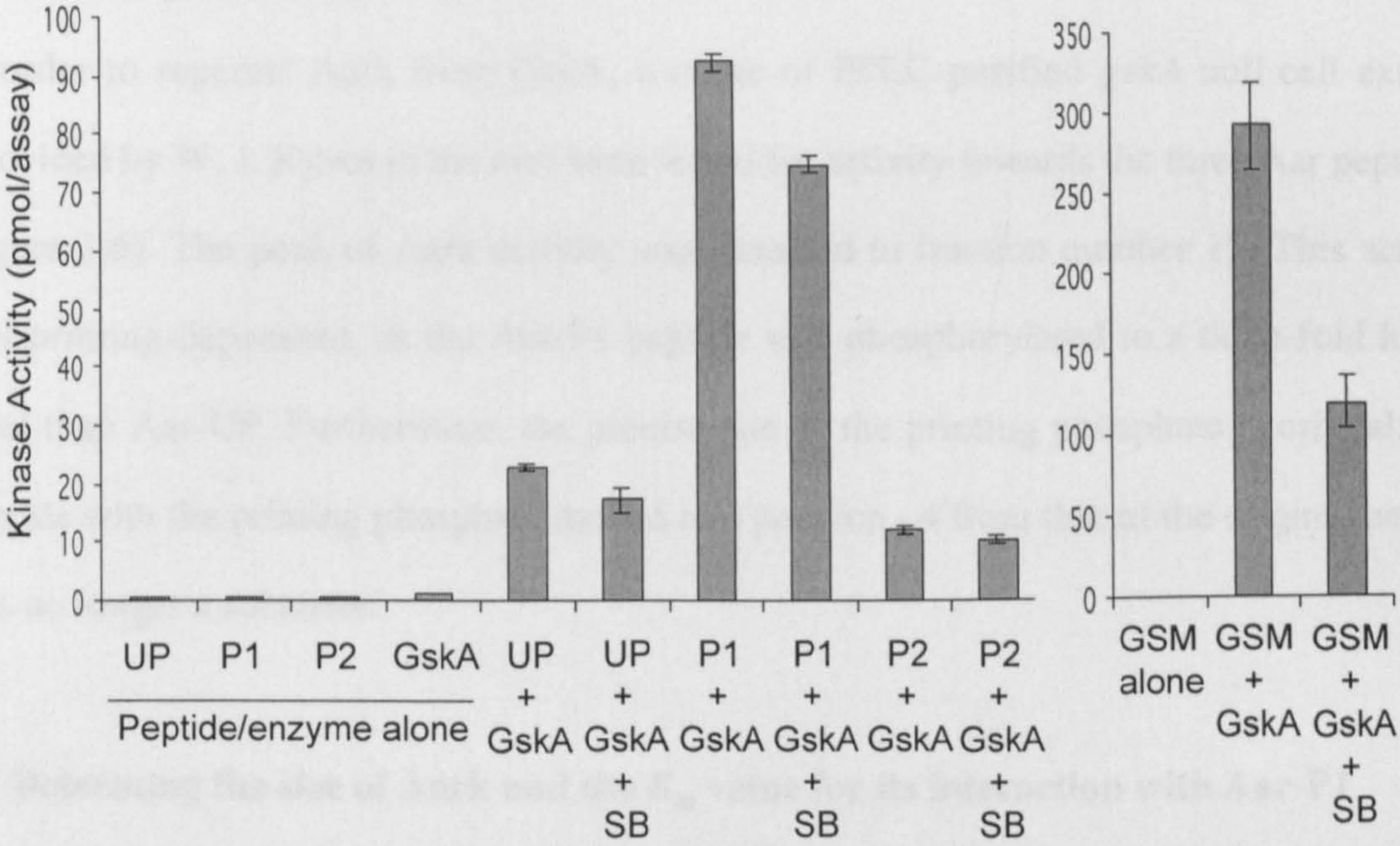

Figure 3.5 GskA phosphorylation of Aar peptides

Activity of a FPLC-purified sample, containing peak kinase activity for GskA, against Aar-UP (UP), Aar-P1 (P1), Aar-P2 (P2) and GSM. All peptides were added at 400μM and SB-415286 (SB) was added at 1μM, where indicated. Although assayed alongside the Aar peptides, the GSM activity is shown separately for greater clarity. The assay was performed in triplicate and results are shown +/- SEM.

3.6 Further purification of Aark

In order to separate Aark from GskA, a range of FPLC-purified *gskA* null cell extracts (provided by W. J. Ryves in the lab) were tested for activity towards the three Aar peptides (figure 3.6). The peak of Aark activity was detected in fraction number 15. This activity was priming-dependent, as the Aar-P1 peptide was phosphorylated to a three-fold higher level than Aar-UP. Furthermore, the precise site of the priming phosphate is critical, as a peptide with the priming phosphate moved to a position –4 from that of the original peptide was no longer a substrate.

3.7 Determing the size of Aark and the K_m value for its interaction with Aar-P1

The peak *gskA* null fraction for Aark activity was subjected to further FPLC separation both to estimate the size of Aark and determine the K_m value for its interaction with Aar-P1. The peak Aark fraction was passed through a size gradient column (see section 2.4.3). Prior calibration of the system with molecular weight standards allowed the determination of the approximate molecular weight of each resulting fraction. Figure 3.7 shows the activity of the resulting fractions towards Aar-P1. The peak of Aark activity is in the apparent size range of 30-35kDa.

To calculate the K_m value for the interaction between Aark and Aar-P1, serial dilutions of 3.2mM Aar-P1 were made and an *in vitro* kinase assay performed with the newly-purified Aark. Figures 3.8 (a) and (b) show the activity of Aark towards each dilution of Aar-P1, and the Lineweaver-Burk plot is shown in (c). The K_m value was calculated from the plot to be 365µM.

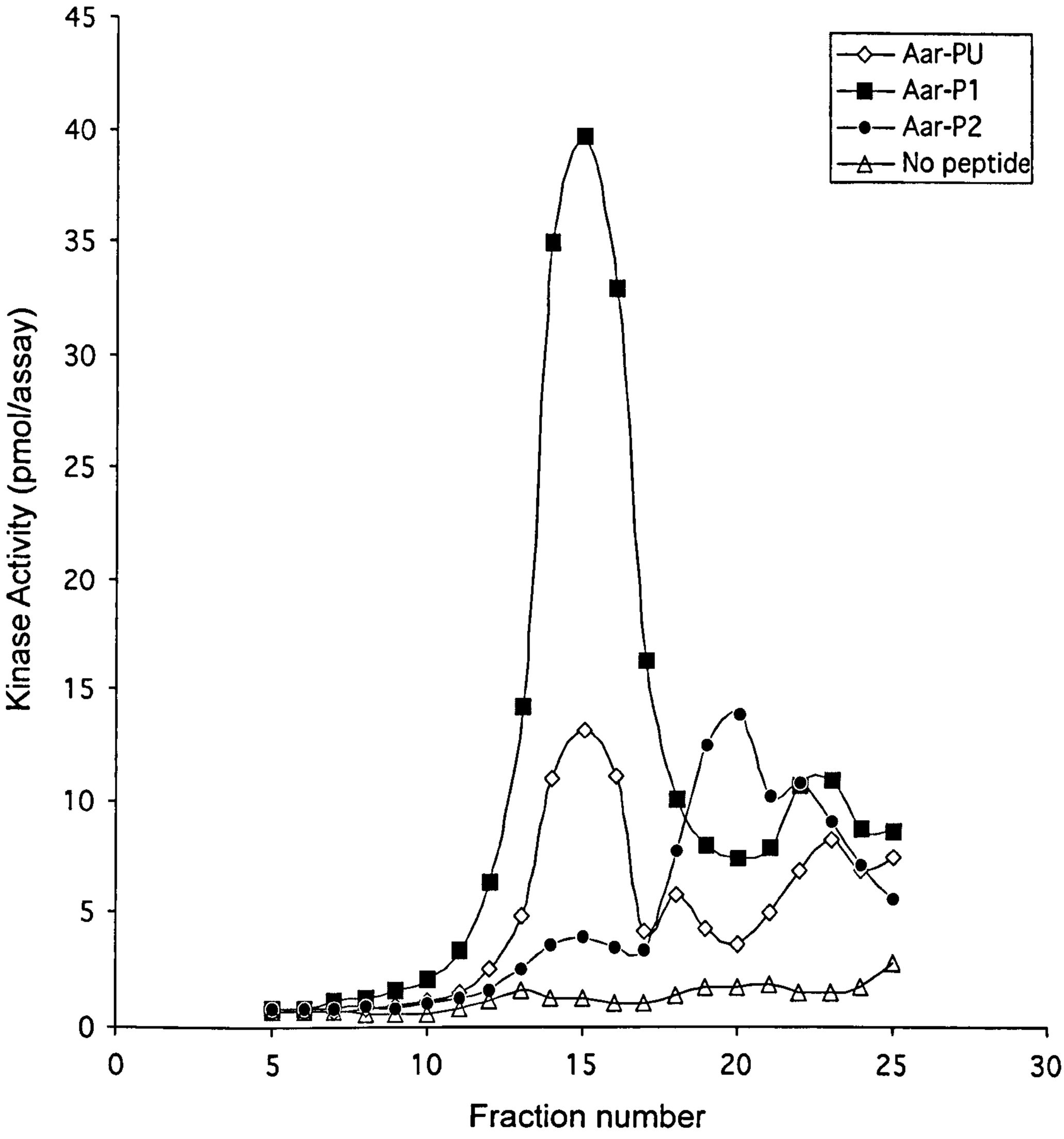

Figure 3.6 Activity of purified *gskA* null fractions against Aar peptides
Proteins from a *gskA* null *Dictyostelium* cell extract were separated by FPLC, on the basis of ion exchange and interaction with phosphocellulose. This separation was via a P11 phosphocellulose exchange column (Whatman), across a 0-500mM NaCl gradient (this purification was performed by W. J. Ryves in the lab). The resulting fractions were assayed for activity towards each of the Aar peptides by *in vitro* kinase assay.

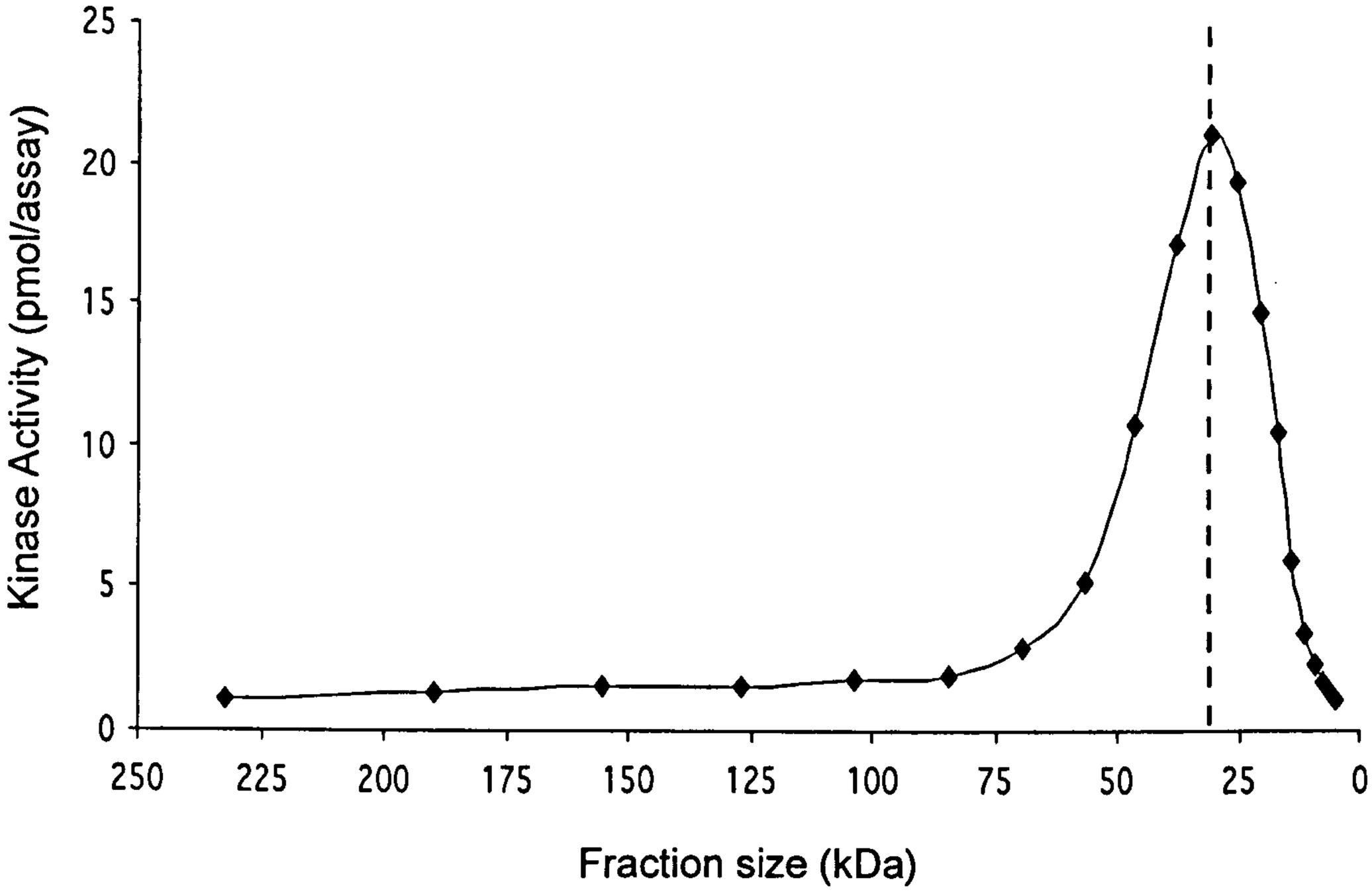

Figure 3.7 Activity of size-separated FPLC *gskA* null fractions against Aar-P1
Proteins from a *Dictyostelium gskA* null cell extract were separated by FPLC, on the basis of size, through a Superose 12 column. The system was previously calibrated with molecular weight markers, which allowed an estimate of the size of Aark to be made. The fraction which corresponded to 30-35kDa showed peak Aark activity, as determined by activity towards Aar-P1 in an *in vitro* kinase assay.

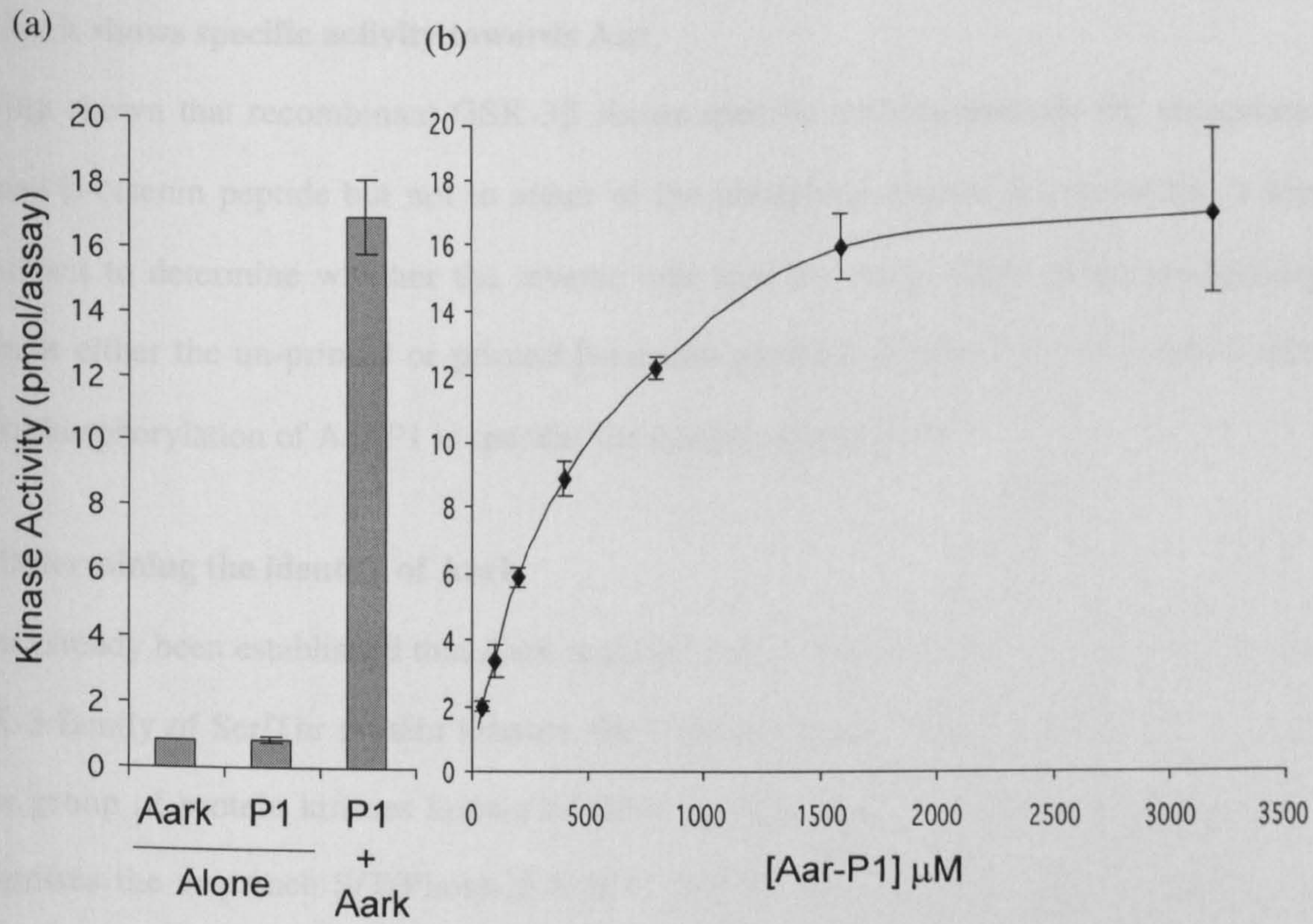

(c)

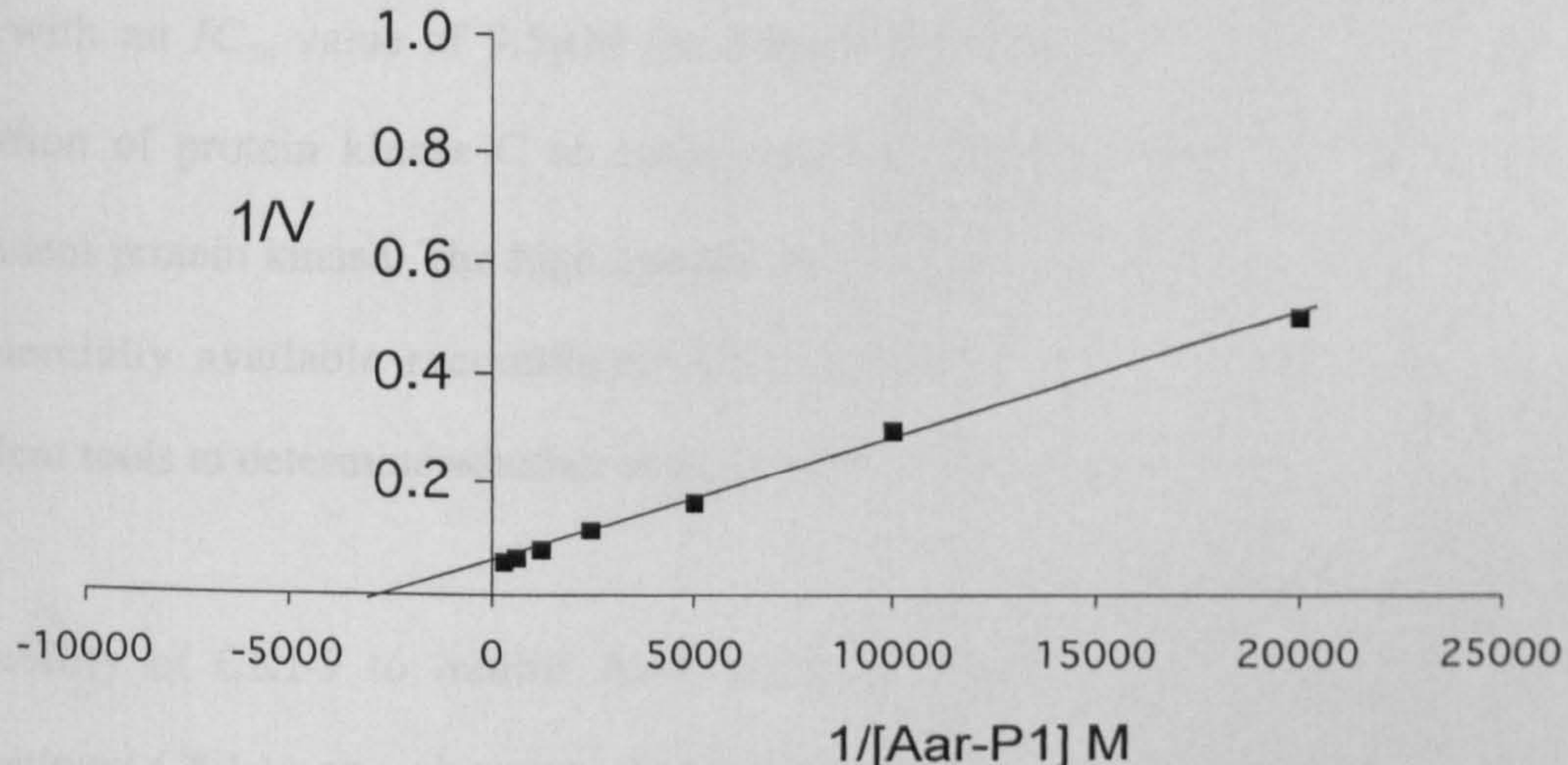

Figure 3.8 Calculating the *K*m value for Aark phosphorylation of Aar-P1

a) Phosphorylation of 3.2mM Aar-P1 by Aark

b) Serial dilutions of Aar-P1 from 3.2mM down to 200µM

c) Double-reciprocal plot of Aark activity against [Aar-P1]. *K*m value = 365µM

■ = Aar-P1 —— = linear Aar-P1. The assay was performed in triplicate. Results are shown +/- SEM.

3.8 Aark shows specific activity towards Aar

Having shown that recombinant GSK-3β shows specific activity towards the phosphate-primed β-catenin peptide but not to either of the phosphate-primed Aar peptides, it was important to determine whether the reverse was true for Aark. Aark shows no activity towards either the un-primed or primed β-catenin peptides (figure 3.9). This shows that Aark phosphorylation of Aar-P1 is specific for this phosphopeptide.

3.9 Determining the identity of Aark

It has already been established that Aark requires Aar to be phosphate-primed. Besides the GSK-3 family of Ser/Thr protein kinases, the Casein Kinase 1 (CK1) family are the only other group of protein kinases known to show a preference for primed substrates. CK1 recognises the sequence S/T(Phos)-X-X-S/T, putting the phosphate onto a Ser or Thr residue at +3 to the priming phosphate.

CKI-7, *N*-(2-aminoethyl)-5-chloroisoquinoline 8-sulfonamide, exerts potent inhibition of CK1 with an IC_{50} value of 9.5μM (Seikagaku Corporation). CKI-7 causes only weak inhibition of protein kinase C at 1mM, and has an IC_{50} value of 550μM for cAMP-dependent protein kinase. The high specificity of CKI-7 inhibition of CK1, along with the commercially available recombinant CK1 and its cognate peptide substrate provide excellent tools to determine whether Aark is a CK1 family member.

The ability of CKI-7 to inhibit Aark phosphorylation of Aar-P1 and the ability of recombinant CK1 to phosphorylate Aar-P1 were tested (figure 3.10). Aark was unable to phosphorylate the CK1 peptide substrate (CK1-P), but CKI-7 (10μM) reduced the activity of Aark towards Aar-P1 by 45%. However, CK1 was unable to phosphorylate Aar-P1, whilst CKI-7 reduced CK1 activity towards the CK1 peptide by almost 80%.

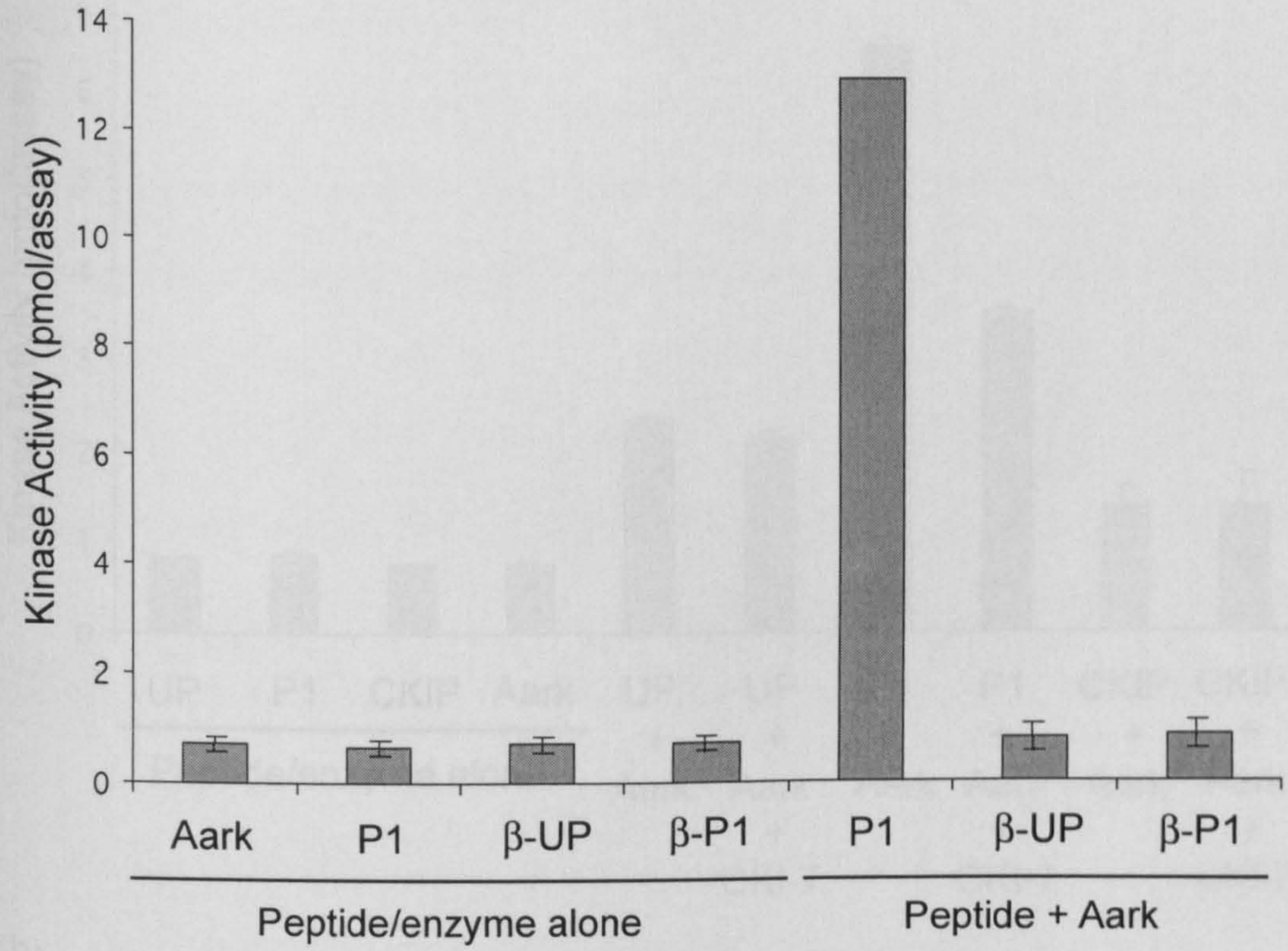

Figure 3.9 Comparison of Aark activity towards Aar and β-catenin peptides
400μM Aar-P1 (P1), β-catenin-UP (β-UP) and β-catenin-P1 (β-P1) were all added alone or with Aark in an *in vitro* kinase assay. The results shown are from one assay performed in triplicate, +/- SEM. The assay was repeated, with the same trend seen.

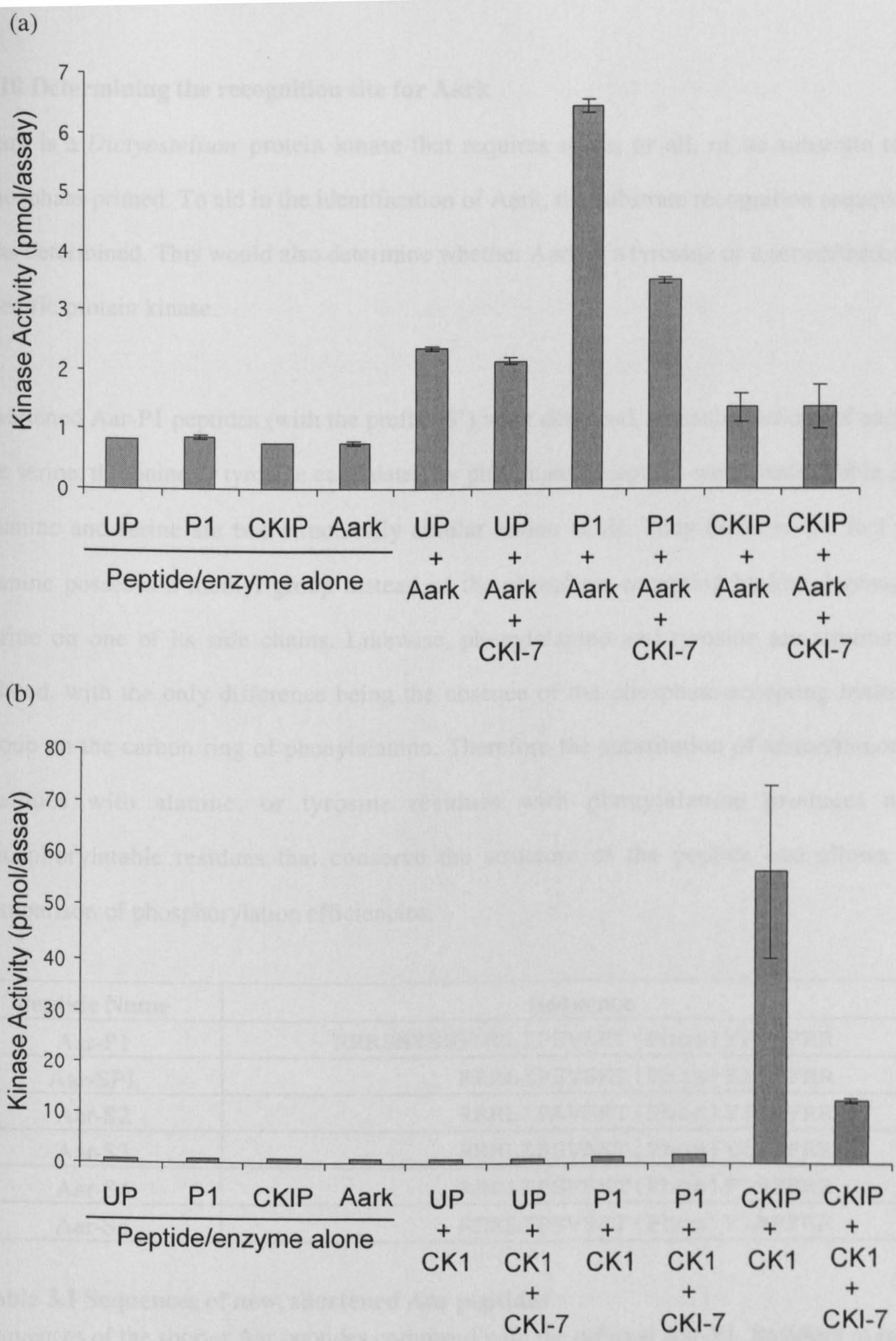

Figure 3.10 Aark and CK1 phosphorylation of Aar and CKIP peptides
All peptides were added at 400μM in the *in vitro* kinase assay. UP = Aar-UP; P1 = Aar-P1; CKIP = Casein Kinase 1 peptide substrate. The CK1 inhibitor, CKI-7, was used at 10μM, where indicated. The results of one assay, performed in triplicate, are shown +/- SEM. The assay was repeated and the same trends seen.

3.10 Determining the recognition site for Aark

Aark is a *Dictyostelium* protein kinase that requires some, or all, of its substrate to be phosphate-primed. To aid in the identification of Aark, the substrate recognition sequence was determined. This would also determine whether Aark is a tyrosine or a serine/threonine specific protein kinase.

Shortened Aar-P1 peptides (with the prefix 'S') were designed, and substitutions of each of the serine, threonine or tyrosine candidates for phosphate-acceptors, were made (Table 3.1). Alanine and serine are two structurally similar amino acids. They differ in the fact that alanine posseses a methyl group instead of the phosphate-accepting hydroxyl group of serine on one of its side chains. Likewise, phenylalanine and tyrosine are structurally related, with the only difference being the absence of the phosphate-accepting hydroxyl group on the carbon ring of phenylalanine. Therefore the substitution of serine/threonine residues with alanine, or tyrosine residues with phenylalanine produces non-phosphorylatable residues that conserve the structure of the peptide and allows the comparison of phosphorylation efficiencies.

Peptide Name	Sequence
Aar-P1	RRRSNYSSPNTLIPSVSKT(Phos)YISPFRR
Aar-SP1	RRRLIPSVSKT(Phos)YISPFRR
Aar-S2	RRRLIP**A**VSKT(Phos)YISPFRR
Aar-S3	RRRLIPSV**A**KT(Phos)YISPFRR
Aar-S4	RRRLIPSVSKT(Phos)**F**ISPFRR
Aar-S5	RRRLIPSVSKT(Phos)YI**A**PFRR

Table 3.1 Sequences of new, shortened Aar peptides

Sequences of the shorter Aar peptides compared with the original Aar-P1. Residues in red highlight the non-phosphorylatable substitutions. The sequence of the original Aar-P1 is included for comparison.

The ability of Aark to phosphorylate the new, shortened, peptides was tested (figure 3.11). A high degree of activity towards Aar-SP1 was seen, which showed that shortening the peptide by removing the first eight amino acids had no effect on the ability of Aark to phosphorylate it. At 400μM, Aar-S4 and Aar-S5 were phosphorylated to an equal level as Aar-SP1. This meant that the sites of their substitutions could not be the phosphate-accepting residues. This also confirms that Aark is a Ser/Thr kinase and not a tyrosine kinase, as the substitution contained in Aar-S4 has replaced the only tyrosine in the peptide.

Aark showed low activity towards both Aar-S2 and Aar-S3, meaning that at least one (or both) of the substituted residues represents the phosphate-accepting residue(s). One explanation could be that one of the residues is the phosphate-accepting residue, whilst the other is required in a structural capacity to enhance the peptide-kinase interaction. To test this possibility, the assay was repeated with Aar-S2 and Aar-S3, but this time an 8-fold increase in peptide concentration was used. If one of the serine residues is required to optimise the enzyme-substrate binding, then a large increase in peptide concentration might be able to overcome the block, whilst an increase in peptide concentration should have little effect on the peptide whose substitution represents the phosphate-accepting residue. For this experiment, the assay time was increased from 10 minutes to 30 minutes as an additional aid to enhance the kinetics of the reaction. The repeated assay is included in figure 3.11 to allow a direct comparison of the two peptide concentrations. Whilst the phosphorylation of both the Aar-SP1 control and Aar-S2 increased by greater than 400%, the phosphorylation of Aar-S3 increased only by about 50%, relative to the control. This suggests that the substituted serine residue in Aar-S3 is the phosphate acceptor, and that the substituted serine in Aar-S2 is required for the optimum substrate recognition site. This proposes a recognition site for Aark of S-X-S-X-T(Phos), with the highlighted serine being the phosphate acceptor.

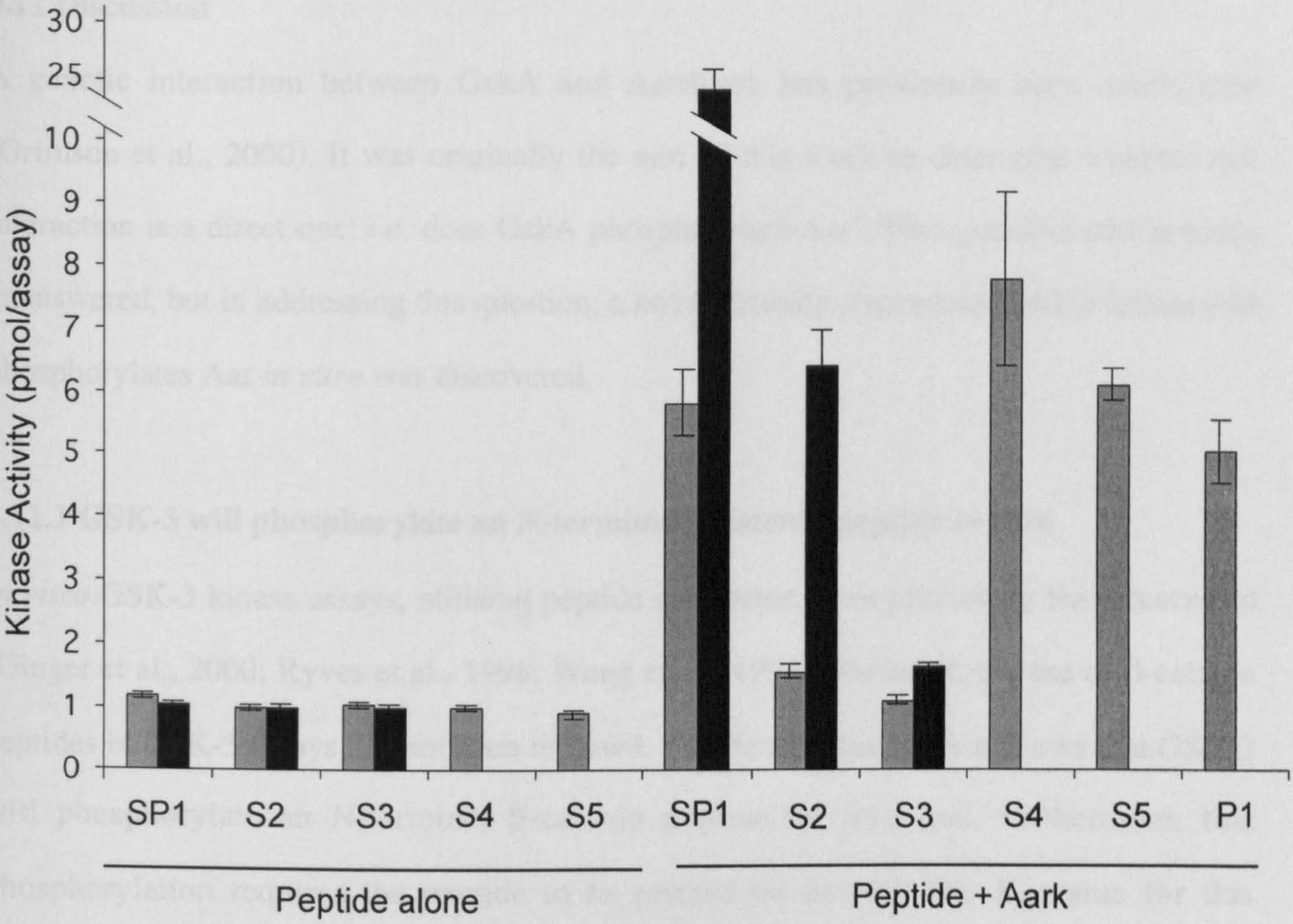

Figure 3.11 Aark phosphorylation of shortened Aar peptides

The ability of Aark to phosphorylate Aar peptides with alanine or phenylalanine substitutions, plus the original Aar-P1 (P1), was tested in an *in vitro* kinase assay. Grey columns represent activity towards 400μM peptides; black columns represent activity towards 3.2mM peptides in an extended, 30 minute, assay (only selected peptides were repeated at 3.2mM, see text for details). The results of a single assay, performed in triplicate are shown, +/- SEM.

3.11 Discussion

A genetic interaction between GskA and Aardvark has previously been established (Grimson et al., 2000). It was originally the aim of this work to determine whether that interaction is a direct one, i.e. does GskA phosphorylate Aar? That question still remains unanswered, but in addressing this question, a novel priming-dependent Ser/Thr kinase that phosphorylates Aar *in vitro* was discovered.

3.11.1 GSK-3 will phosphorylate an N-terminal β-catenin peptide *in vitro*

In vitro GSK-3 kinase assays, utilising peptide substrates, have previously been described (Ginger et al., 2000; Ryves et al., 1998; Wang et al., 1994). However, the use of β-catenin peptides in GSK-3 assays has not been reported. The data presented here shows that GSK-3 will phosphorylate an N-terminal β-catenin peptide *in vitro* and, furthermore, this phosphorylation requires the peptide to be primed on Ser-45. The K_m value for this interaction was established as 85μM. This figure falls within the range of values previously reported for GSK-3 peptide substrates.

3.11.2 Is Aar a GSK-3 substrate?

Peptides based on the putative GSK-3 phosphorylation sites of Aardvark were synthesised commercially, with and without a priming phosphate. These peptides were not substrates for GSK-3 *in vitro*. However, the possibility that GskA, but not GSK-3, would phosphorylate at these sites *in vitro* still remained. To address this, FPLC-purified *Dictyostelium* cell extracts with high levels of GskA activity were tested for activity towards the Aar peptides. Activity was observed, but the specific GSK-3 inhibitor, SB-415286 , reduced the activity by only about 20%. This suggested that the activity in the extracts was not due to GskA.

These experiments, however, can not exclude the possibility that GskA phosphorylates Aar protein *in vivo*. Additional potential GSK-3 phosphorylation sites are also present in the Aar sequence, within the Arm domain and also within the N-terminus. Like the N-terminal sites of β-catenin, the GSK-3 sites in Arm repeat number two of Aar contain multiple residues that could be phosphorylated by GskA. Further peptide synthesis and kinase assays would be required to establish whether these are genuine GSK-3 phosphorylation sites.

3.11.3 Aark phosphorylates Aar *in vitro*

The discovery that a kinase other than GskA (named Aark) was able to phosphorylate Aar peptides *in vitro* was unexpected and further characterisation work was performed.

The charge-separated fraction containing the peak of Aark activity was subjected to further FPLC purification. This time separation was performed on the basis of size, and it was established that Aark has an apparent molecular weight of 30-35kDa. In addition to estimating the size of Aark, the K_m value for its interaction with Aar-P1 was calculated to be 365μM. This figure may be high compared to other kinase-substrate interactions, but several reasons for this could exist. If Aark phosphorylates Aar *in vivo*, it may be that scaffold proteins and/or other additional factors are required. This would bring the kinase and substrate into close proximity and reduce the effective K_m. Also, the conformation of Aar *in vivo*, compared with that of the Aar peptides, may be such that the phosphate-accepting residues are better presented to the kinase.

Having established the size of Aark and a K_m value for its interaction with Aar-P1, the focus shifted towards the identification of the kinase. Several approaches were taken. The preference for phosphate-primed substrates, and the lack of inhibition by SB-415286, suggested that Aark might be Casein Kinase 1. The casein kinase 1 (CK1) family are the

only kinase family, other than the GSK-3 family, that are known to show a preference for phosphate-primed substrates and some family members are 35kDa. The notion that Aark could be CK1 is further enhanced by the finding that CK1α phosphorylates β-catenin, at Ser-45, *in vitro* (Amit et al., 2002,Liu et al., 2002).

3.11.4 Is Aark Casein Kinase 1?

Two parallel approaches were taken to establish whether Aark could be CK1. The CK1 specific inhibitor CKI-7 was used in an attempt to block Aark activity towards Aar-P1 and purified CK1 was used in an attempt to phosphorylate Aar-P1 *in vitro*.

The CK1 inhibitor, CKI-7, reduced CK1 activity towards its synthetic peptide substrate CKI-P by approximately 80% and reduced Aark activity towards Aar-P1 by 45%. However, the manufacturers quote an IC_{50} value of 9.5μM for CKI-7 interaction with CK1, but 80% inhibition was observed with 10μM CKI-7. If the correct IC_{50} value for CKI-7 inhibition of CK1 was calculated for these conditions and added to Aark, it may be that little inhibition is observed. In other words, the 45% inhibition seen in this assay may have been non-specific inhibition associated with the high concentration of inhibitor used.

Furthermore, purified CK1 failed to phosphorylate either the unprimed (Aar-UP) or primed (Aar-P1) peptides *in vitro*. This suggests that Aark is not to a CK1. However, the CK1 isoform used in these assays was CK1δ, whereas the CK1 isoform that has been shown to phosphorylate β-catenin is CK1α. The two isoforms will phosphorylate some, but not all, of the same substrates *in vitro*. CK1δ is the only isoform of CK1 that is commercially available, which puts limitations on the experiments. However, only one CK1 has been identified in *Dictyostelium* and this has been shown to have a molecular weight of 49kDa (Moreno-Bueno et al., 2000), which is much larger than the apparent size of Aark.

The strongest argument against Aark being CK1 comes from an examination of the substrate recognition site. A closer inspection of the amino acids that surround the Aark recognition site of Aar reveals conservation with the CKI-P peptide. This conservation is X-X-G-L, at +1 to the phosphate-accepting serine/threonine residue. However, the Aar-P1 peptide is terminated after X-X, and therefore an extended Aar peptide containing the conserved Gly and Leu residues may be phosphorylated by CK1 *in vitro*, and CK1 phosphorylation of Aar could be of *in vivo* relevance.

3.11.5 Aark's recognition site

The recognition site of Aark was determined. Peptides containing single amino acid substitutions that produced non-phosphorylatable residues were synthesised commercially. The ability of Aark to phosphorylate each of these was tested. Initial results showed that two different substitutions abolished Aark phosphorylation. The block caused by one of the substitutions could be overcome by increasing the concentration of the peptide and the incubation time of the assay. This led to the determination of Aark's phosphorylation site as S-X-S-X-T(Phos), with the highlighted Ser residue being the phosphate acceptor. It would be interesting to observe the effects of expressing a mutant Aar protein which contains amino acid substitutions at this site, and to observe the effects in wild type cells and the *aar* null mutant.

3.11.6 A GSK-3-like kinase is present in *Dictyostelium*

If the evidence presented thus far argues against Aark being GSK-3 or CK1, what is the identity of Aark? The *gskA* null mutant shows no significant activity towards the GSM substrate *in vitro* (Ryves et al., 1998). However, a kinase that shows greatest homology with the GSK-3 family has been discovered in the *Dictyostelium* genomic database. This

kinase has been named GLK, for GSK-3-like kinase. An examination of the GLK amino acid sequence shows complete conservation of the Arg-96, Arg-180, Lys-205 residues which have been shown to be essential for the binding of GSK-3β to phosphate-primed substrates (Dajani et al., 2001,Harwood, 2001). However, the GLK sequence is not conserved at the Axin-binding site of GSK-3β. It has a Val-267Gly and a Glu-268Arg substitution. These exact substitutions have been shown to abolish Axin-binding in GSK-3β and have multiple effects on GskA in *Dictyostelium* (Fraser et al., 2002). Aark may be GLK, but further analysis is needed. However, if Aark is GLK, then it would be expected to phosphorylate Aar in an Axin-independent manner.

Addition: Both GSK-3 and GskA are unable to phosphorylate Aar at the putative N-terminal GSK-3 sites *in vitro*. This does not preclude that the two proteins do not interact *in vivo*; the protein may be a much better substrate for the kinase than the peptides. Alternatively, the phosphorylation of Aar by GskA may require interaction with scaffold proteins, for example, or other additional activating factors. However, it may also be that Aar is not a substrate for GskA at all. The evidence for a genetic interaction between the two proteins has already been established (Grimson et al, 2000; Fraser et al, 2002), but this interaction may prove to be indirect. Either way, the interaction would appear to be unconventional in comparison with that of GSK-3 and β-catenin, but this is not unique. The interaction between GSK-3 and the β-catenin homologue WRM-1 in *C. elegans*, for example, is a positive one (see Korswagen 2002), unlike that seen in flies and mammals.

Further potential GSK-3 phosphorylation sites do exist within the Aar sequence. These sites are present within the second armadillo repeat of the protein and align with putative GSK-3 phosphorylation sites within the second armadillo repeat of β-catenin (Yost et al, 1996). Furthermore, complete loss of the N-terminal GSK-3 sites of β-catenin does not lead to total loss of GSK-3 phosphorylation, suggesting that the protein is indeed phosphorylated at

additional sites. Phosphate-primed and unprimed peptides based on the sequence of these second sites in Aar have been synthesised. The phosphate-primed and not the unprimed peptide has recently been demonstrated to be a substrate for both GSK-3 and GskA *in vitro* (W. J. Ryves, pers. commun.). It has yet to be established whether an interaction occurs between GskA and Aar *in vivo*, but it would appear that any interaction is unconventional, but may turn out to be a universal mechanism for β-catenin regulation.

Chapter 4

Deletion Analysis of Aardvark

4.1 Introduction

It has previously been established that, like its mammalian counterpart, Aar plays important roles in both adhesion and signalling processes within the cell. Aark has been discovered as a kinase that will phosphorylate Aar at a defined site *in vitro*, but is this phosphorylation of Aar actually significant to the protein's function?

In order to answer this question, but also to increase the understanding of the role that Aar plays in both adhesion and signalling in *Dictyostelium*, a series of DNA constructs for the expression of Aar and Aar deletion mutants were created. The full-length *aar* cDNA, or deletions encoding N-terminal or C-terminal Aar truncations were cloned into a modified version of the pDXA-3C vector (Manstein et al., 1995). The pDXA vector is an extrachromosomal, high copy number plasmid, which expresses transgenes from the constitutively-expressed actin15 promoter. This vector was previously modified to allow for translation from the *aar* initiator codon (Grimson et al., 2000).

aar and each of its deletion derivatives were also fused to a sequence encoding a C-terminal green fluorescent protein (GFP) 'tag' so that the localisation of the proteins could be followed in living cells. Figure 4.1 highlights the features of the modified pDXA-3C expression vector.

Figure 4.1 The 9.335Kb pDXA-aar-gfp expression vector
The 861bp Amp^r gene allows for selection in bacteria, whilst the 831bp Neo^r gene allows for positive selection of eukaryotic transformants. The vector also contains a *Dictyostelium* origin of replication, for extrachromosomal replication.

Aar is required in both a signalling and adhesion capacity within the *Dictyostelium* cell. Thus, multiple phenotypes are associated with the loss of Aar. These include the collapse of fruiting bodies and ectopic stalk formation – both associated with the loss of adherens junctions; a reduction of *pspA* gene expression, both during development and in isolated cells; and a reduction of spore and stalk cell production in monolayer culture (Coates, 1999; Coates et al., 2002; Grimson et al., 2000).

The two simplest assays were chosen as independent indicators of Aar function. A comparison of the morphology of mature fruiting bodies was chosen as a marker for adhesion, whilst the expression of the prespore marker gene *pspA* in isolated cells was chosen as a marker for signalling activity.

4.2 Aar-GFP is functional in the both the *aar* mutant and wild type *Dictyostelium* with respect to development

To test that the GFP fusion had no effect on Aar function within the cell, both *aar* mutant and wild type *Dictyostelium* were transformed with pDXA-aar-gfp. Transformants were starved for 24 hours and the morphology of the resulting fruiting bodies examined by light microscopy.

Upon starvation, *aar* mutant cells will aggregate, but produce fruiting bodies that differ from those of wild type cells. Stalks appear thinner and weaker than in wild type structures, and the majority of fruiting bodies collapse onto the substratum (Coates, 1999; Grimson et al., 2000). These collapsed fruiting bodies are often seen to reculminate from within the fallen fruiting body. In addition, *aar* null mutants form ectopic stalk structures (Coates et al., 2002). Over-expression of *aar* in the *aar* mutant partially rescues the collapse, but fruiting bodies remain weaker than wild type ones (Coates, 1999).

Transmission electron microscopy (TEM) of cross sections of fruiting bodies of the *aar* mutant revealed a loss of actin fibres at the adherens junctions (Grimson et al., 2000). This suggests that Aar is necessary for the formation of *Dictyostelium* adherens junctions, which itself may be a necessary process in the creation of a rigid fruiting body. Conversely, TEM of *aar* mutants over-expressing *aar* revealed the adherens junctions to possess abnormally high levels of actin filaments, leading to a buckling of the membrane. Thus the collapse of structures in the *aar* mutant could be explained by the total absence of adherens junctions, whilst the weakness of the *aar* over-expressing culminants could be explained by an excess of adherens junctions. In short, loss or over-expression of Aar upsets the balance of a highly regulated adhesion process.

If over-expression of *aar* affects fruiting body morphology by causing a disruption to regulated cell-cell adhesion, the effect should also occur in wild type cells. This is indeed the case. Over-expression of *aar* in wild type *Dictyostelium*, causes the stalks of culminants to become twisted, leading, in some instances to a collapse of the structures, as seen with the *aar* mutant (Coates, 1999).

In order to show that the C-terminal GFP fusion does not affect the function of Aar, both *aar* mutant and wild type cells were transformed with the full-length pDXA-aar-gfp expression construct. Cells were starved, and allowed to develop on nitrocellulose filters. After 24 hours, their morphology was examined by light microscopy. Transforming *aar* mutant cells with pDXA-aar-gfp rescued the collapse of many fruiting bodies, but some collapse was also seen (figure 4.2b). Expression in wild type cells led to contortion of the stalk tube, smaller spore heads and instability and often collapse of the fruiting body (figure 4.2d). Both of these observations are consistent with the phenotypes of *aar* overexpression.

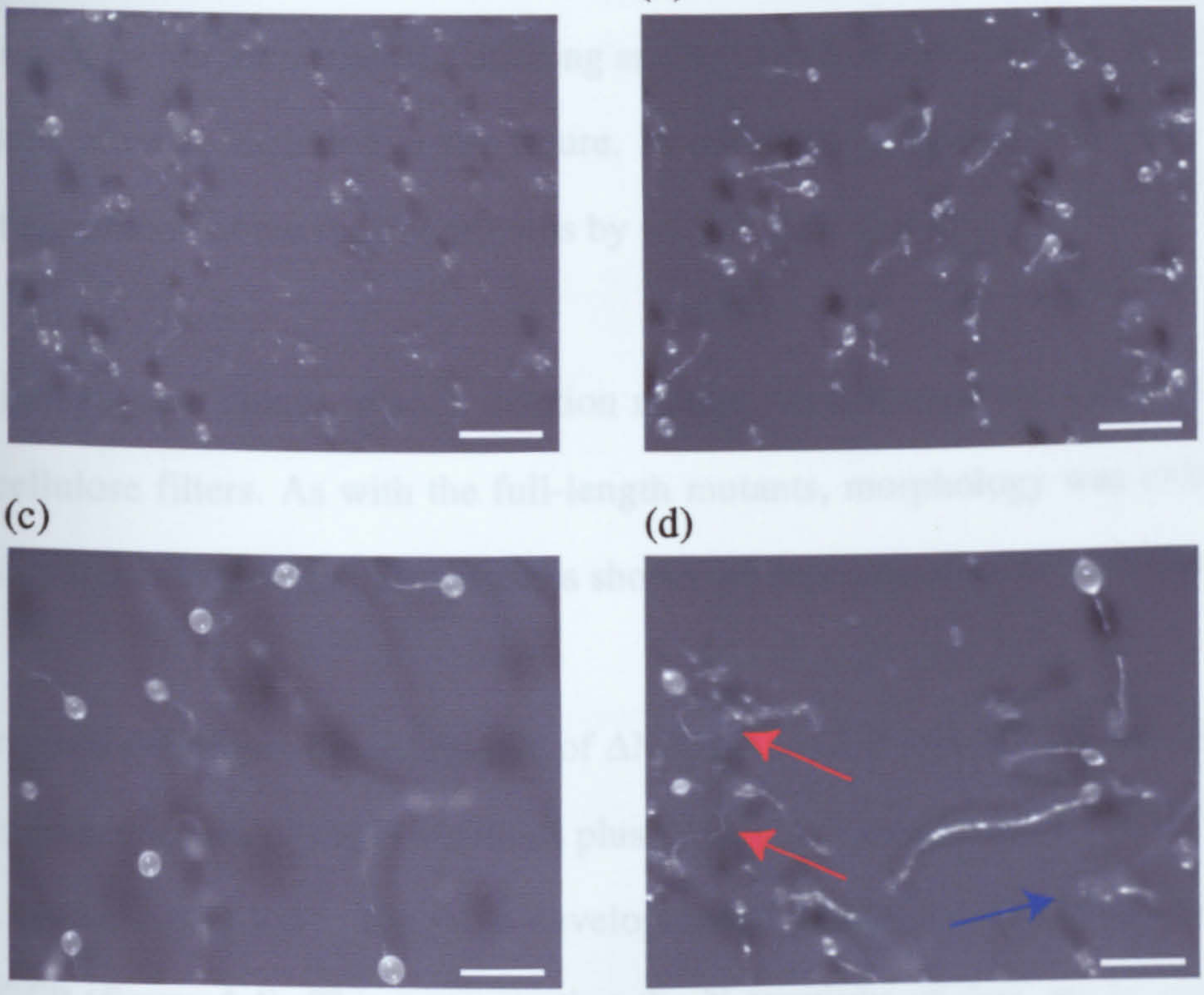

Figure 4.2 Cells transformed with pDXA-aar-gfp display the *aar* overexpression phenotype in both *aar*- and wild type cells

(a) *aar- Dictyostelium.* Most culminants have collapsed onto the substratum.

(b) *aar- Dictyostelium* overexpressing *aar-gfp*. Expression of *aar-gfp* partially rescues the collapsed fruting body phenotype but also leaves culminants unstable.

(c) Wild type *Dictyostelium*

(d) Wild type *Dictyostelium* overexpressing *aar-gfp*. Note the twisted stalk tubes, denoted by the red arrows, and the collapsed fruiting body (blue arrow) in the *aar* overexpressors. Scale bar represents 0.5mm.

4.3 Rescue of the *aar* mutant phenotype by N-terminal and C-terminal Aar-GFP deletions

Each of the deletion constructs were transformed into the *aar* mutant, and expression was determined by northern analysis, utilising an *aar* cDNA probe (figure 4.3). Maps of the Aar deletions are also included in the figure. In addition, western blot analysis was used to detect expression of the mutant proteins by way of their C-terminal GFP tags (figure 4.3a).

Two independent clones of each deletion mutant were starved and allowed to develop on nitrocellulose filters. As with the full-length mutants, morphology was examined after 24 hours by light microscopy. The pictures shown are representative of both clones tested.

N-terminal deletions: the expression of ΔN201 Aar-GFP and ΔN258 Aar-GFP (loss of the N-terminus and loss of the N-terminus plus the region containing the Aark phosphorylation sites, respectively) led to the same developmental phenotype as expression of full-length Aar-GFP (figure 4.4). This suggests that the N-terminus of Aar, up to and including the Aark sites, is not required for rescue of the *aar* fruiting body morphology. However, ΔN371 and ΔN587 mutants (loss of the putative α-catenin binding site and loss of the first 7 arm repeats, respectively) resemble the *aar* mutant (figure 4.4).

C-terminal deletions: the morphology of all three of the C-terminal deletion mutants of Aar resembled the *aar* mutant (figure 4.5). This suggests that the C-terminus of Aar is not essential for developmental rescue.

The minimum sequence of Aar that will rescue the mutant morphology, from these results, is therefore the ΔN258 mutation

(a)

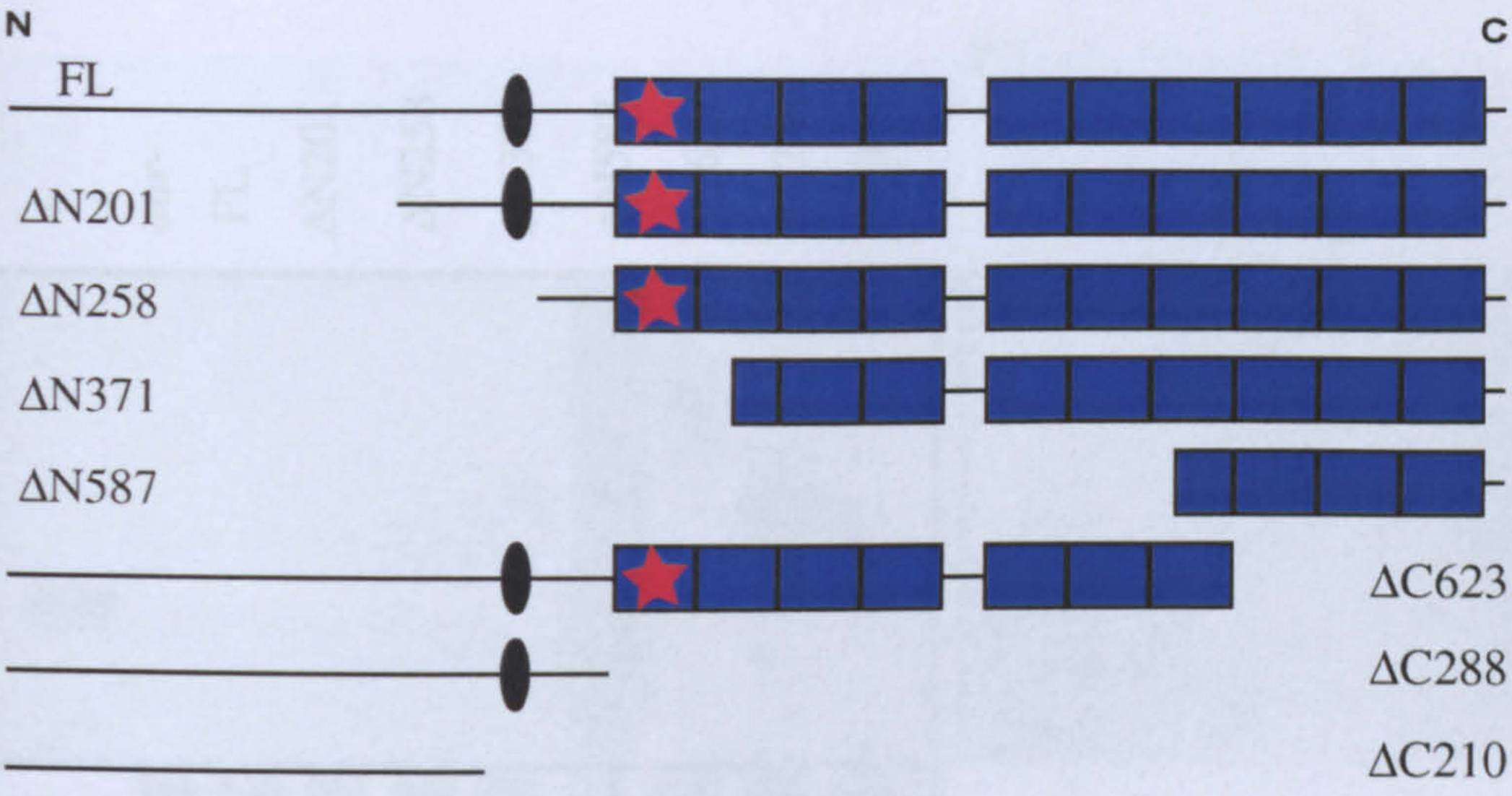

(b)

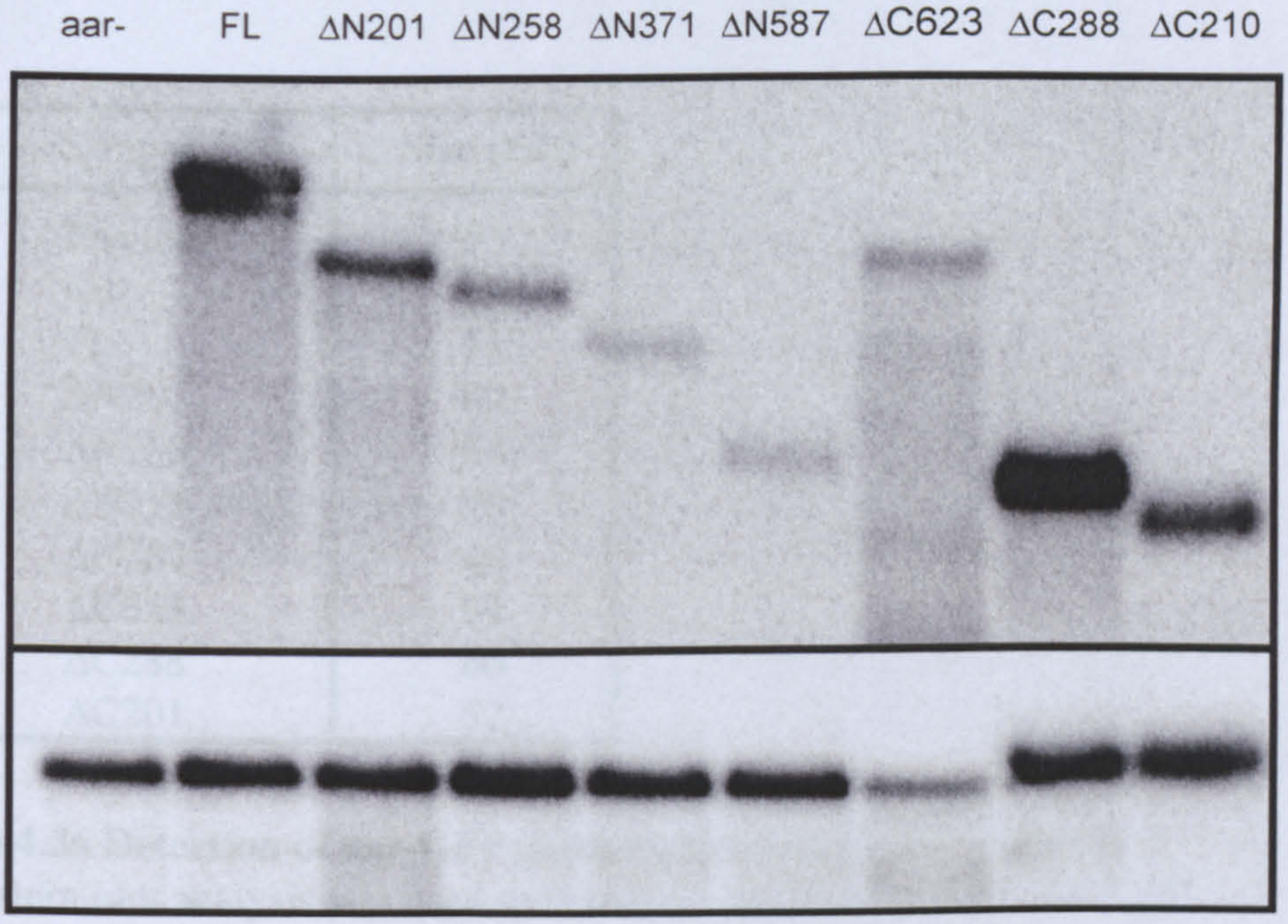

Figure 4.3 Detecting expression of Aar-GFP deletions by northern analysis
(a) Nomenclature of N-terminal and C-terminal Aar-GFP deletions.
ΔNxxx = deletion of Aar from the N-terminus as far as amino acid xxx
ΔCxxx = deletion of Aar from the C-terminus as far as amino acid xxx
Black ovals and red star mark the Aark phosphorylation and putative α-catenin binding sites, respectively.
(b) Northern analysis of Aar-GFP deletion mutants, expressed in *aar-* cells. Top panel shows *aar* expression, whilst the bottom panel shows the ubiquitously-expressed *Ig7* message, shown here as a loading control. FL = full-length.

(a)

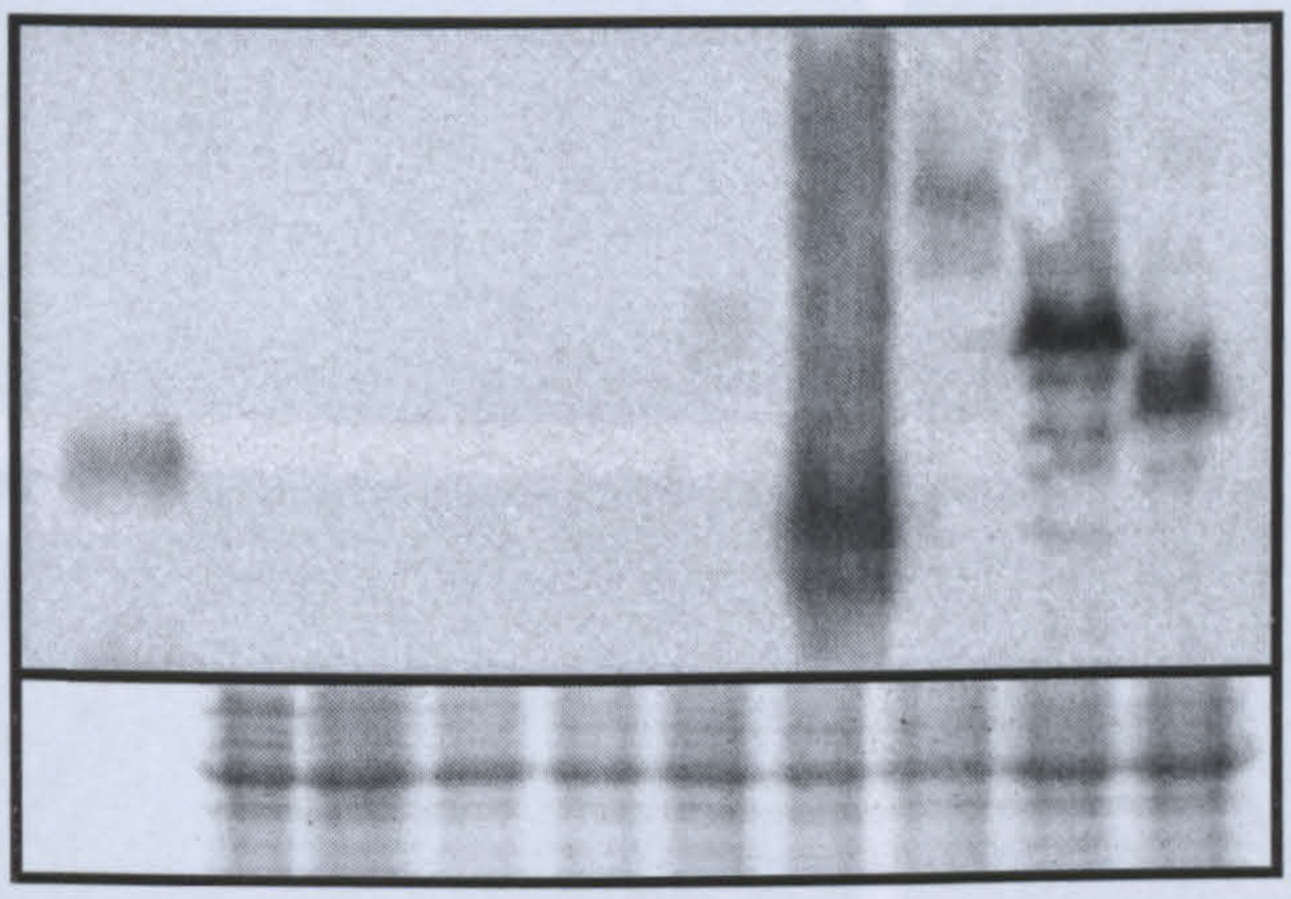

(b)

(c)

(d)

Sample	Size (kda)
Positope	53
aar-	N/A
FL	113
ΔN201	90
ΔN258	84
ΔN371	70
ΔN587	46
ΔC623	94
ΔC288	60
ΔC201	52

Figure 4.3a Detection of aar-GFP deletion mutants in cell lysates
(a) Western blot analysis was used to detect the expression of the Aar-GFP deletion mutants in *Dictyostelium* cell lysates. + = positope positive control protein; FL = full-length Aar-GFP.
(b) Coomassie blue staining was used to compare loadings
(c) The blot in (a) was subjected to a greater period of exposure in order to detect bands of weaker intensity. Only the first 6 lanes are shown.
(d) Table of predicted sizes for each Aar deletion mutant, as determined by their amino acid sequences.

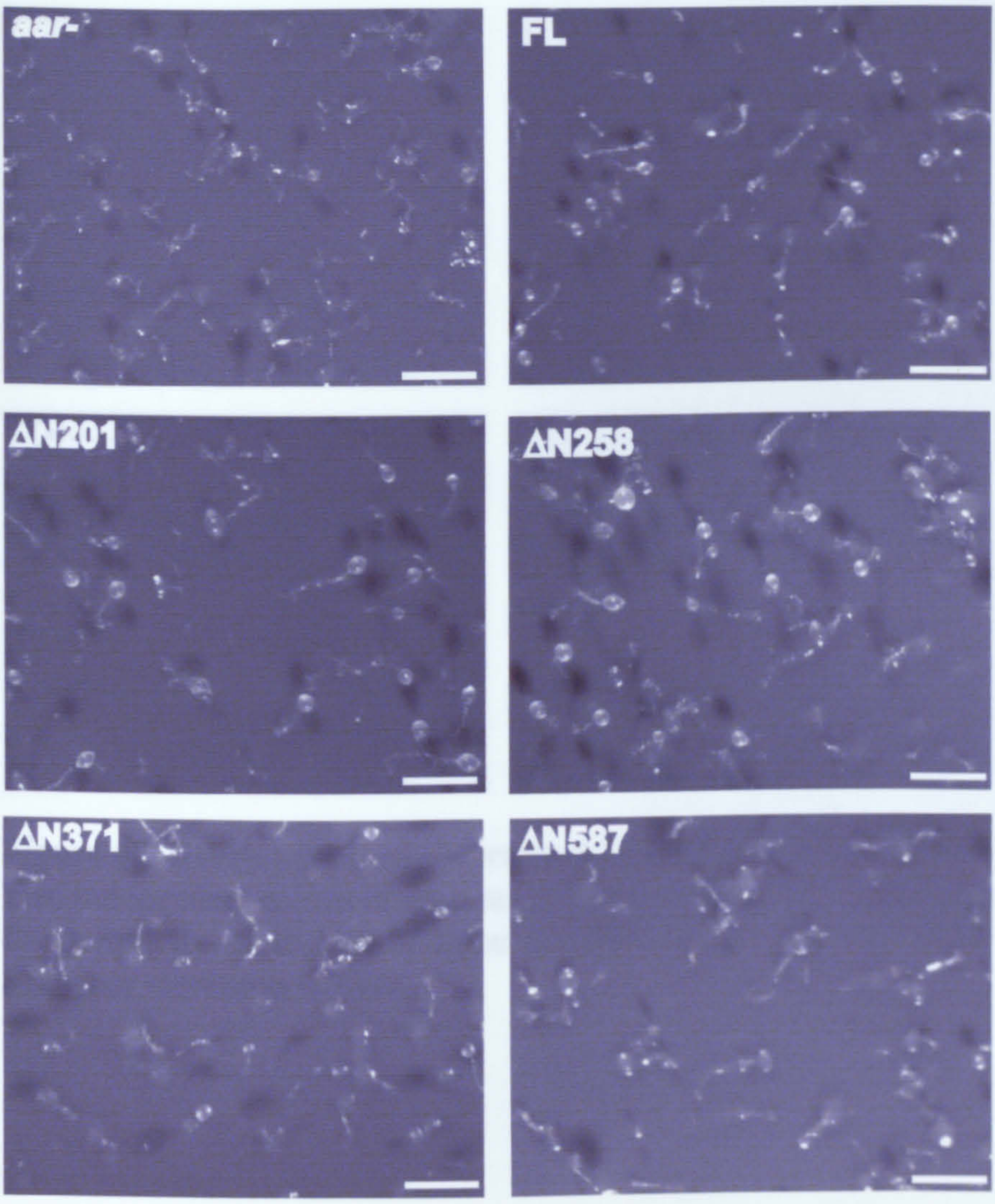

Figure 4.4 Development of N-terminal Aar-GFP deletion mutants
Two independent clones of each mutant were developed on nitrocellulose filters for 24h. Note that whilst FL, ΔN201 and ΔN258 all partially rescue the *aar*- phenotype, ΔN371 and ΔN587 mutants display the *aar*- phenotype. Scale bar represents 0.5mm.

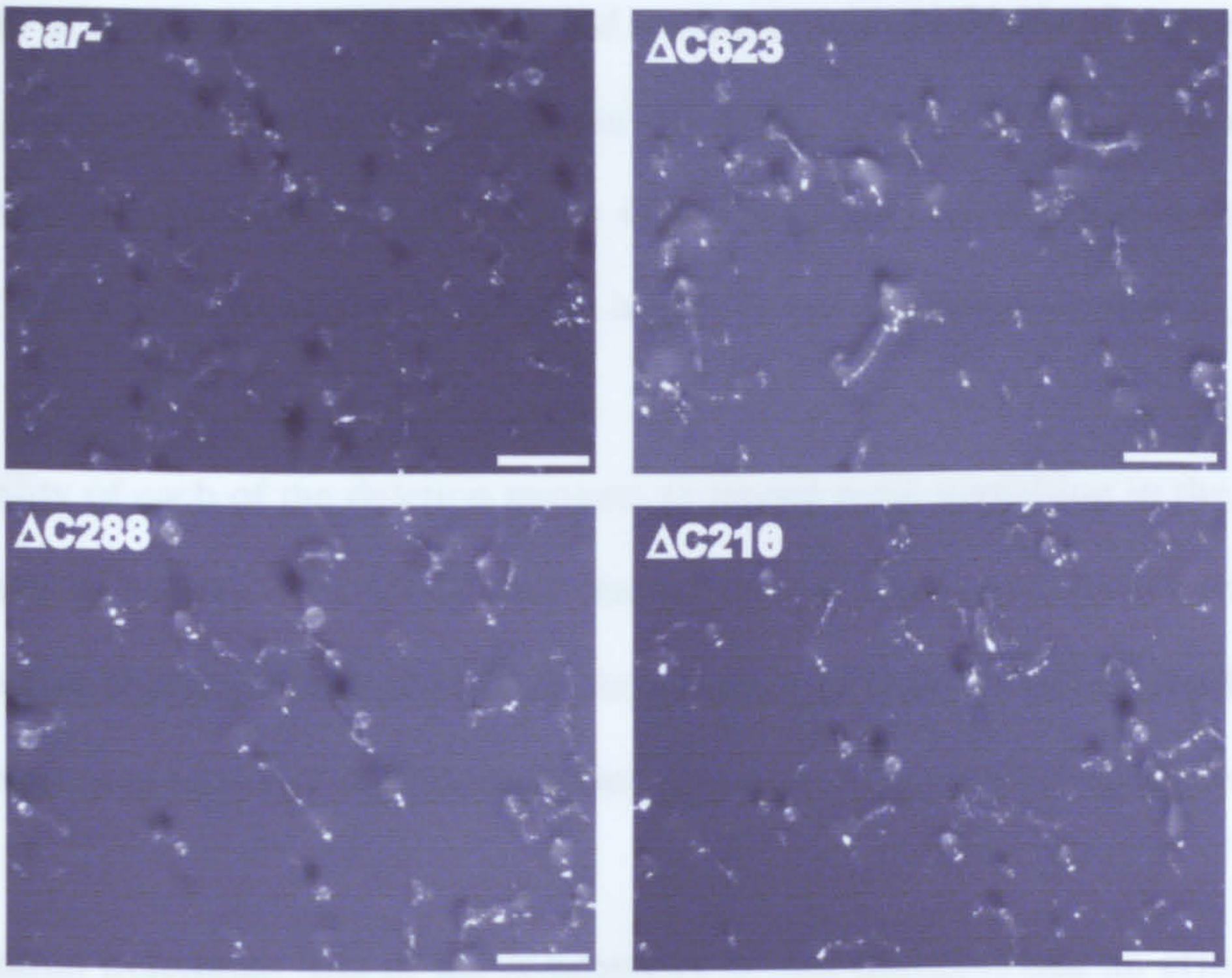

Figure 4.5 Development of C-terminal Aar-GFP deletion mutants
Two independent clones of each mutant were developed on nitrocellulose filters for 24h. Note that all three mutants display the *aar-* phenotype. Scale bar represents 0.5mm.

4.4 *pspA* expression in the Aar-GFP deletion mutants (*aar*- background)

The loss of *aar* leads to both a delay and a reduction in the levels of expression of the pre-spore gene *pspA* during development (Coates, 1999). These observed effects are exaggerated in isolated cells (Grimson et al., 2000). Over-expression of *aar* in the *aar* mutant rescues this reduction, leading to higher levels of expression than in wild type cells.

The ability of each of the deletion mutants to rescue *pspA* signalling in the *aar* mutant was examined in isolated cells. Cells were starved by shaking at low density in KK_2 buffer for 6-8h, before shaking with 1mM cAMP for a further 15 hours to induce *pspA* signalling. The experiment was repeated with independent clones and comparable results were obtained.

N-terminal deletions: loss of the N-terminus of Aar (ΔN201) had no effect on the ability of Aar to rescue the null phenotype (figure 4.6). However, the level of *pspA* expression in the ΔN258 mutant was close to that of the *aar* mutant, whilst the ΔN371 and ΔN587 mutants appeared to show reduced levels of *pspA* expression (figure 4.6b and c). This shows the region of Aar containing the Aark phosphorylation sites to be necessary for the full rescue of *pspA* signalling, suggesting a requirement for Aark phosphorylation.

C-terminal deletions: loss of the final three Arm repeats of Aar (ΔC623) appeared to increase the protein's ability to rescue *pspA* signalling over and above that of the full-length protein (figure 4.6). This suggests that not only is the C-terminus of Aar not required for full *pspA* rescue, but it may actually be inhibitory to Aar signalling function when the protein is over-expressed. The ΔC288 and ΔC210 mutants showed *pspA* expression levels that were lower than those of the *aar* mutant, but this will be discussed in section 4.7.

Figure 4.6 Northern analysis of *pspA* expression in *aar* deletion mutants
(a) A reminder of the Aar-GFP deletions.
(b) Northern analysis of *pspA* expression in *aar* deletion mutants, expressed in an *aar*- background. Top panel represents *pspA* expression. The bottom panel represents *Ig7* expression, included for comparison of loadings. WT = wild type; FL = full-length.
(c) A repeat of the northern analysis in (b), performed with independent clones.
(d) Table of statistics based upon the densitometry readings for each northern (calculated using Quantity One software). Each *pspA* figure was normalised to *Ig7* levels, before being expressed as a percentage of FL expression. SD = standard deviation.

4.5 Development of Aar-GFP deletions in wild type cells

Each of the deletion constructs were transformed into wild type cells and expression determined by northern analysis, probing for *aar* as in section 4.3 (figure 4.7).

Two independent clones of each mutant were starved and developed on nitrocellulose filters for 24 hours, before examining the morphology of the fruiting bodies. The pictures are representative of both clones.

N-terminal deletions: loss of the N-terminus of Aar (ΔN201) and loss of the Aark phosphorylation sites (ΔN258) still gave the characteristic *aar* over-expression phenotype (figure 4.8). Stalk tubes were twisted, spore heads smaller, and many fruiting bodies collapsed onto the substratum. The ΔN371 and ΔN587 mutants (loss of the putative α-catenin binding site and loss of the first seven arm repeats, respectively) both displayed wild type morphology (figure 4.8). These observations are comparible to the results of expression of the same deletions in the *aar* mutant. This suggests that the region of Aar between the N-terminus of ΔN258 and ΔN371 Aar-GFP is important for protein function, and. This would be consistent with α-catenin binding at the predicted site.

C-terminal deletions: wild-type cells over-expressing the C-terminal Aar truncations, ΔC288 & ΔC210 showed no visible phenotype; that is, development appeared normal in comparison with that of wild type cells (figure 4.9).

(a)

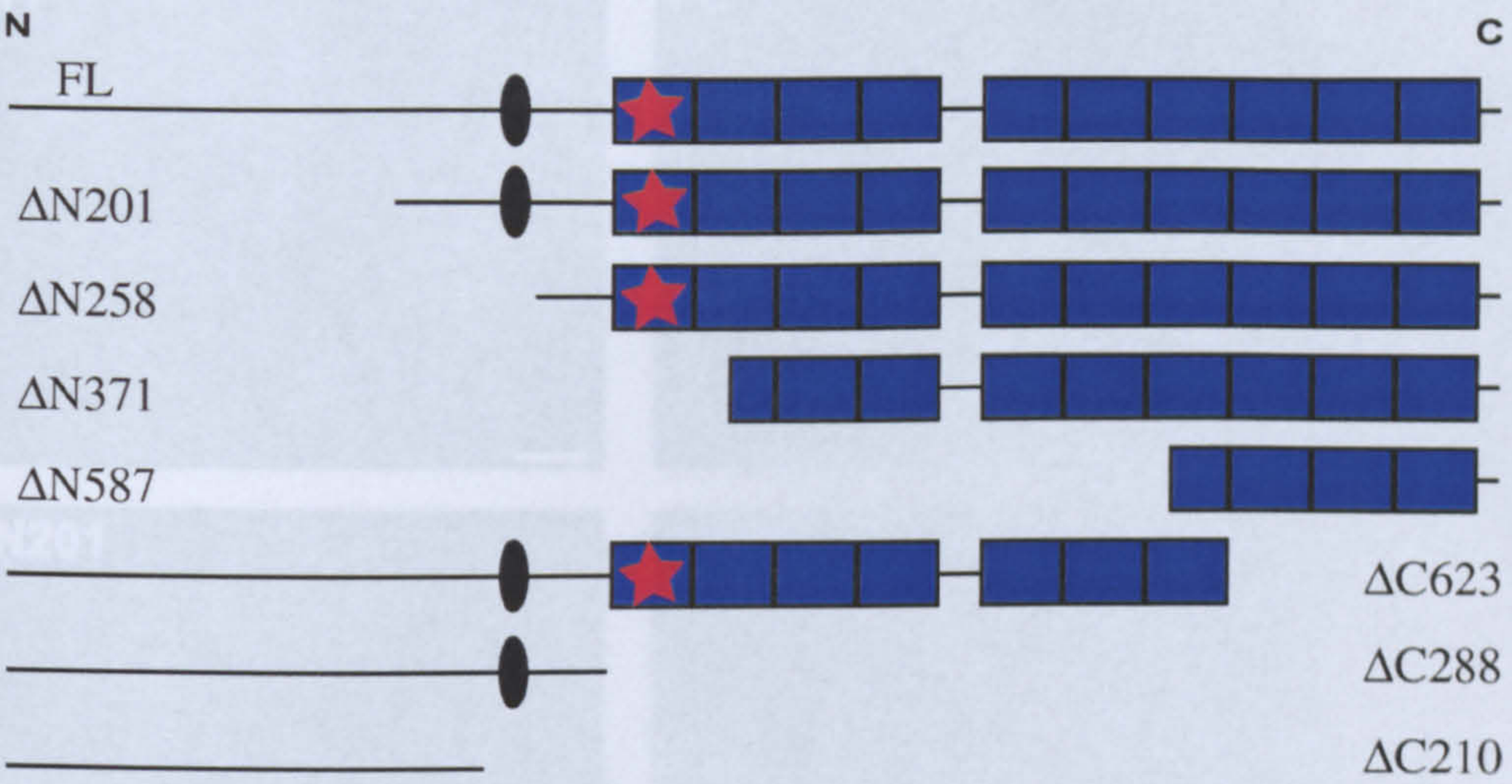

(b)

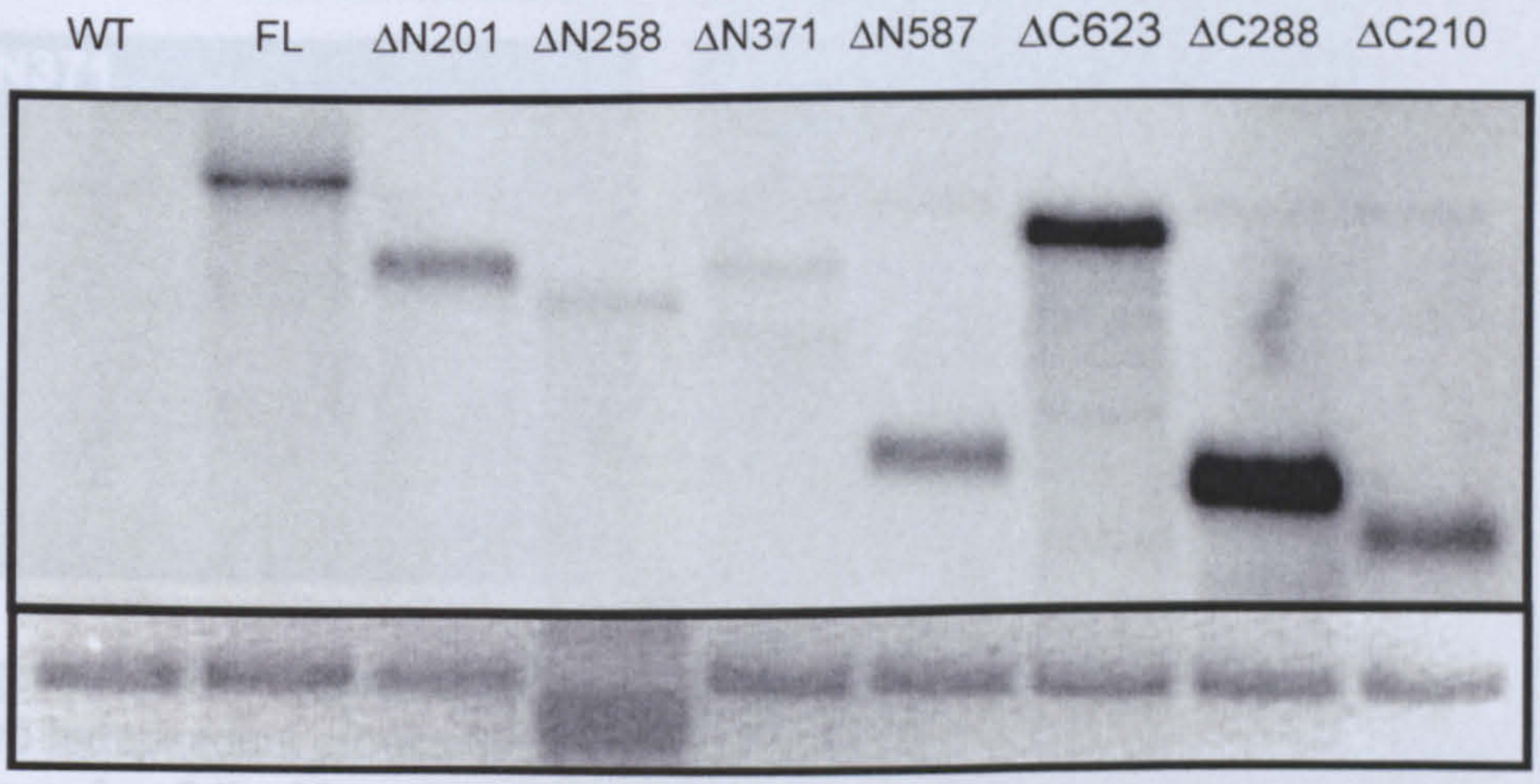

Figure 4.7 Detecting expression of *aar* deletions by northern analysis
(a) A reminder of the Aar-GFP deletions
(b) Northern analysis of Aar-GFP deletions. The top panel represents *aar* expression, whilst the bottom panel represents the 28s rRNA band (shown as a loading control). WT = wild type; FL = full-length.

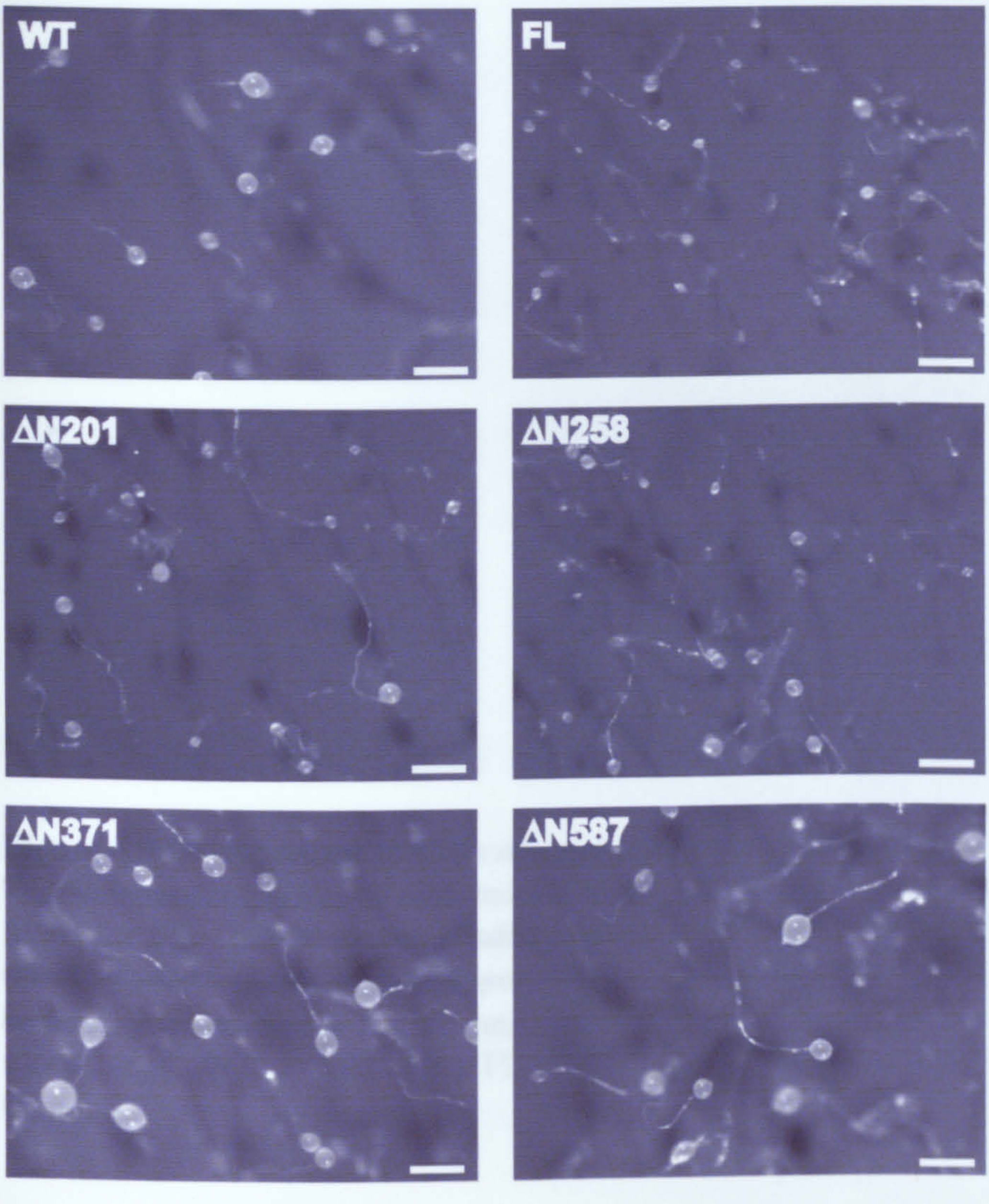

Figure 4.8 Development of N-terminal Aar-GFP deletion mutants
Two independent clones of each mutant were developed on nitrocellulose filters for 24h. Note that whilst ΔN201 and ΔN258 display the *aar* over-expression phenotype, ΔN371 and ΔN587 appear wild type. WT = wild type; FL = full-length. Scale bar represents 0.5mm.

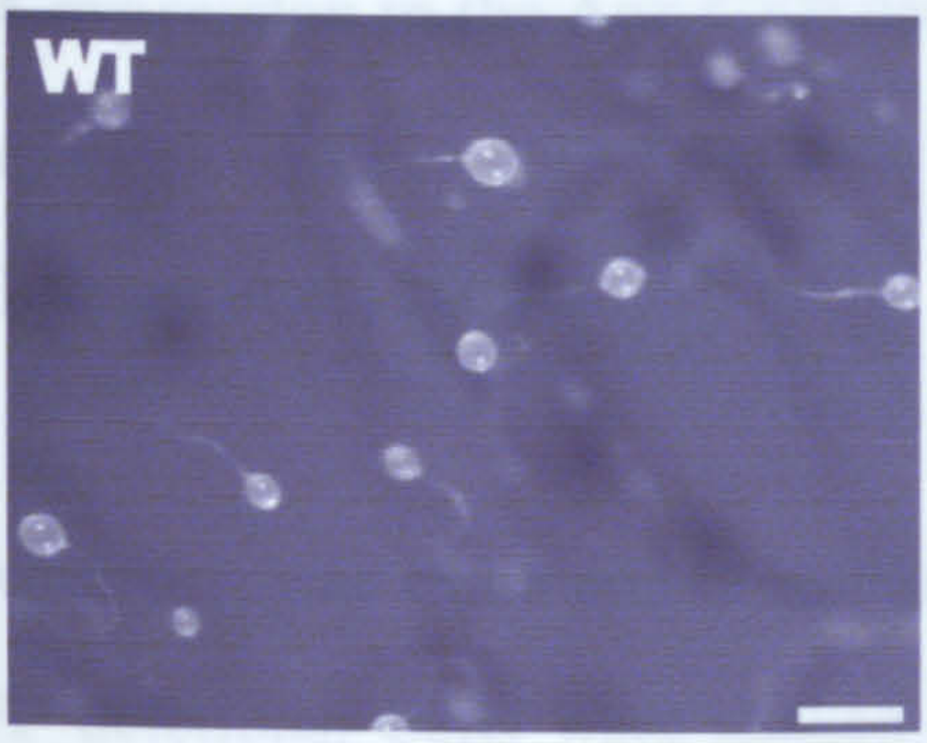

Data not available

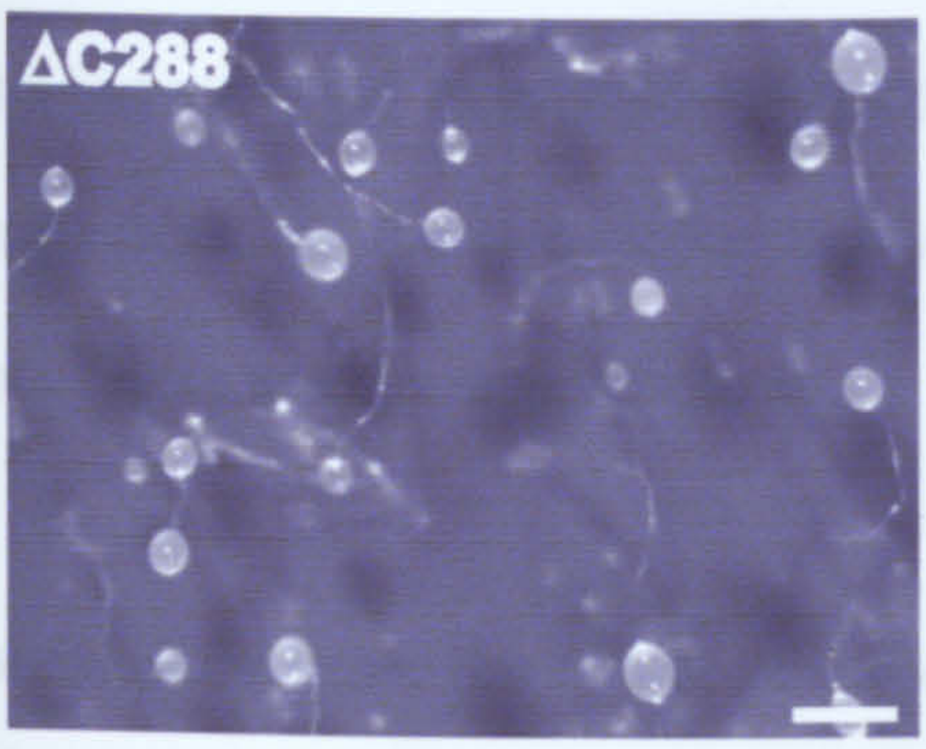

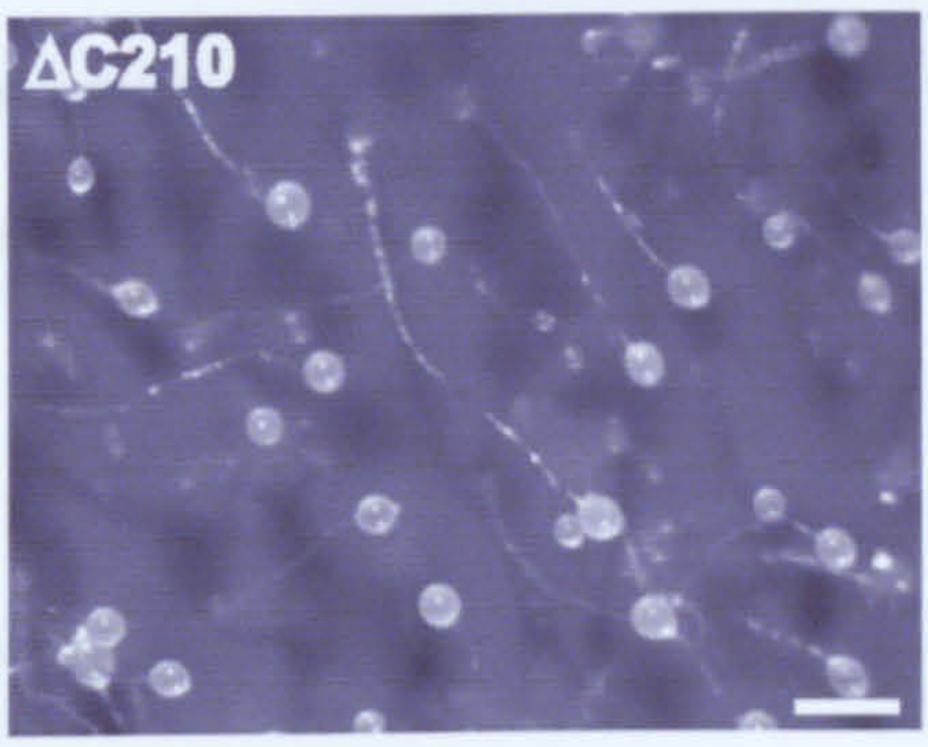

Figure 4.9 Development of C-terminal Aar-GFP deletion mutants
Two independent clones of each mutant were developed on nitrocellulose filters for 24h. ~~ΔC623 mutants exhibited a morphology similar to that of the *aar* overexpression phenotype. Stalks were contorted, but fruiting bodies did not collapse.~~ ΔC288 and ΔC210 developed with wild type morphology. WT = wild type; FL = full-length. Scale bar represents 0.5mm.

4.6 *pspA* expression in the Aar-GFP deletion mutants (wild type background)

Over-expresssion of *aar* in isolated wild type cells leads to an increase in the expression of *pspA* (Grimson et al., 2000).

pspA expression was examined in isolated cells of wild type *Dictyostelium* expressing the Aar-GFP deletions. Cells were shaken at low density as before, and treated with 1mM cAMP to induce *pspA* expression. The experiment was repeated, using independent clones. The results between the two experiments varied; some results were reproducible and others were not. These are discussed below.

N-terminal deletions: the effect of the ΔN201 and ΔN258 truncations (deletion of the N-terminus and deletion of the Aark phosphorylation sites, respectively) on *pspA* expression differed little from the expression of full-length *aar* in one northern (figure 4.10c), yet showed dominant negative effects in the other (figure 4.10b). The effects of expression of ΔN371 and ΔN587 however, were more reproducible. The former showed a drastic reduction in *pspA* levels, whilst expression of the latter had little effect in both northerns.

C-terminal deletions: expression of the ΔC623 mutants appeared to have little effect on *pspA* levels in both experiments, whilst expression of both the ΔC288 and ΔC210 mutants caused a drastic reduction in *pspA* expression levels.

(a)

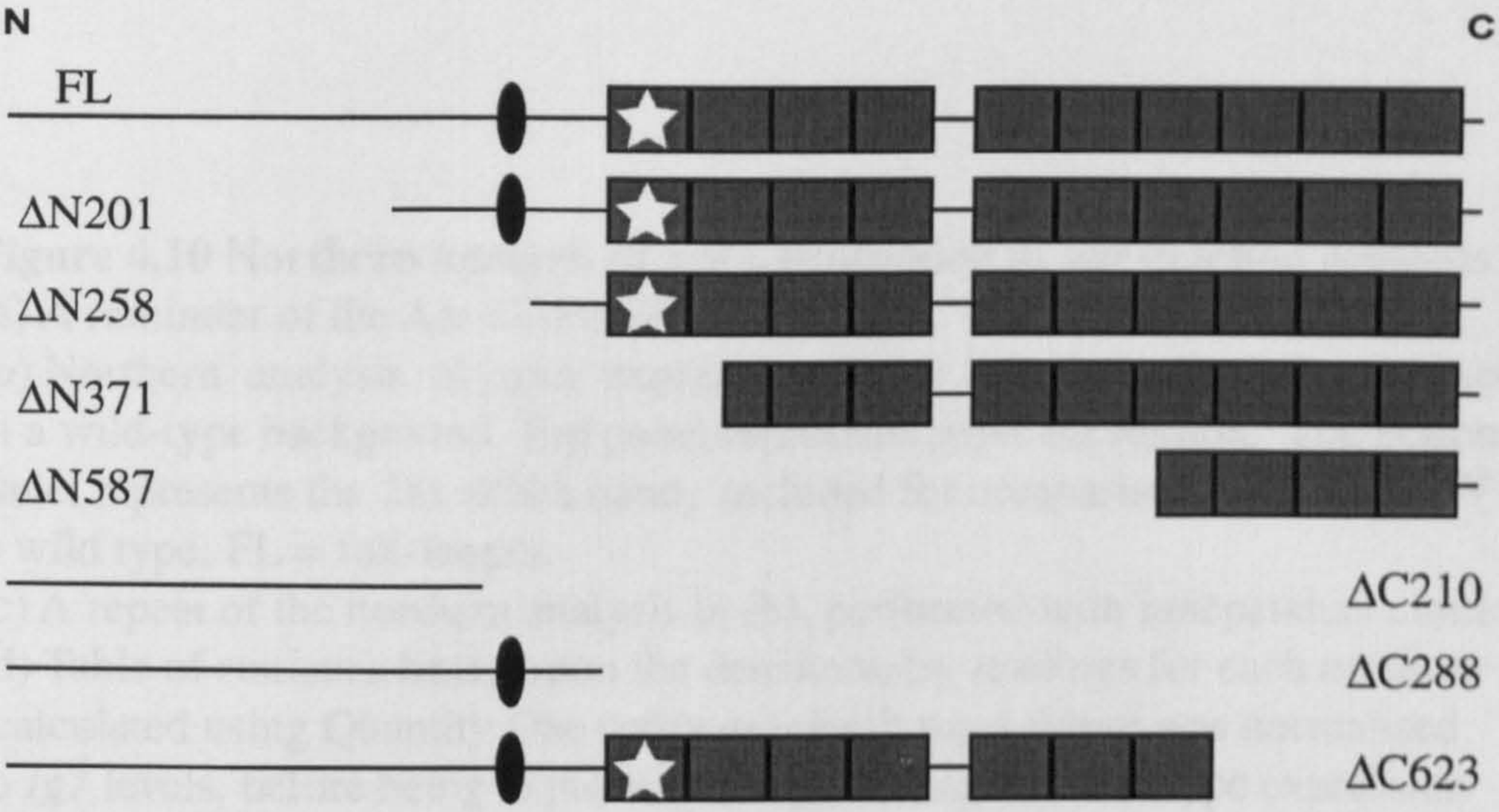

(b)

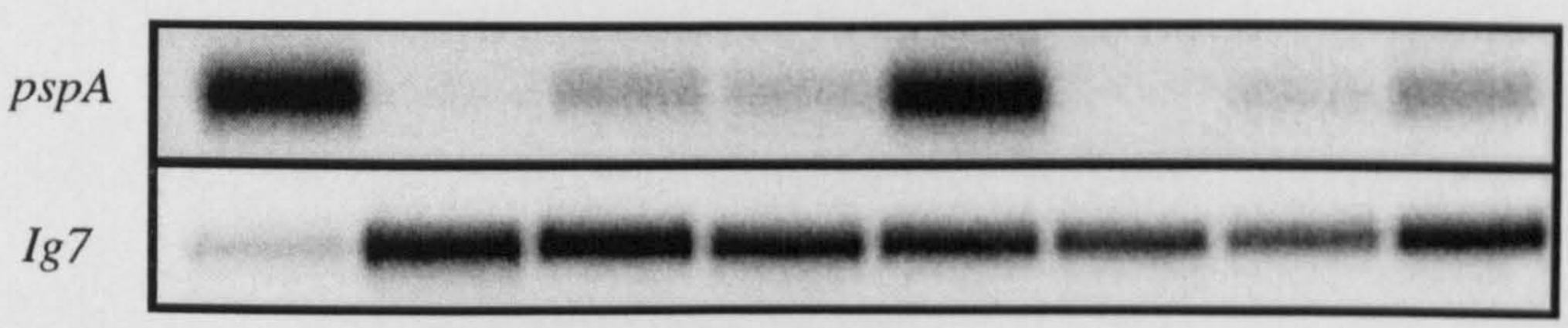

(c)

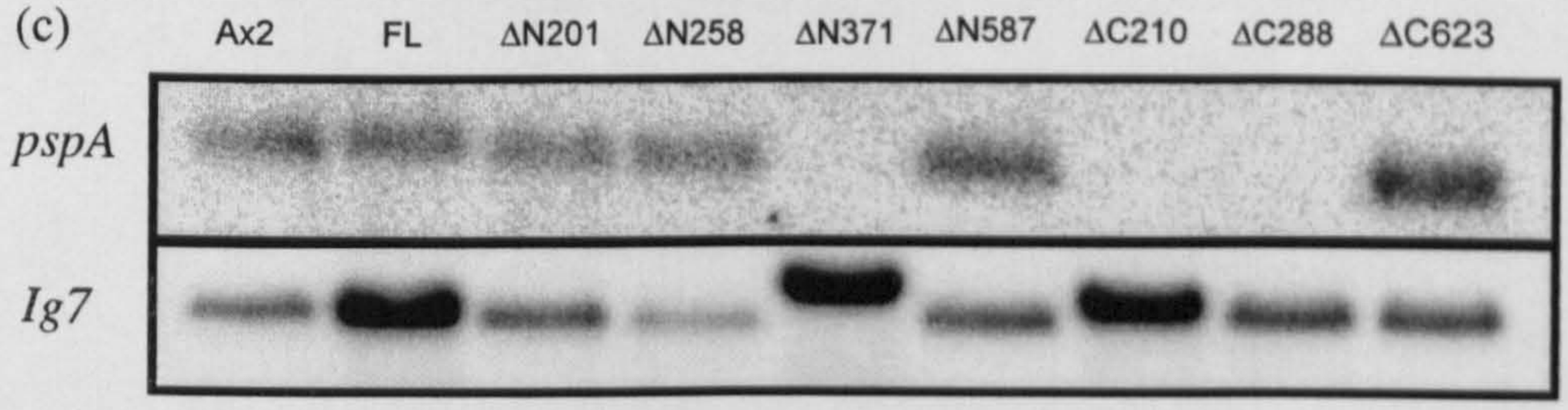

(d)

Mutant	Value			
	blot (b)	blot (c)	Mean	SD
Ax2	100	100	100	0
FL	N/A	30	N/A	N/A
ΔN201	3	76	40	52
ΔN258	6	159	82	109
ΔN371	6	0.5	3	4
ΔN587	23	105	64	58
ΔC210	10	137	73	96
ΔC288	7	-5	1	9
ΔC623	3	-0.5	1	3

Figure legends on next page

Figure 4.10 Northern analysis of *pspA* expression in *aar* deletion mutants
(a) A reminder of the Aar-GFP deletions.
(b) Northern analysis of *pspA* expression in *aar* deletion mutants, expressed in a wild-type background. Top panel represents *pspA* expression. The bottom panel represents the 28s rRNA band, included for comparison of loading. WT = wild type; FL = full-length.
(c) A repeat of the northern analysis in (b), performed with independent clones.
(d) Table of statistics based upon the densitometry readings for each northern (calculated using Quantity One software). Each *pspA* figure was normalised to *Ig7* levels, before being expressed as a percentage of wild type expression levels. SD = standard deviation.

4.7 Discussion

4.7.1 Aar and cell adhesion

The expression of N-terminal and C-terminal Aar-GFP deletions affects adhesion and signalling processes in both the *aar* mutant and wild type *Dictyostelium*. To summarise the adhesion effects, table 4.1 lists the morphology of the deletion mutants, whilst table 4.2 summarises the signalling effects by listing the *pspA* expression levels.

Mutant	**Effect in *aar* mutant cells**	**Effect in wild type cells**
FL	rescue/*aar* over-expression phenotype	*aar* over-expression phenotype
ΔN201	rescue/*aar* over-expression phenotype	*aar* over-expression phenotype
ΔN258	rescue/*aar* over-expression phenotype	*aar* over-expression phenotype
ΔN371	*aar*- phenotype	wild type
ΔN587	*aar*- phenotype	wild type
ΔC623	*aar*- phenotype	N/A
ΔC288	*aar*- phenotype	wild type
ΔC210	*aar*- phenotype	wild type

Table 4.1 Summary of morphological phenotypes
The resulting morphology of expression of each deletion mutant in both the *aar* mutant and wild type cells are included.

Loss of the N-terminus has no effect on the ability of Aar to rescue the *aar* mutant fruiting body morphology, nor its ability to cause the over-expression phenotype. The same is true of further deletion to remove the Aark phosphorylation sites. Deletion of the putative α-catenin binding sites does, however, affect both of these processes. This supports the idea that amino acids 301-331 of Aar contain a binding site for α-catenin. In support of this, a vinculin/α-catenin-like protein has recently been identified in *Dictyostelium* (T. Soldati,

pers. commun). If Aar functions like β-catenin in the formation of adherens junctions, then cadherin binding would be expected in the C-terminus of Aar. Deletion of the final 3 arm repeats of Aar created a protein that was unable to rescue the *aar* mutant, and therefore further deletions were also unable to rescue. The last three Arm repeats are therefore important for Aar function and it is possible that they could contain a binding site for a cadherin-like molecule, although as yet no such protein has been identified in *Dictyostelium.*

In terms of overexpression phenotypes, deletions with loss of the N-terminus of Aar, including the Aark phosphorylation sites, acted like full-length Aar. These results are consistent with the *aar* mutant rescue experiments, which suggest that the N-terminus up to and including the Aark phosphorylation sites are not required for Aar's role in adhesion. Loss of the putative α-catenin binding site and further deletion from the N-terminus prevented the over-expression phenotype, again supporting the *aar* mutant data. Deletion of the final three Arm repeats caused a phenotype that was partially reminiscent of the overexpression phenotype. However, this truncated protein fails to function properly in the *aar* null mutant, suggesting that a different mechanism is acting. The observed phenotype may be explained by a reduction in the number of adherens junctions. The truncated protein may bind α-catenin, but not a *Dictyostelium* cadherin. This would mean that it would compete with the endogenous Aar protein for α-catenin. But, as it would be unable to bind cadherin it would not lead to more recruitment of actin to the adherens junctions, and hence this is not an overexpression phenotype. Instead this would prevent the correct formation of the adherens junctions through competition for one of the constituent proteins.

Using these results, a minimum length of the protein that is required for Aar's adhesion function can be defined; both from the *aar*- and wild type data (figure 4.11).

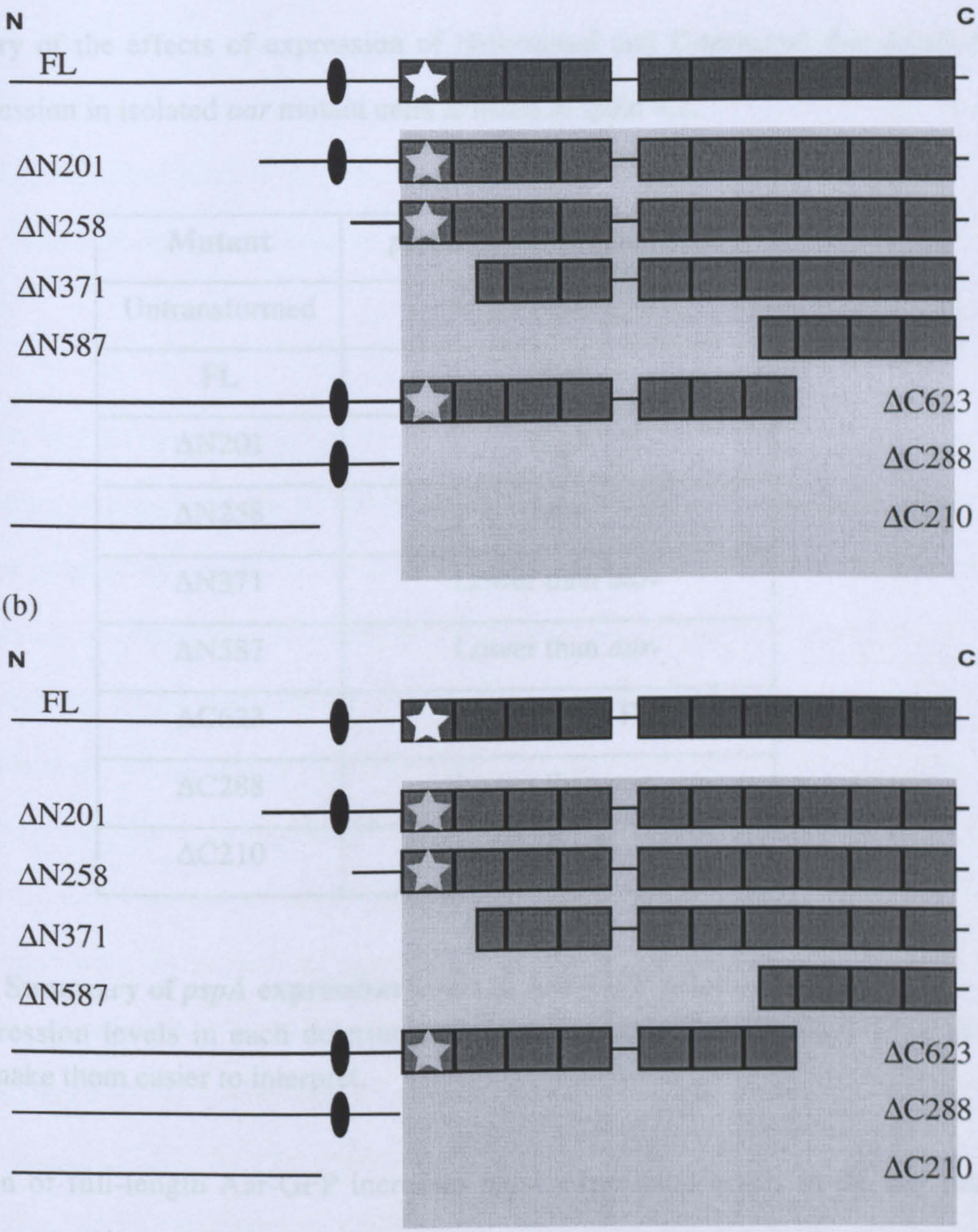

Figure 4.11 Summary of the morphology analysis of deletion mutants in both *aar*- and Ax2 backgrounds.

(a) *aar* mutant background: schematic of Aar deletions. FL = full-length. The shaded region of the protein denotes the minimum length of protein that rescues/ gives the over-expression phenotype in the *aar* mutant, with respect to morphology. This is determined by grouping all of deletions that fail to rescue.

(b) Wild type background: the shaded region of the protein denotes the minimum length of the protein that is required to give an *aar* over-expression phenotype in wild type cells, with respect to morphology. The mutants were grouped as in (a).

4.7.2 Aar and cell signalling

A summary of the effects of expression of N-terminal and C-terminal Aar deletions on *pspA* expression in isolated *aar* mutant cells is listed in table 4.2.

Mutant	*pspA* in *aar* mutant cells
Untransformed	Low
FL	High
ΔN201	High
ΔN258	Low
ΔN371	Lower than *aar*-
ΔN587	Lower than *aar*-
ΔC623	Higher than FL
ΔC288	Lower than *aar*-
ΔC210	Lower than *aar*-

Table 4.2 Summary of *pspA* expression levels in Aar-GFP deletion mutants
pspA expression levels in each deletion mutant are summarised in relationship to each other, to make them easier to interpret.

Expression of full-length Aar-GFP increases *pspA* expression levels in the *aar* mutant. Deletion of the N-terminus (ΔN201) did not prevent the increase and, in fact, led to greater levels of *pspA* expression. Deletion of the Aark phosphorylation sites (ΔN258) made a protein that was no longer able to rescue *pspA* expression. Further N-terminal deletions (ΔN371 and ΔN587), not only failed to rescue *pspA* signalling, but also reduced levels to below those observed with the *aar* mutant. These dominant negative effects on *pspA* expression, in the absence of Aar, suggest that a second Aar-like protein could be involved, or at least partially compensates in the *aar* mutant. This idea is further supported by the fact that *pspA* expression is not entirely lost in the *aar* mutant.

Figure 4.12 defines the minimum length of the protein that is required for Aar function, with respect to *pspA* expression. This shows that the region of the protein containing the Aark phosphorylation sites is required for full *pspA* expression. This hints that Aark phosphorylation of Aar may occur *in vivo* and, furthermore, may be required for *pspA* expression.

A reduction in the expression levels of *pspA* was associated with several of the Aar-GFP deletions when expressed in the *aar* null mutant. This could be an overexpression artefact. If Aar were to bind both negative and positive regulators of a the *pspA* signalling pathway, overexpression of certain deletion mutants could sequester out just the negative regulator, which would lead to an overload of the pathway. Conversely, the opposite could be true, and expression of certain deletion mutants could be leading to inhibition of the pathway by way of competing out a co-regulator of *pspA* expression. This second scenario could be explained by involvement of a second *Dictyostelium* catenin molecule in the *pspA* signalling pathway. In support of this, antisera raised to amino acids 5-304 of human plakoglobin recognises a 69 kDa protein in *aar*- whole cell lysates (Coates, 1999). Antiserum raised to the C-terminus of human plakoglobin does not cross-react with this protein, named DdPlako. In wild type cells, Aar may be the sole GskA downstream target in the *pspA* signalling pathway of wild type cells but, in the absence of Aar, a DdPlako could replace Aar in the *pspA* signalling pathway. Such cross-talk would not be unique to the *Dictyostelium* pathway. The functions of β-catenin and plakoglobin are not mutually exclusive. As examples, over-expression of plakoglobin induces axes duplication in Xenopus (Karnovsky and Klymkowsky, 1995) whilst β-catenin localises to the desmosomes in plakoglobin null-mutant mice (Bierkamp et al., 1999).

(a)

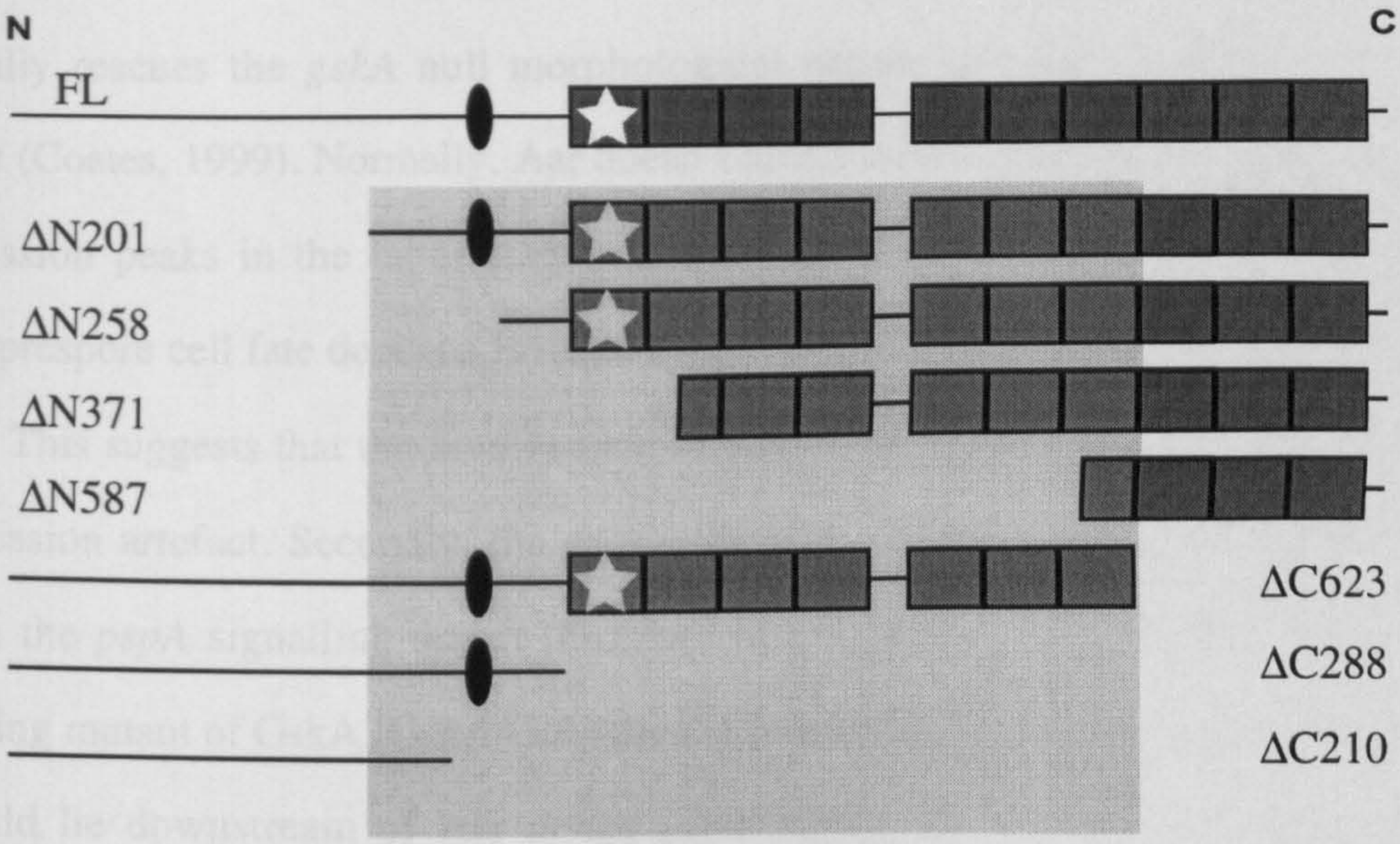

Figure 4.12 Summary of the *pspA* northern analysis of *aar* deletion mutants in the *aar* mutant background.

(a) Schematic of Aar deletions. FL = full-length. The shaded region of the protein is the minimum length required for full rescue of *pspA* signalling in the *aar* null mutant. The minimum length was determined by overlapping the mimum N-terminal deletion that still gives full rescue, with the minimum C-terminal deletion that still gives full rescue. As the ΔC210 mutant showed higher levels of *pspA* expression than the full-length protein, the last 3 Arm repeats were deemed to be in some way inhibitory. (The data for Ax2 mutants is excluded from this analysis, as results were not sufficiently reproducible).

Evidence for cross-talk already exists in *Dictyostelium* also. Firstly, the over-expression of Aar partially rescues the *gskA* null morphological phenotype, via a reduction of *ecmB* expression (Coates, 1999). Normally, Aar doesn't affect *ecmB* expression or stalk cell fate. *aar* expression peaks in the latter stages of development, whereas the GskA-mediated prestalkB:prespore cell fate decision is made much earlier, at the mound stage (Harwood et al., 1995). This suggests that the involvement of Aar in the GskA/prestalkB pathway is an over-expression artefact. Secondly, the over-expression of GskA in the *aar* mutant does not rescue the *pspA* signalling defect (Grimson et al., 2000), but over-expression of an Axin-binding mutant of GskA (GskA G/R) does (Fraser et al., 2002). One possibility is that GskA could lie downstream of Aar in the *pspA* signalling pathway, but given all the evidence that seems unlikely. No Axin-like protein has been discovered in *Dictyostelium* to date, but the fact that there is a phenotype associated with the expression of GskA G/R in *Dictyostelium*, it seems attractive to think that one may exist. Loss of binding to an Axin-like protein could allow GskA to interact with other substrates, which could include DdPlako.

Aark phosphorylation of Aar could be required for Aar binding to this possible Axin-like protein. GskA phosphorylation could then be required for activation of Aar. In this hypothesis, binding of cAMP to the cAR3 receptor may lead to activation of GskA and, in a multistep process, GskA and Aark phosphorylation would be required for activation of Aar. This activation would promote *pspA* expression. However, if the interaction between GskA and this possible Axin-like protein was lost, then GskA would become promiscuous and may activate other factors, which could include DdPlako.

Chapter 5

Overexpression of Aardvark

5.1 Introduction

Aark has been identified as a kinase that phosphorylates Aar at a defined site *in vitro*. Deletion of a short region of Aar that contains the site of Aark phosphorylation creates a protein that is no longer able to mediate *pspA* expression. Further N-terminal and C-terminal deletions of Aar have identified regions of the protein that are required for the correct morphology of the fruiting body. These sites are assumed to be binding sites that mediate the formation of adherens junctions. It was the aim at the outset of this chapter to examine the subcellular localisation of full-length Aar, and also its deletions, to further investigate the function of these possible interactions.

5.2 Aar-GFP cannot be visualised in living cells

As a control, unfused GFP was expressed from the actin15 promoter in *aar* mutant cells and examined by confocal microscopy. The GFP protein showed a diffuse pattern of fluorescence, suggesting no restriction of the GFP protein within the cell. As seen in many other cases, there was a slight enrichment in the nucleus (figure 5.1a). In contrast, examination of *aar*- Aar-GFP cells by confocal microscopy showed only background levels of fluorescence (figure 5.1b). Fixed wild type cells stained with anti-Aar antisera showed that endogenous Aar has a diffuse pattern of staining throughout the cytoplasm (figure 5.1c).

Several possible explanations exist to explain why the over-expressed protein cannot be detected. One reason could be that the transgene is not expressed. Northern analysis was used to address this question (figure 5.1d). Total RNA was isolated from both *aar* mutant cells and *aar* mutant cells transformed with pDXA-aar-gfp. Aar cDNA was used to probe the blot, and demonstrated the prescence of the transgene in transformed cells only.

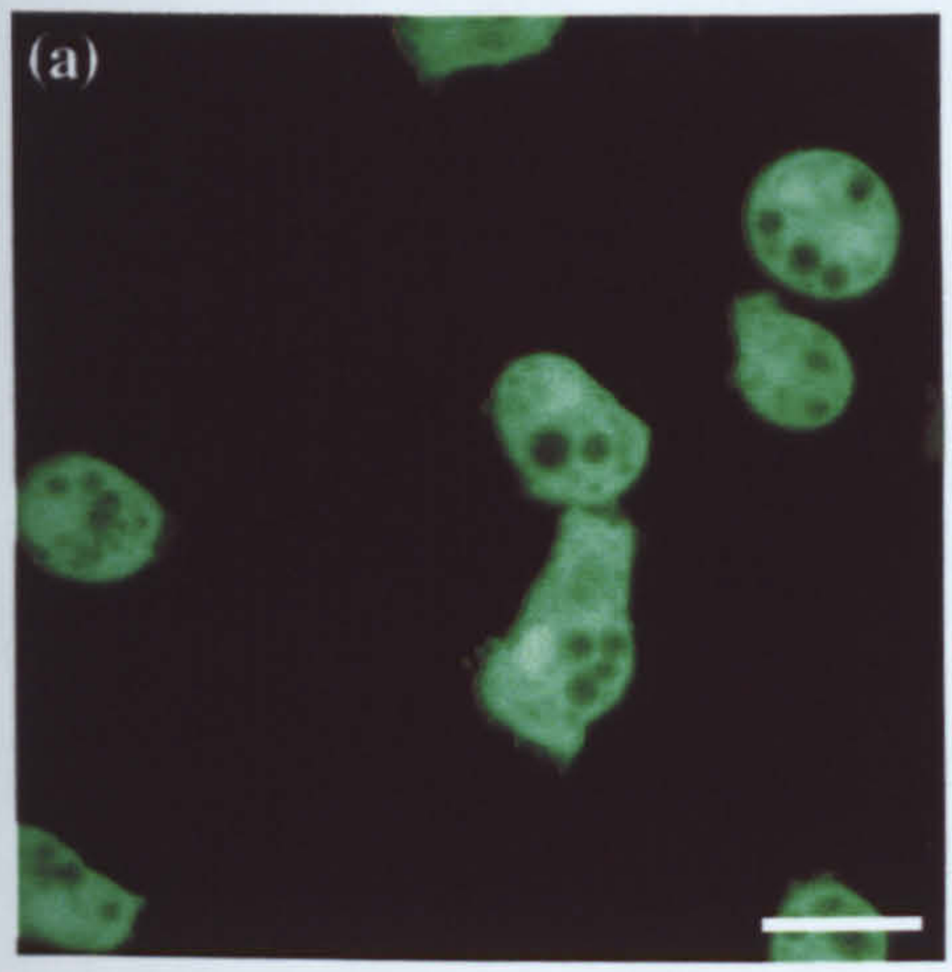

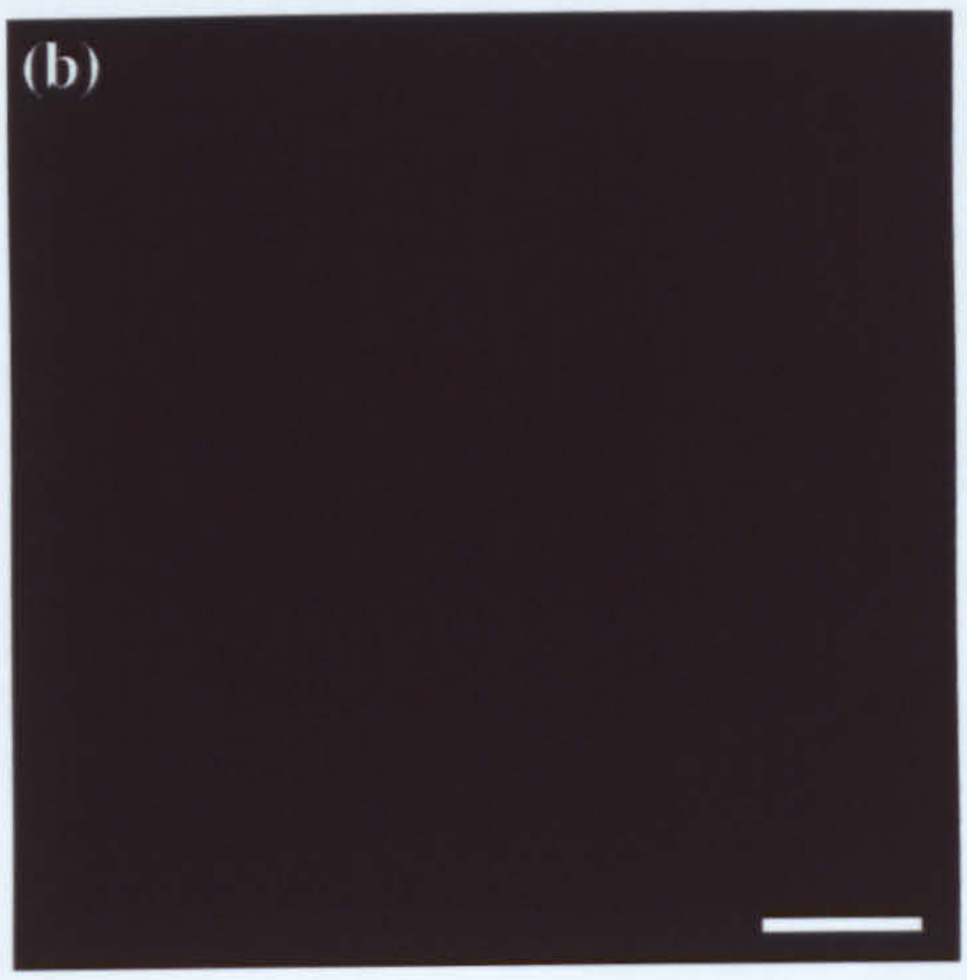

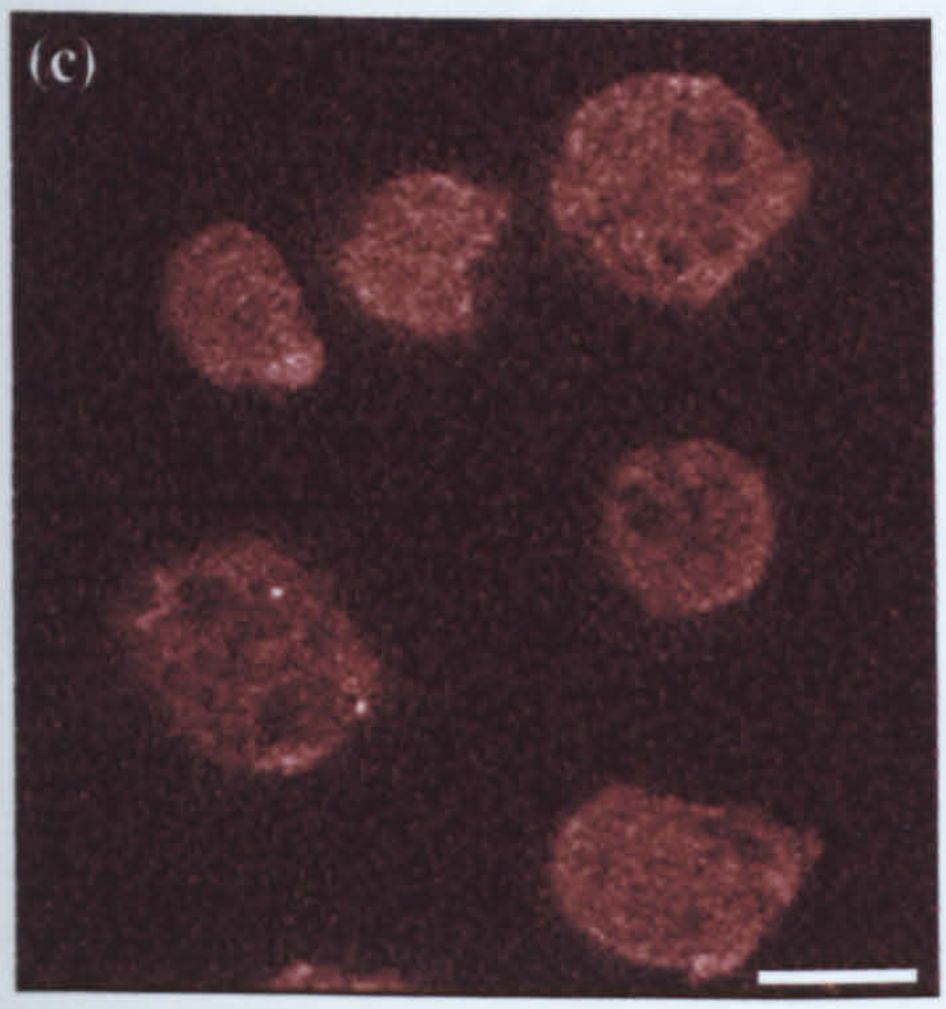

(d)

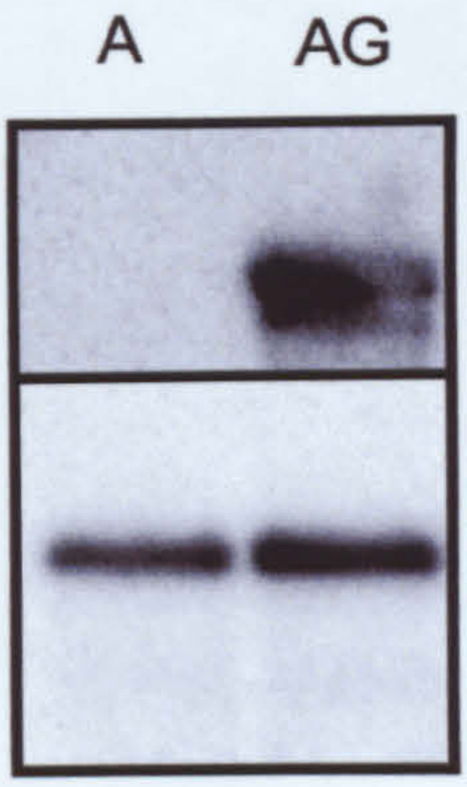

Figure 5.1 Expression of a full-length GFP-tagged version of Aar
(a) Confocal microscopy image of *aar-* cells transformed with GFP alone (false-coloured green)
(b) Confocal microscopy image of *aar-* cells transformed with pDXA-aar-gfp (false-coloured green)
(c) Anti-Aar anti-sera staining of wild type *Dictyostelium* (false-coloured red)
The scale bars in (a), (b) and (c) represent 10μm.
(d) Northern analysis to detect the expression of Aar-GFP. A = *aar-* cells, AG = *aar-* cells transformed with pDXA-aar-gfp
Top panel shows *aar-gfp* expression, whilst the bottom panel shows expression of the ubiquitously-expressed *Ig7* for comparison of loadings.

5.3 Expression of Aar-V5-His

As the *aar-gfp* mRNA was present, then it is possible that it was not translated. The use of anti-GFP antisera to detect the fusion protein failed due to the high level of non-specificity shown by the antisera towards whole cell lysates (data not shown). The GFP sequence of pDXA-aar-gfp was removed and replaced with a double tag comprising the V5 epitope and 6x His residues, making pDXA-aar-V5-his (figure 5.2). The V5 epitope facilitates easy detection of the protein, which could be purified via its 6x His tag on immobilised cobalt resin (Talon™, BD Clontech). The presence of this fusion protein in *aar* mutant cells was detected by western analysis. Figure 5.3a shows the presence of Aar-V5-His, present in the transformed cell lysate (AV), but absent in the untransformed *aar*- cell lysate (A).

Aar-V5-His is predicted to have a molecular weight of 88kDa. However, a second methionine residue, i.e., another putative translational start site, exists at the end of the additional N-terminal sequence that Aar posseses compared with β-catenin. The western blot analysis in figure 5.3 reveals that the cell must translate this additional sequence *in vivo*, as the size of Aar-V5-His appears to be approximately 88kDa. In addition to detecting the protein, the ability of Aar-V5-His to induce higher levels of *pspA* expression was demonstrated by northern analysis (figure 5.3b), showing that this fusion protein is functional, at least with respect to *pspA* signalling.

Figure 5.2 The 8.675Kb pDXA-aar-V5-his expression vector

The 861bp Amp^r gene allows for selection in bacteria, whilst the 831bp Neo^r gene allows for positive selection of eukaryotic transformants. The *Dictyostelium* origin of replication is also present for extrachromosomal expression.

(a)

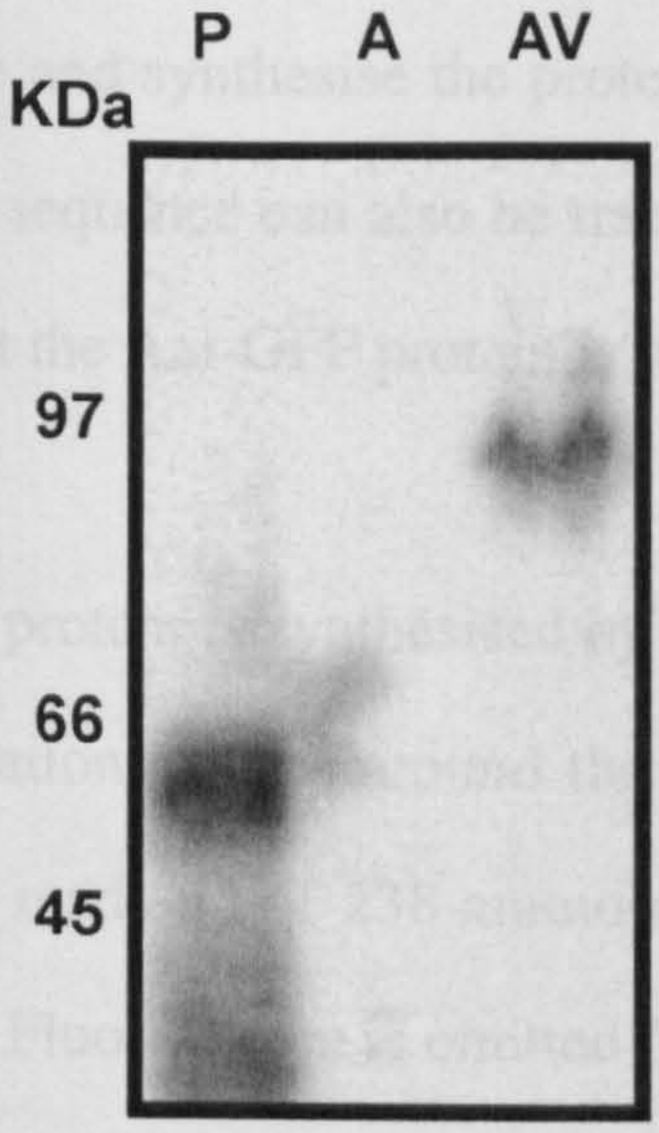

(b)

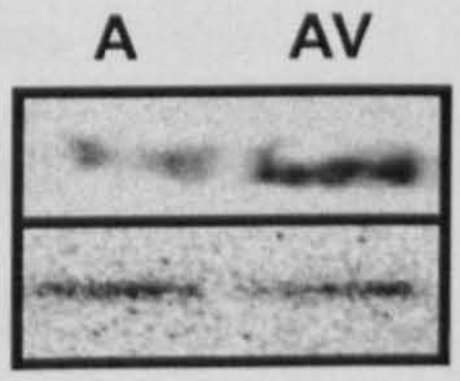

Figure 5.3 Expression of pDXA-aar-V5-his in the *aar* mutant

(a) Expression of Aar-V5-His can be detected in *aar*- cells by western blot analysis: P = positope positive control protein (53kDa), A = *aar*- cell lysate, AV = *aar*- Aar-V5-His cell lysate. Aar-V5-His has a predicted moleular weight of 88kDa.

(b) Northern analysis of *aar*- Aar-V5-His transformants shows that the protein is functional, as determined by an increase in *pspA* expression. A= *aar*- cells, AV= *aar*- Aar-V5-His cells. Top panel shows *pspA* expression. Bottom panel shows expression of the ubiquitously-expressed *Ig7*, included for comparison of loadings.

5.4 Aar-GFP is destabilised within the cell

Detection of unfused GFP by confocal microscopy demonstrated that the cells can translate the message and synthesise the protein. Likewise, the use of the V5-His tag demonstrated that the *aar* sequence can also be translated and the protein synthesised. This makes it very unlikely that the Aar-GFP protein is not being synthesised within the cell.

If Aar-GFP protein *is* synthesised by the cell, then why could no fluorescence be detected? One explanation centres around the intrinsic fluorescence of the GFP protein. The GFP molecule is made up of 238 amino acids arranged in one single polypeptide that is non-fluorescent. Fluorescence is emitted from an intrinsic chromophore formed by cyclisisation and oxidation of three adjacent amino acids (Ser-65, Tyr-66, Gly-67) (Cody et al., 1993). From the synthesis of the polypeptide to completion of the final fluorophore takes approximately 4 hours at 22°C *in vitro* (Cody et al., 1993). This presents two ways in which Aar-GFP fluorescence could be prevented. Firstly, the correct folding of GFP is of paramount importance to its fluorescence. In other words, any attachment to the protein that interferes with the protein's folding may either reduce or abolish fluorescence. It may be that the Aar-GFP fusion protein folds in such a way as to hinder the cyclisation and oxidation of amino acids 65-67 of GFP, thus affecting fluorescence. The successful GFP 'tagging' of armadillo repeat-containing proteins, however, has been described many times, which makes errors in folding an unlikely reason for the lack of fluorescence.

The second, and more likely scenario is that Aar is under tight post-translational control within the cell, such that the turnover of the protein is high. In mammalian cells, β-catenin is targeted for breakdown via the proteasome following GSK-3 phosphorylation. It is only upon Wnt stimulation of the cell that β-catenin is allowed to accumulate and induce expression of downstream genes. Aar-GFP may be subject to a similar mechanism of

control in *Dictyostelium*. This would mean that although Aar-GFP is expressed at high levels, each individual molecule is not present for a sufficient amount of time to produce the fluorophore and hence fluoresce. If this were the case, then western blot analysis should detect the protein. However, the poor specificity of the antisera when tested against *Dictyostelium* whole cell lysates made this difficult.

5.5 Is Aar-GFP under developmental regulation?

Both *aar* mutant and wild type cells expressing Aar-GFP were starved and allowed to develop for 24 hours. The resulting fruiting bodies were examined by epifluorescence UV microscopy. The level of fluorescence in Aar-GFP over-expressing cells was comparable to that of untransformed cells (figures 5.4a & c). Fluorescence could however, be detected in fruiting bodies of cells transformed with *gfp* alone (figure 5.4b). This suggests that even if Aar-GFP is under developmental regulation, the levels of protein are insufficient to be detected by these methods.

5.6 Expression of Aar-GFP in *fbxA- Dictyostelium*

As discussed in chapter 1, following GSK-3 phosphorylation, the F-box protein βTrcp binds β-catenin, thus targeting it for breakdown via the proteosome. At least one *Dictyostelium* βTrcp homologue, FbxA, exists. pDXA-aar-gfp (and pDXA-aar-V5-his as a positive control) were transformed into *Dictyostelium* cells null for *fbxA*. As with the *aar* mutant, Aar-GFP could not be detected by confocal microscopy (figure 5.5b). Northern analysis confirmed that the message was present (figure 5.5c). The presence of Aar-V5-his was confirmed by western blot analysis (figure 5.5d), which was consistent with the findings in the *aar* mutant. If Aar-GFP is subject to degradation within the cell, it would appear that it is via an FbxA-independent mechanism.

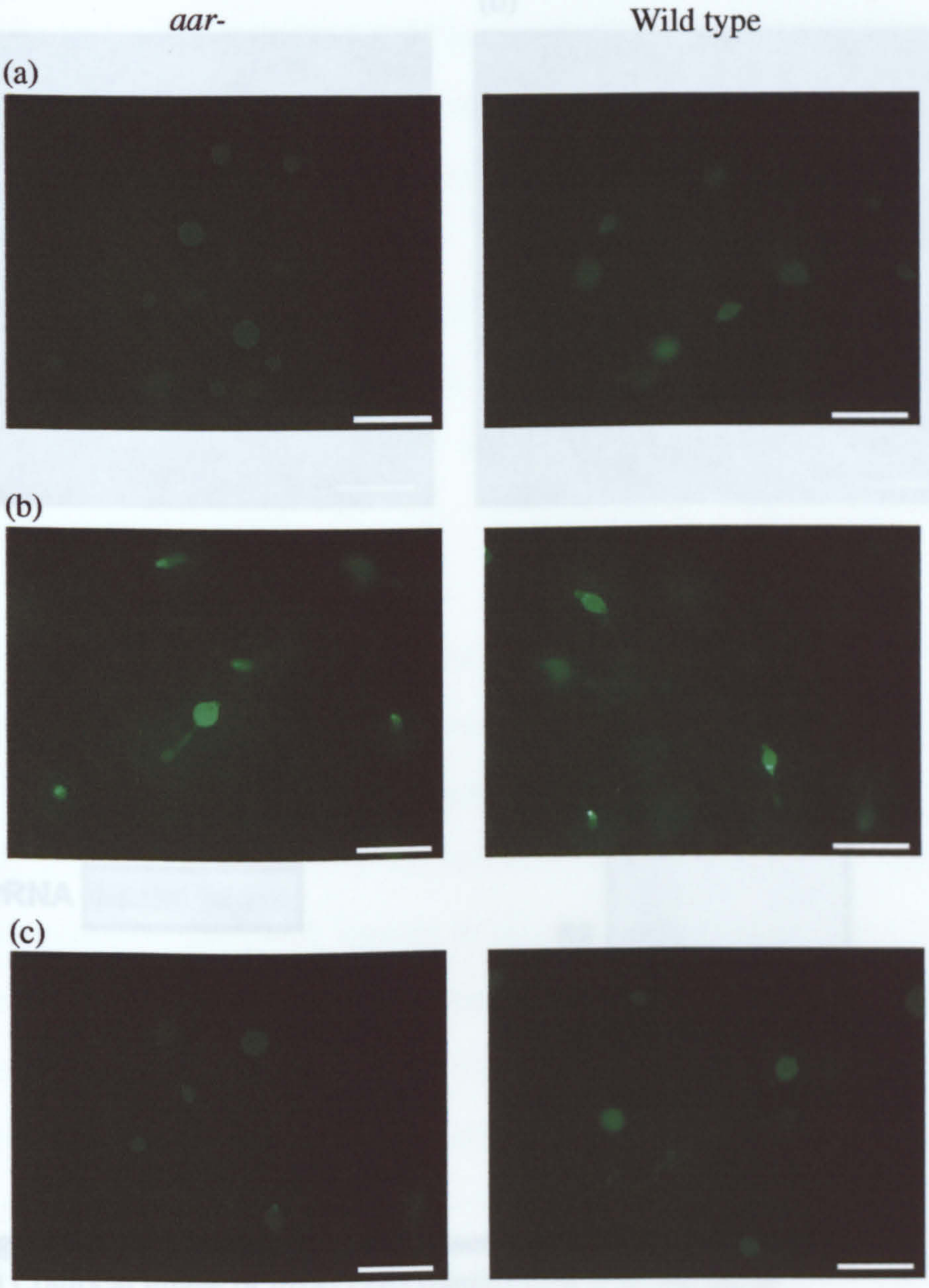

Figure 5.4 Development of Aar-GFP transformants
Cells were developed on nitrocellulose filters for 24h, and viewed under a UV dissecting microscope.
(a) Untransformed cells
(b) Cells transformed with *gfp* alone
(c) Cells transformed with pDXA-aar-gfp
Scale bar represents 0.5mm

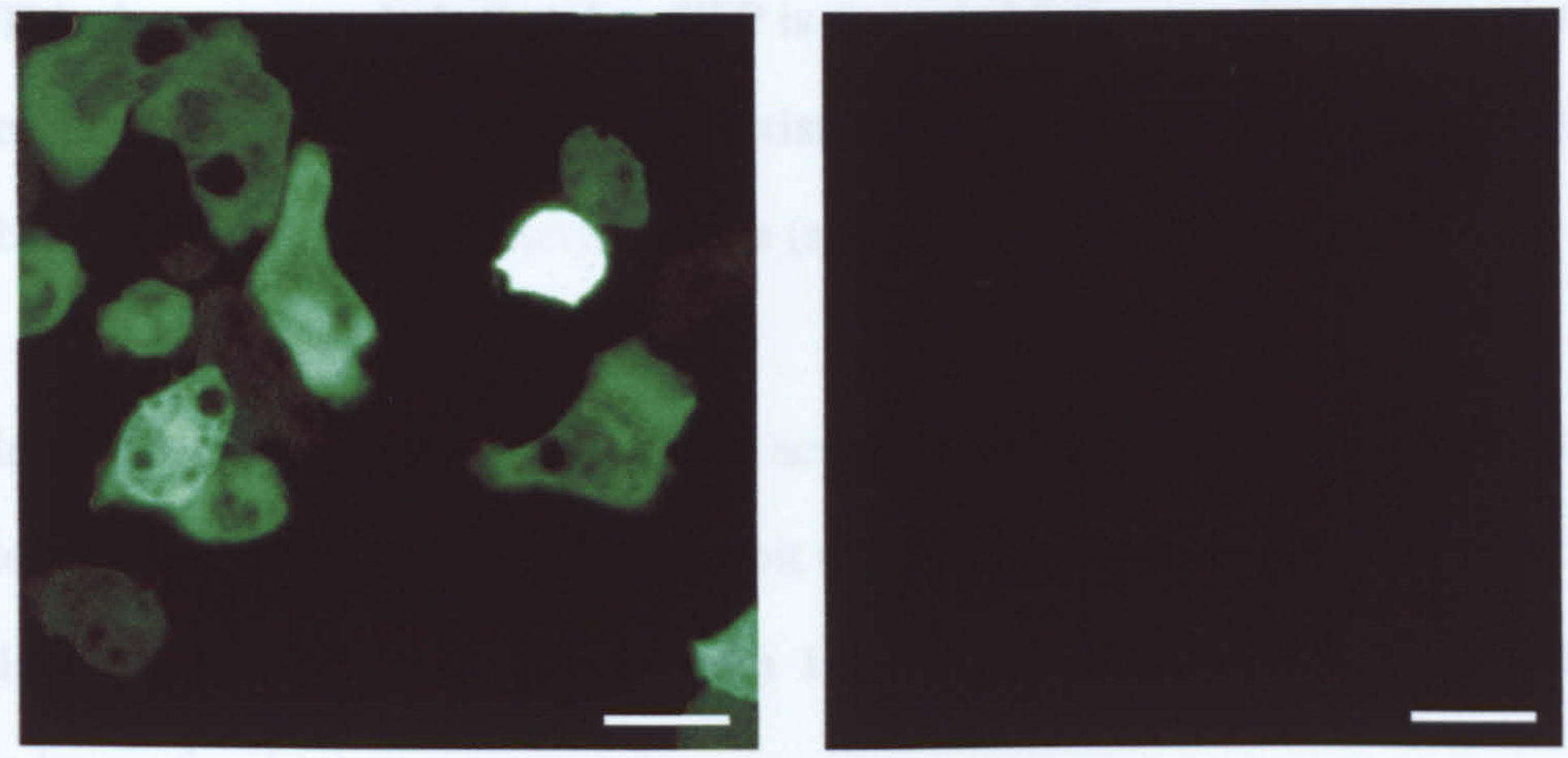

Figure 5.5 Detection of overexpressed Aar in *fbxA*- cells
(a) Confocal image of *fbxA*- cells transformed with *gfp* alone
(b) Confocal image of *fbxA*- cells transformed with pDXA-aar-gfp
Scale bars in (a) and (b) represent 10μm
(c) Northern analysis to detect *aar-gfp* message, F = *fbxA*- cells,
FG = *fbxA*- cells transformed with pDXA-aar-gfp. Top panel shows *aar* expression, whilst the bottom panel shows levels of the 28s rRNA subunit, shown for comparison of loadings.
(d) Western analysis to detect Aar-V5-his (predicted molecular weight of 88kDa) in *fbxA*- cells. P = positope positive control protein (53kDa);
F = *fbxA*- cell lysate; FV = *fbxA*- Aar-V5-his cell lysate.

5.7 Inhibition of GskA by treatment with lithium chloride

If Aar-GFP is broken down within cells, it would appear not to be via the F-box protein FbxA. This does not preclude that Aar-GFP is degraded following the binding of another F-box protein, as multiple F-box proteins exist in mammals, flies and plants and so more would be predicted to exist in *Dictyostelium* (see Kipreos and Pagano, 2000)

To address the question of whether GskA activity leads to Aar-GFP degradation, lithium chloride (LiCl) treatment was used to inhibit the kinase. *aar* mutant cells containing either GFP alone or Aar-GFP were treated with 10mM lithium chloride and viewed after 30 minutes by confocal microscopy.

Treatment of GFP-only transformants caused the cells to become more rounded, and also appeared to increase their fluorescence (figure 5.6). However, no difference in fluorescence was observed between the treated and untreated Aar-GFP transformants. This would suggest that inhibition of GskA does not stabilise Aar-GFP. This is also consistent with previous observations that GskA appears to act positively on Aar (Fraser et al., 2002; Grimson et al., 2000). On two independent occasions, however, a very small number (less than 1:100) of Aar-GFP fluorescent cells were detected (figure 5.7). The fluorescence within these cells was very diffuse, but was absent from a subcellular compartment with the appearance of the nucleus. Upon treatment of these cells with lithium chloride the fluorescence pattern changed, from diffuse to a more concentrated pattern, in the subcellular compartment that appears to be the nucleus. The same effect was not observed with sodium chloride controls or with treatment with IMPase inhibitors. This would suggest that this effect is due to the inhibition of GskA, and not the alternative LiCl target within the cell, which is IMPase. Unfortunately, it was not possible to repeat this experiment further, as no fluorescent cells have since been detected.

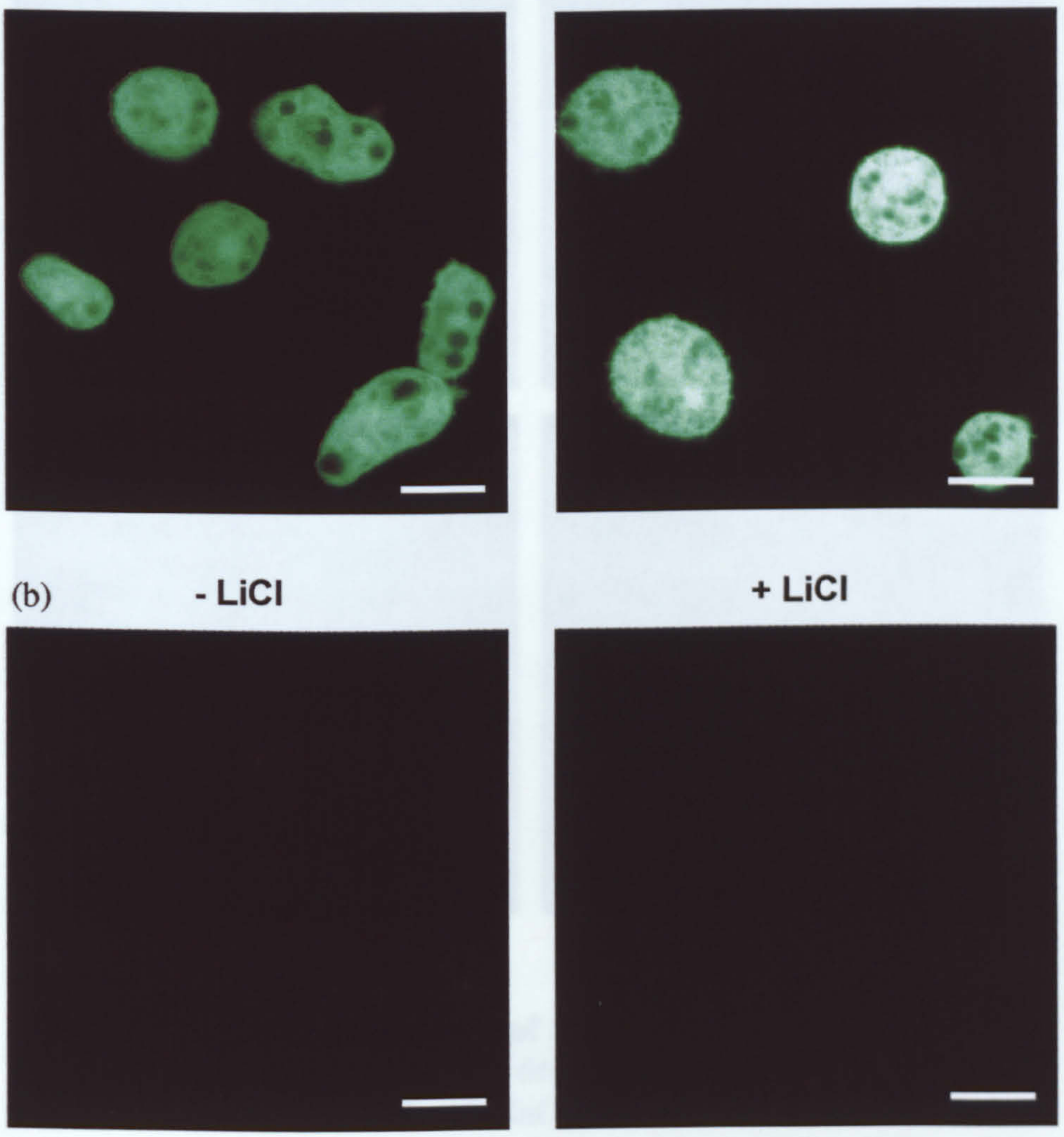

Figure 5.6 Inhibition of GskA by treatment with lithium chloride
Treatment of *aar*- cells transformed with pDXA-aar-gfp with 50mM LiCl for 30 minutes failed to restore fluorescence.
(a) *aar*- GFP only cells - note the increase in roundedness and fluorescence after treatment with LiCl.
(b) *aar*- Aar-GFP cells
Scale bar represents 10μm

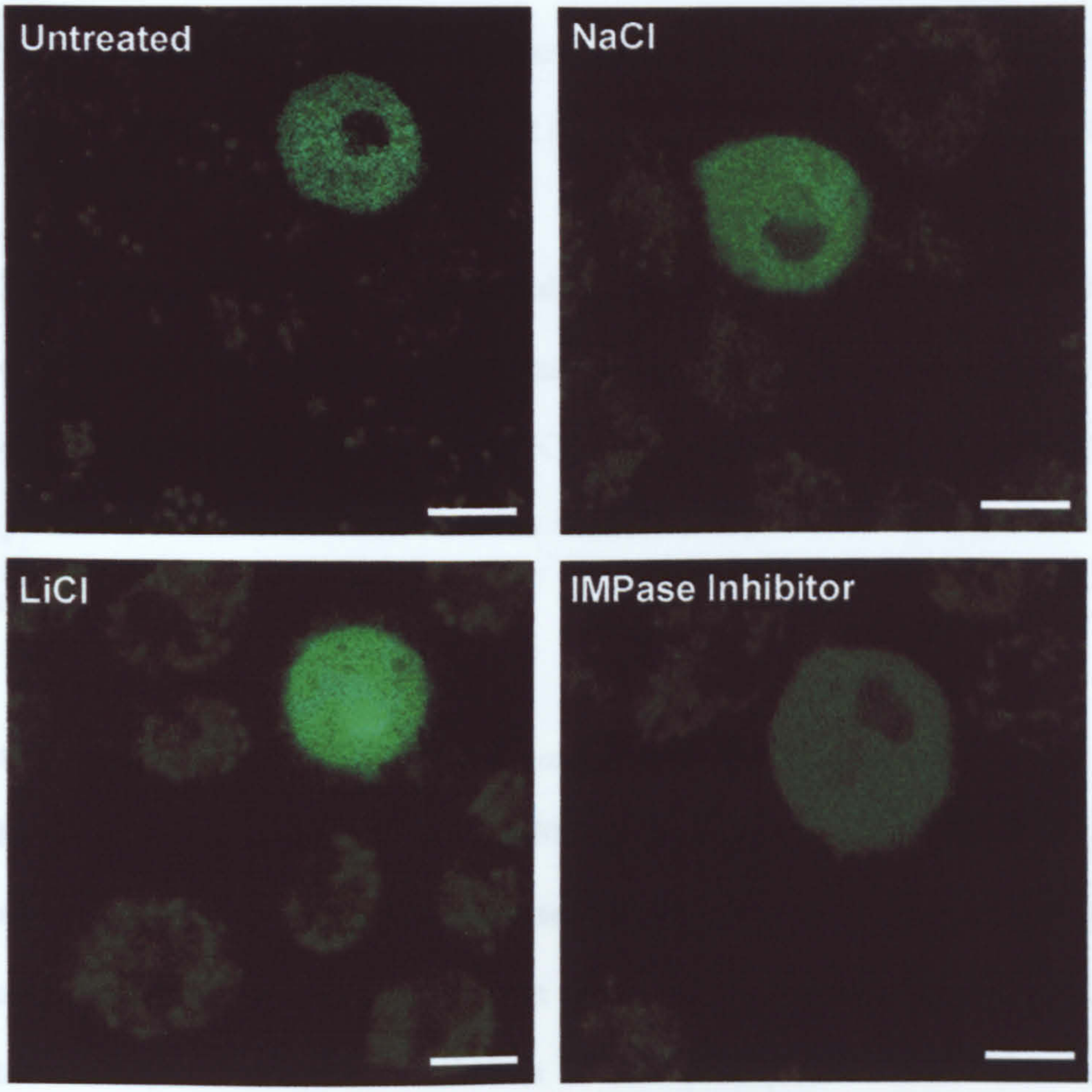

Figure 5.7 Nuclear translocation of Aar-GFP
Confocal microscopy was used to detect fluorescence of Aar-GFP cells. Untreated cells, cells treated with NaCl and cells treated with the IMPase inhibitor all showed a diffuse fluorescence pattern, with exclusion from what would appear to be the nucleus. Treatment with LiCl, led to the translocation of Aar-GFP to the nucleus. Scale bars represent 10μm.

5.8 Proteasome inhibition

The ubiquitin-proteasome pathway is responsible for the degradation of the vast majority of both short and long-lived proteins synthesised within the cell. Therefore, if Aar-GFP becomes degraded shortly after synthesis, it is highly likely that the proteasome is involved.

MG-132 is a potent, reversible, cell-permeable proteasome inhibitor (Tsubuki et al., 1996). The use of MG-132 to inhibit the proteasome in *Dictyostelium* has previously been described (Pukatzki et al., 2000). If Aar-GFP is degraded via the ubiquitin-proteasome pathway, then treatment of transformants with MG-132 would be expected to produce fluorescence.

aar mutant cells transformed with pDXA-aar-gfp were treated with MG-132 for 6 hours, to allow the protein to accumulate and the GFP fluorophore to form. In addition to Aar-GFP transformants, GFP only controls were also treated. Cells were viewed after 6 hours by confocal microscopy and cell lysates were produced for western blot analysis with anti-ubiquitin antisera. Successful inhibition of the proteasome leads to a build up of ubiquitinated proteins within the cell, seen as a smear on a western blot. Whilst the successful inhibition of the proteasome was observed (figure 5.8c), no fluorescence was detected in the Aar-GFP transformants (figure 5.8b). This would suggest that the sequence of Aar responsible for preventing fluorescence – the 'destabilisation motif' - leads to a conformation of the fusion protein that prevents the production of the GFP fluorophore. Alternatively, this sequence contains a degradation motif, responsible for targetting Aar-GFP for breakdown independently of the ubiquitin-proteasome pathway.

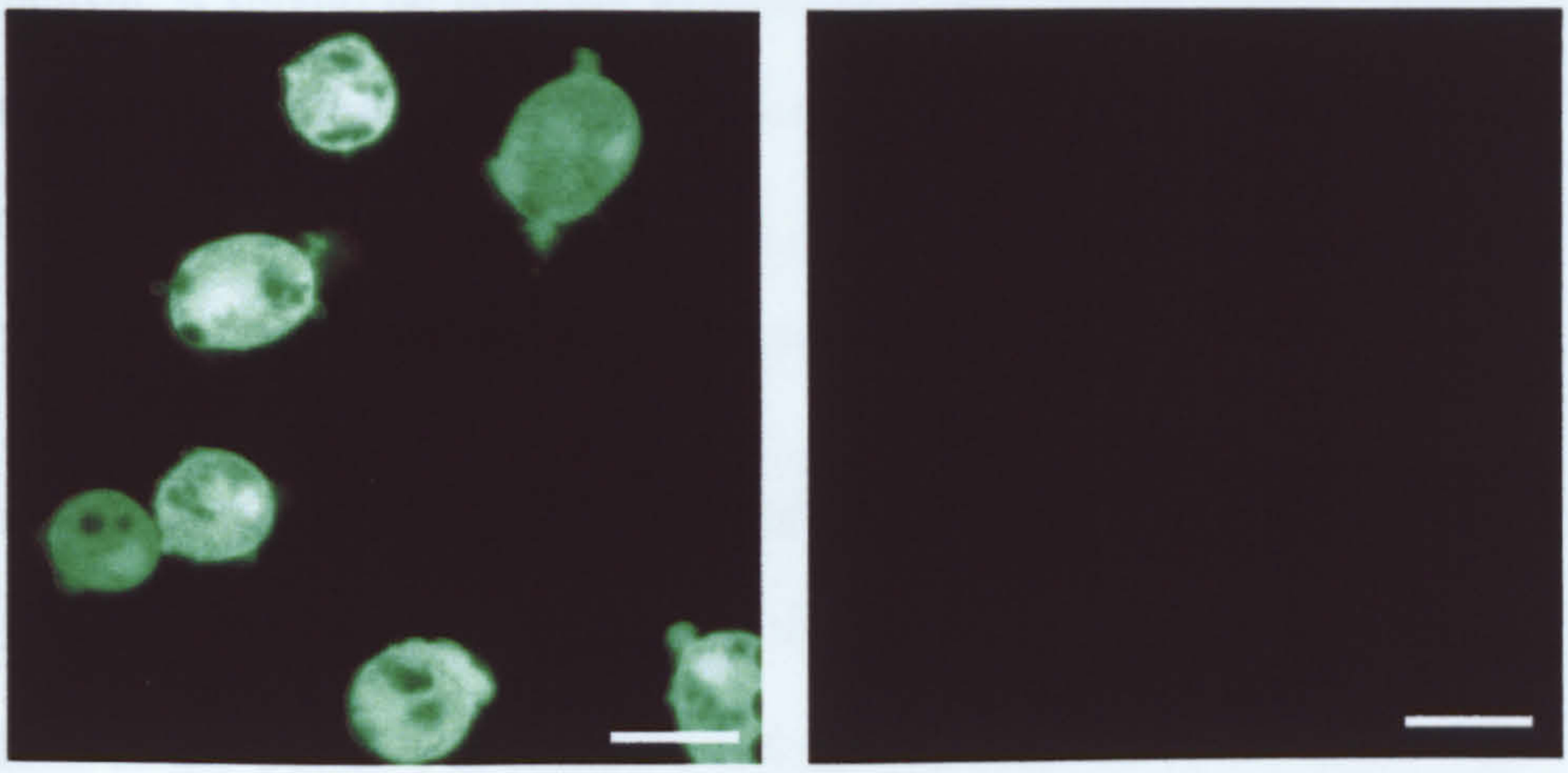

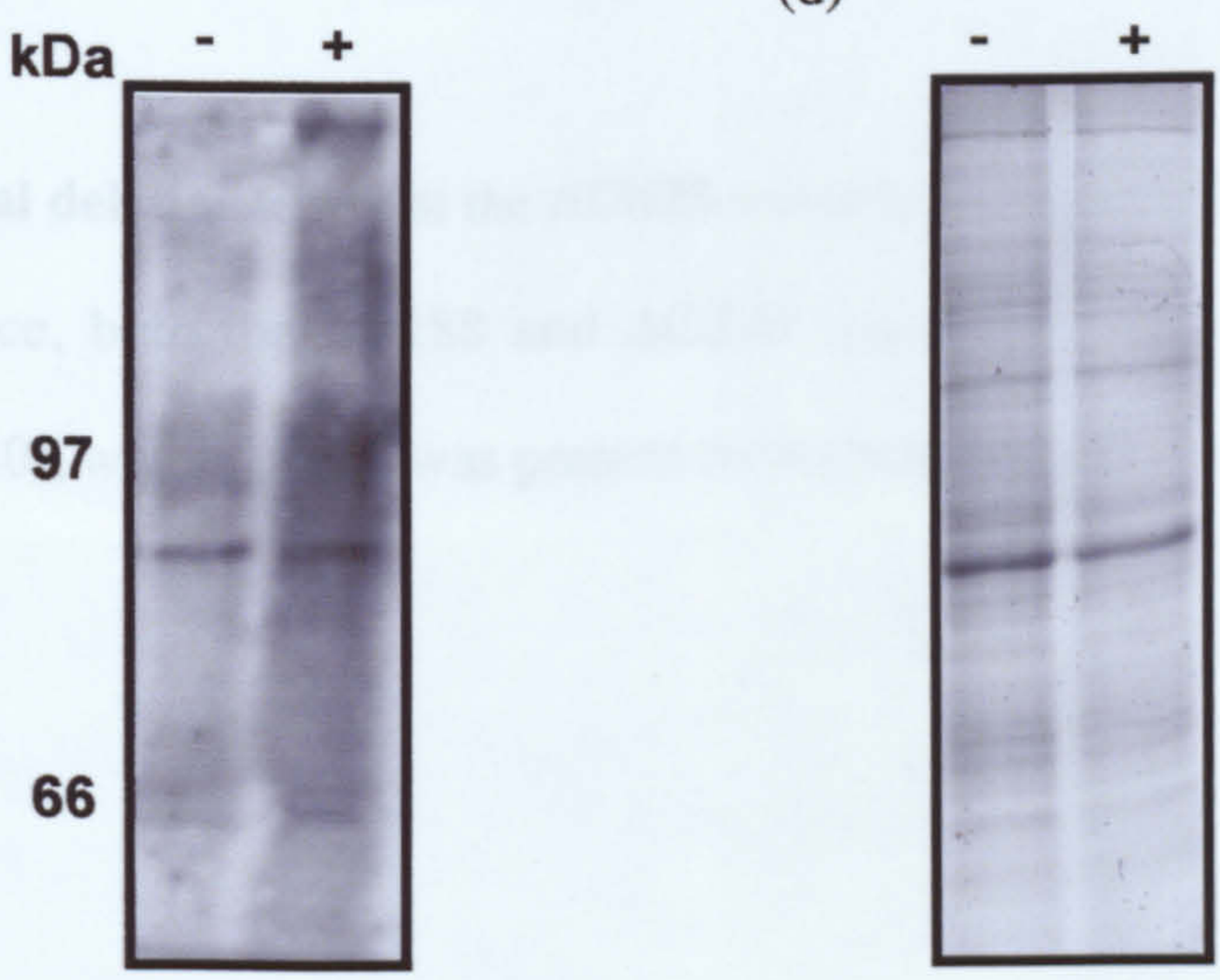

Figure 5.8 Treatment of cells with the proteasome inhibitor MG-132
Confocal microscopy was used to detect Aar-GFP
(a) *aar*- cells transformed with GFP alone
(b) *aar*- cells transformed with pDXA-aar-gfp
Scale bar represents 10μM
(c) MG-132-treated *aar*- Aar-GFP cell lysates, probed with anti-ubiquitin antibody. - = untreated, + = treated for 6h with 100μM MG-132
(d) Coomassie blue staining of a duplicate of the gel used in (c), to demonstrate equal loading.

5.9 Aar-GFP deletions in *aar* mutant cells

Direct evidence for Aar-GFP destabilisation remains elusive. However, if this is an active mechanism, it should be possible to identify a part of Aar that is responsible for protein destabilisation. To test this, confocal microscopy was used to examine the N-terminal and C-terminal Aar deletions (see chapter 4) at the subcellular level. Deletion mutants in both *aar* mutant and wild type backgrounds were examined.

N-terminal deletions: in *aar* mutant cells, no fluorescence was detectable with the ΔN201, ΔN258 and ΔN371 mutants (loss of the N-terminus, loss of the Aark phosphorylation sites and loss of the putative α-catenin binding site, respectively) (figure 5.9). However, the ΔN587 mutants (loss of arm repeats 1-7) displayed fluorescence comparable to the levels of the GFP-only transformants, which was present throughout the cell.

C-terminal deletions: whilst the ΔC623 mutants (deletion of the final 3 arm repeats) failed to fluoresce, both the ΔC288 and ΔC210 mutants showed high levels of fluorescence (figure 5.10), which, again, was present throughout the cell.

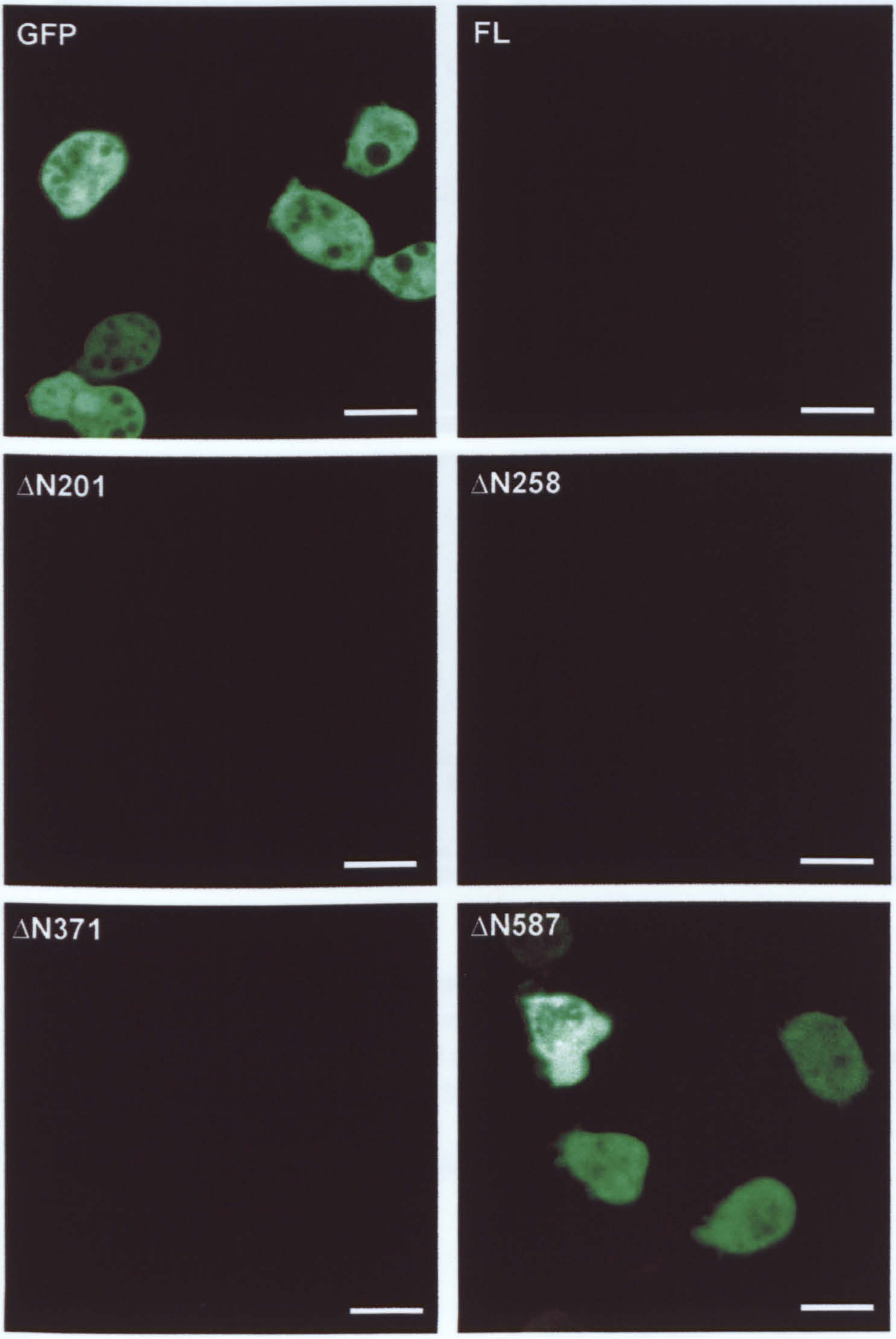

Figure 5.9 N-terminal deletions of Aar-GFP in the *aar* mutant
Confocal microscopy was used to detect fluorescence. The most C-terminal fragment of Aar (ΔN587) displayed GFP fluorescence. GFP = *aar*- cells transformed with *gfp* alone. FL = *aar*- cells transformed with full-length pDXA-aar-gfp. Scale bars represent 10μm.

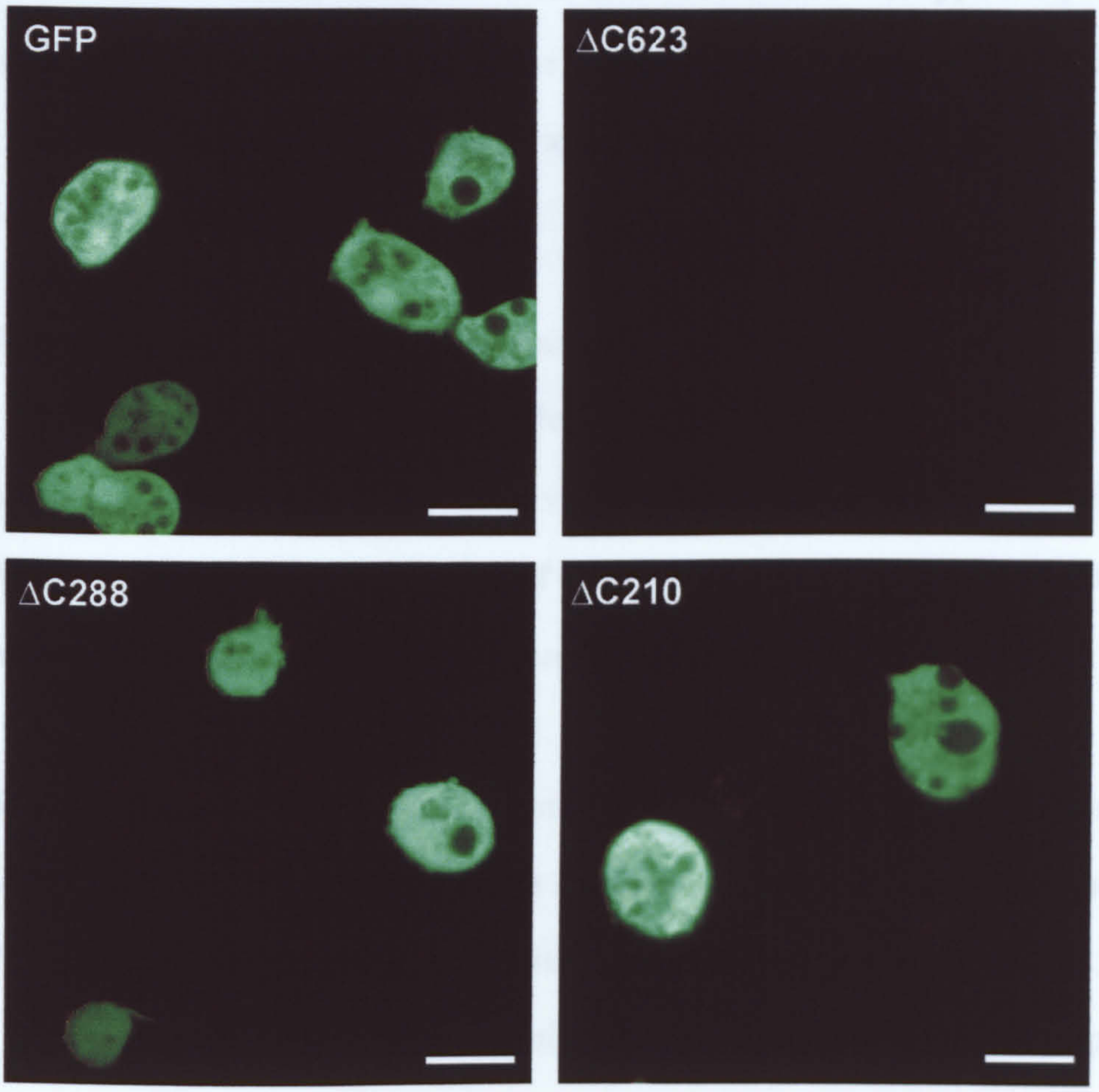

Figure 5.10 C-terminal deletions of Aar-GFP in the *aar* mutant

Confocal microscopy was used to detect fluorescence. Deletion of the final 3 arm repeats (ΔC623) had no effect on fluorescence, but further deletion of the C-terminus (ΔC288 and ΔC210) led to levels of fluorescence comparable with control cells. GFP = *aar-* cells transformed with *gfp* alone. Scale bars represent 10μm.

5.10 Aar-GFP deletions in wild type cells

The same deletions as used in section 5.9 were also examined in wild type *Dictyostelium*, to see if endogenous Aar has any effect on the localisation of the truncated proteins. As the anti-Aar antisera used in figure 5.1c was no longer available, the GFP tags were relied upon for further localisation studies.

N-terminal deletions: as with the *aar* mutant cells, no fluorescence was detectable in the ΔN201, ΔN258 and ΔN371 mutants (loss of the N-terminus, loss of the Aark phosphorylation sites and loss of the putative α-catenin binding site, respectively) (figure 5.11). However, the ΔN587 mutants (loss of arm repeats 1-7) again displayed fluorescence comparable to the levels of the GFP-only transformants.

C-terminal deletions: whilst the ΔC623 mutants (deletion of the final 3 arm repeats) failed to fluoresce, both the ΔC288 and ΔC210 mutants showed high levels of fluorescence (figure 5.12). Again, this was consistent with the results seen in the *aar* mutant. With the ΔC288 mutants, both diffuse cytoplasmic fluorescence and a punctate pattern of fluorescence were observed (figure 5.12).

By aligning the deletion sequences and comparing those which fluoresced, the boundaries of the minimum sequence that abolishes Aar-GFP fluorescence was determined (figure 5.13). This sequence makes up the putative 'destabilisation motif' of Aar.

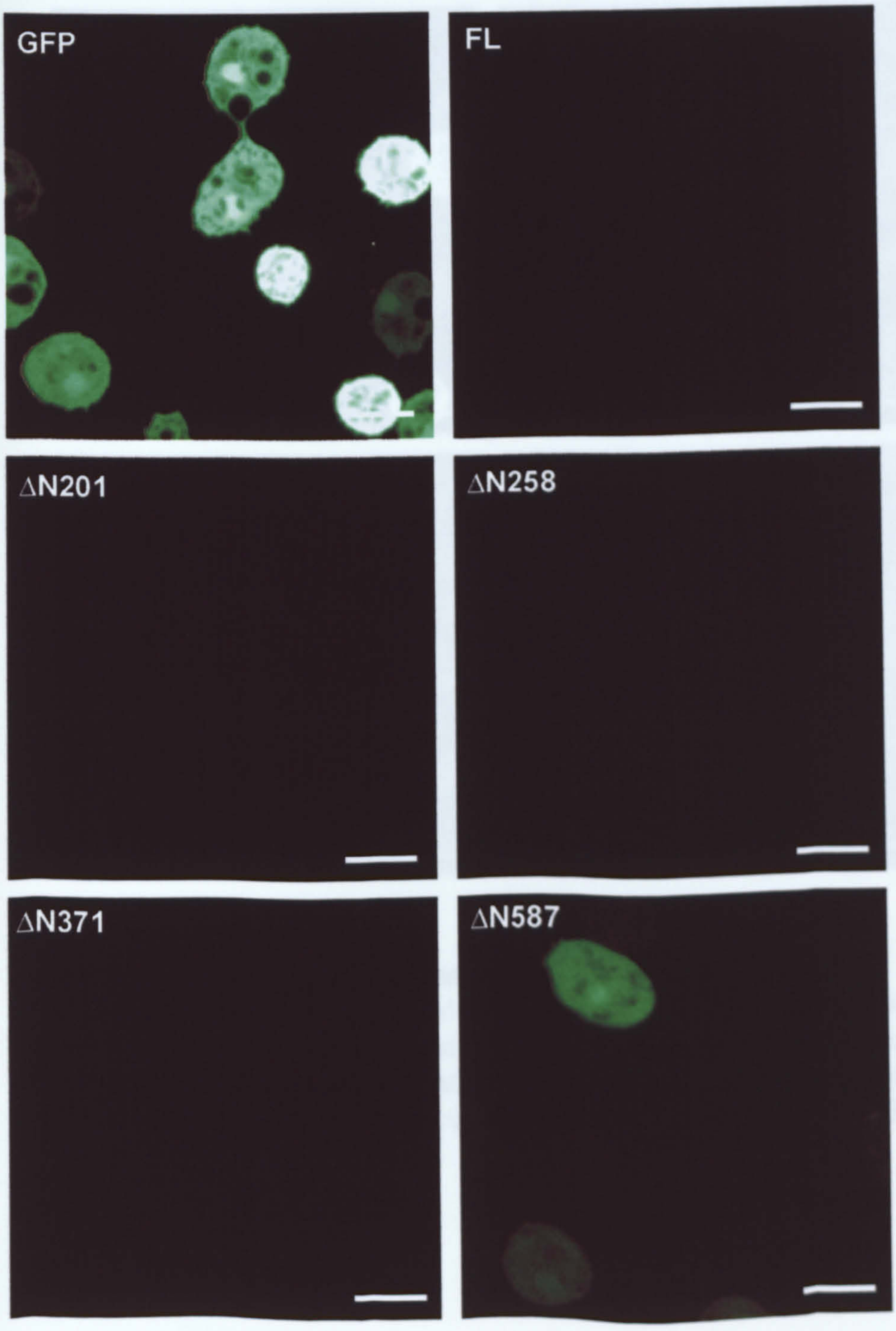

Figure 5.11 N-terminal deletions of Aar-GFP in wild type cells
Confocal microscopy was used to detect fluorescence. The most C-terminal fragment of aar (ΔN587) displayed GFP fluorescence. GFP = *aar*- cells transformed with *gfp* alone. FL = *aar*- cells transformed with full-length pDXA-aar-gfp. Scale bars represent 10μm.

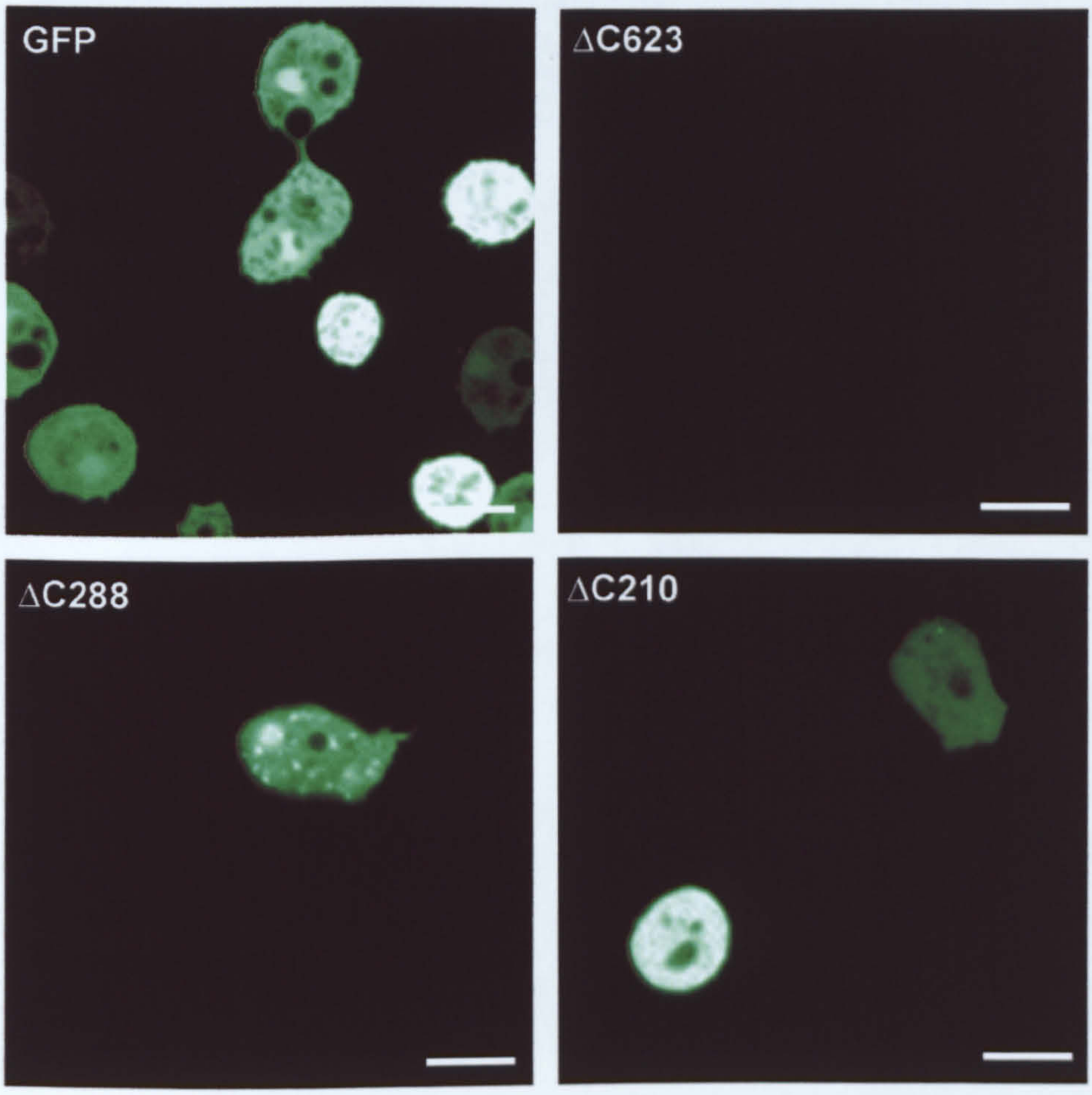

Figure 5.12 C-terminal deletions of Aar-GFP in wild type cells
Confocal microscopy was used to detect fluorescence. Deletion of the final three arm repeats (ΔC623) had no effect on fluorescence, but further deletion of the C-terminus (ΔC288 and ΔC210) led to levels of fluorescence comparable with control cells. GFP = *aar*- cells transformed with GFP alone. Scale bars represent 10μm.

(a)

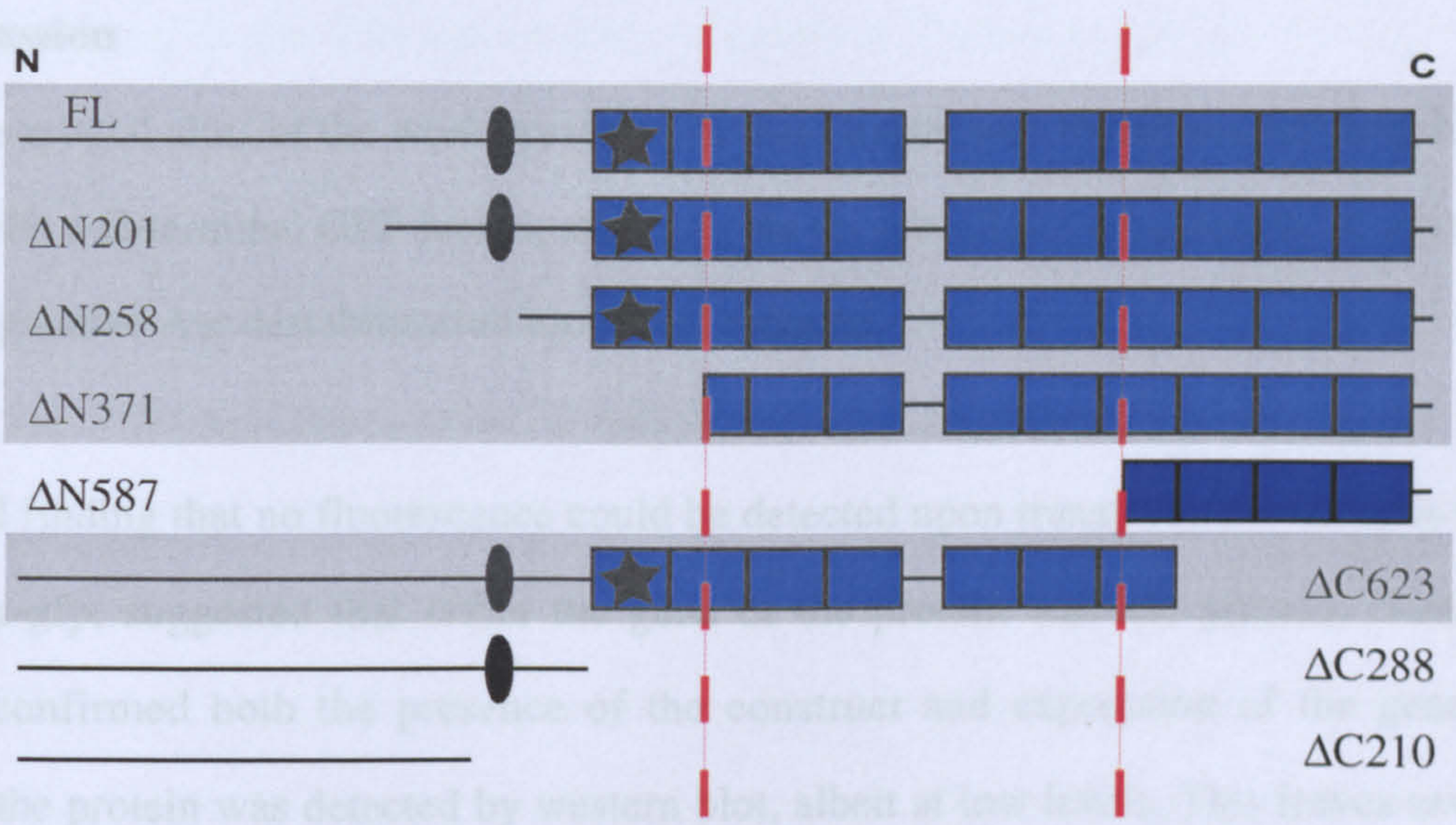

(b)

N-srwsnpts fqskmilcyi drlptdnykn fdksdesgqi kkiigvmnen
lhnpmilret cyilkrlsyr qrkedehesl iaryggisli lqamknhpyd
agvqedacga lgnltcdspn nmglysndny lsvveqggiq lilqamknhm
mnpgvqynts fvlrnlarnd vseskvaieg giqsiatamk nhpnhigiqt
qgcgalrnl-**C**

Figure 5.13 Defining the minimum sequence required for Aar destabilisation
(a) Full-length Aar and each deletion have been aligned. Those that fail to fluoresce have been shaded out. This allows the boundaries of the destabilisation sequence to be defined (broken red lines).
(b) Amino acid sequence of the 'destabilisation motif' of Aar.

5.11 Discussion

One of the crucial aims of the work presented in this chapter was to express full-length Aar protein, with a C-terminal GFP fusion, and examine its subcellular localisation. In trying to do this, a putative Aar destabilisation motif was mapped.

The initial finding that no fluorescence could be detected upon transformation of cells with pDXA-aar-gfp, suggested that either the gene or the protein was not present. Northern analysis confirmed both the presence of the construct and expression of the gene. In addition, the protein was detected by western blot, albeit at low levels. This leaves several possible explanations as to why a GFP fusion protein could be expressed, yet fluorescence not be detected. Each explanation is individually addressed below.

- The GFP polypeptide is not being synthesised correctly, i.e. there are mutations in the DNA construct which lead to a truncated protein. The entire length of the *aar-gfp* gene was sequenced commercially, and the use of DNA analysis software showed that no mutations were present. There is no reason to believe that the sequence of the transgene does not correctly encode for an Aar-GFP fusion.
- A part of the *aar-gfp* mRNA sequence inhibits its own translation. Several factors argue against this being the case. Firstly, the Aar over-expression morphology is observed when cells containing pDXA-aar-gfp are allowed to develop. Secondly, the detection of Aar-V5-his by western blot and the detection of GFP alone by confocal microscopy proves that both the *aar* and *gfp* sequences can be translated. There is no reason why the combination of *aar* with *gfp* should lead to a great reduction in the levels of protein that are synthesised within the cell.
- As the evidence presented so far suggests that Aar-GFP is, in fact, synthesised by the ribosomes at the normal rate, then another explanation is that the GFP protein is incorrectly folded due to the Aar fusion. The intrinsic fluorescence of GFP relies on the

correct folding of the 238 amino acid polypeptide. Following correct folding, three adjacent amino acids (Ser-65, Tyr-66, Gly-67) become cyclisised and oxidised to form the fluorophore. This process takes up to 4 hours *in vitro*. The possibility of incorrect GFP folding cannot be ruled out from the evidence presented in this chapter. However, successful GFP tagging of other arm repeat-containing proteins has previously been reported (Giannini et al., 2000; Miller and Moon, 1997; Mimori-Kiyosue et al., 2000; Oda and Tsukita, 1999).

- Degradation of Aar-GFP is the remaining explanation for a lack of fluorescence in transformed cells. Several reasons for this may exist. Firstly, the structure of the Arm repeats is α-helical. It may be that some of the deletions disrupt the secondary structure of Aar in such a way as to compromise the protein's folding. This could lead to the protein become degraded. The secondary structure of the protein may possibly not be compromised. In which case, either an insufficient level of Aar-GFP within the cell, or a turnover rate high enough to leave GFP with insufficient time to fold correctly, would prevent fluorescence. β-catenin is under tight post-translational regulation, targeted for breakdown via the proteasome, following GSK-3 phosphorylation and binding of the F-box protein, βTrcp. Expression of Aar-GFP in a strain null for the *Dictyostelium* F-box protein, FbxA, failed to produce fluorescence. Other *Dictyostelium* F-box proteins may exist, and so this method of degradation cannot be ruled out. Inhibition of GskA, the *Dictyostelium* GSK-3 homologue also failed to yield Aar-GFP fluorescence. However, some evidence has been presented which suggests that the inhibition of GskA may lead to a change in the subcellular localisation of Aar-GFP (see chapter 6 for further discussion).

One unexpected finding was the punctate pattern of fluorescence observed when the ΔC288 mutant was expressed in a wild type background. This may be have simply been an over-expression artefact. The spots may represent aggregates of the fusion protein, formed due to

the high levels of protein within the cell, or they could represent the fusion protein localising to the lysosomes, as part of a degradation pathway, again brought about by the high levels of protein present within the cell.

Two plant β-catenin homologues exist in *Arabidopsis thaliana*, Arabidillo-1 and Arabidillo-2 (for 'Arabidopsis Armadillo'). Interestingly, no fluorescence is detected when C-terminal GFP fusions of either are over-expressed in *Arabidopsis* (J. C. Coates, pers. commun.) Both of these proteins contain F-box motifs at their N-terminus. This would suggest these proteins do not require binding of an F-box protein to be targeted by the E3 ubiquitin ligase. On closer inspection of the amino acid sequence, an N-terminal F-box domain can also be found in Aar. However, the ΔN371 truncation lacks the F-box motif, yet does not fluoresce. It may be that both the F-box domain and another site are required for targetting to the E3 ubiquitin ligase. Whatever the case, elucidation of the mechanism of Aar destabilisation should provide further insight into the regulation of this important class of molecule.

Chapter 6

Discussion

6.1 Aims of work

It was the aim of this thesis to answer the following questions:

- Does GskA directly phosphorylate Aar?
- What physiological roles can be assigned to the various features of the Aar sequence?
- What does the subcellular localisation of Aar reveal about Aar protein function?

6.2 Does GskA directly phosphorylate Aar?

The studies presented in this thesis failed to demonstrate that GskA directly phosphorylates Aar. Peptides based upon the putative N-terminal GSK-3 phosphorylation sites of Aar turned out not to be substrates for GSK-3 or GskA *in vitro*. It may be that these sites become better substrates when presented to the kinase as part of the whole protein, or it may be that other proteins need to be in association in order for GskA to phosphorylate Aar *in vivo*. However, recent evidence suggests that Aar is a substrate for GskA, but that it is phosphorylated at alternative sites to those in the N-terminus (W. J. Ryves, unpublished data).

Whilst investigating the phosphorylation of Aar by GskA, a novel, priming-dependent, serine/threonine protein kinase, which phosphorylates Aar at the putative N-terminal GSK-3 sites *in vitro*, has been discovered. This kinase was subsequently named Aark, for Aardvark kinase. Aark has an apparent molecular weight of 30-35kDa. The K_m value for its interaction with Aar-P1 was calculated at 365µM. This figure is high, but it may be that scaffold proteins and/or other additional factors are required for Aark phosphorylation of Aar *in vivo*. Although Aark phosphorylates Aar *in vitro*, it cannot be concluded that Aark phosphorylates Aar *in vivo*, and the high K_m value does not support this. However, deletion of a small region of Aar containing the Aark phosphorylation sites effects the physiological function of the protein (see section 6.4). This suggests that Aark phosphorylation may be

required for proper Aar function. Creating a knockout of Aark in *Dictyostelium* would provide a simple route to determining this.

Due to the priming-dependency of Aark, CK1 was a potential candidate. However, CK1 did not phosphorylate the Aar peptides tested *in vitro*, and the size of Aark differs greatly from that of CK1 isolated from *Dictyostelium*. A closer examination of the Aar amino acid sequence surrounding the Aark recognition site shows conservation with the CK1 peptide substrate CKI-P. This conservation is missing from Aar-P1, suggesting that Aar may be a substrate for CK1 *in vivo*, but that Aar-P1 is not. The phosphorylation site of Aark was determined: S-X-**S**-X-T(Phos), with the Ser residue in bold being the phosphate acceptor. This site differs from both the recognition site of GSK-3 and that of CK 1. Therefore Aark represents a novel serine/threonine protein kinase, which shows a preference for phosphate-primed substrates.

A GSK-3-like kinase (GLK) has been discovered in the *Dictyostelium* genomic database and shows conservation of the Arg-96, Arg-180, Lys-205 residues which determine the priming-dependency of GSK-3 substrates (Dajani et al., 2001; Harwood, 2001). The cloning of GLK may provide a short route to the identification of Aark. GLK does not show conservation of the Axin-binding domain, so if Aark is GLK, then it would be expected to phosphorylate Aar in an Axin-independent manner. It is important to note that only circumstantial evidence exists to support the presence of an Axin-like protein in *Dictyostelium*, as none have been discovered to date.

This work has shown that Aark is able to phosphorylate Aar peptides *in vitro*. This does not mean that Aar is necessarily a substrate for Aark *in vivo*. Of course, if GLK does turn out to in fact be Aark, then it will be relatively simple to determine whether the interaction of Aark with Aar is a true one. A simple way to show this would be to take cell extracts of

GLK mutants and test them for kinase activity towards Aar in the *in vitro* kinase assay, as in section 3.5 of this thesis. Expression of an Aar protein with mutated Aark phosphorylation sites may be expected to exhibit a similar phenotype to the GLK null mutant, if Aark is GLK and Aar lies downstream of the latter.

Another way to investigate whether a physiological role can be assigned to the phosphorylation of Aar by Aark, is to express deletion mutants of Aar, some of which lack the Aark phosphorylation sites. This approach was taken since it had the added advantage of being able to potentially assign functions to other regions of the protein in addition to the Aark phosphorylation sites.

6.3 What physiological roles can be assigned to the various features of the Aar sequence?

A number of N-terminal and C-terminal deletions of Aar-GFP were made and expressed in both the *aar* null mutant and wild type cells. Expression of these truncated proteins was determined by both northern and western analyses. The levels of mRNA detected for each of the mutants varied considerably, and coincidently some of the higher expressors had more drastic phenotypes than the lower expressions. This is coincidental, since the western analysis showed that the protein levels did not reflect the mRNA levels detected. It would thus appear from this work, that Aar is subject to post-translational control, and that certain deletion mutants are able to evade this control (see section 6.4).

Cell-cell adhesion

Deletion of the putative α-catenin binding site prevents both the rescue of the *aar* null mutant morphology and the Aar over-expression phenotype. This suggests that this region of the protein is important for the adhesive function of Aar. This is consistent with amino acids 301-331 of Aar being the binding site for α-catenin and an α-catenin/vinculin-like

protein has recently been cloned in *Dictyostelium* (T. Soldati, pers. commun). For the role of Aar in the formation of adherens junctions to be like that of its mammalian counterpart, a site for the binding of the C-terminus of cadherin would also be needed. Deletion of the final three Arm repeats of Aar created a protein that was unable to rescue the *aar* mutant, and hence further deletions were also unable to rescue. It could be that the last three Arm repeats are required to bind to a cadherin-like molecule, although no such protein has identified in *Dictyostelium* to date. The two sites could be used as bait to identify these respective binding proteins in a yeast two-hybrid screen.

Cell signalling

Deletion of the region of Aar containing the Aark phosphorylation sites made a protein that was no longer able to rescue *pspA* expression. Further N-terminal deletions not only failed to rescue *pspA* signalling, but also reduced levels to below those observed with the *aar* mutant. Some dominant negative effects were also observed in wild type cells, once the Aark phosphorylation sites had been removed from Aar, but these results were unclear. Dominant negative effects on *pspA* expression, in the absence of Aar, suggest that a second Aar-like protein could be involved, or at least can partially compensate in the *aar* mutant. This idea is further supported by the fact that *pspA* expression is not entirely lost in the *aar* mutant. A plakoglobin homologue has been discovered in *Dictyostelium*, and would be a good candidate for this second Aar-like protein.

As loss of the region of Aar containing the Aark phosphorylation sites prevents Aar rescue of *pspA* signalling in the *aar* mutant, suggesting that these sites may be required for Aar function *in vivo*. GskA activity is also known to be required for *pspA* expression, and it may be that Aark phosphorylation is required for the GskA-Aar interaction. The second site of Aar that was discovered to be important for *pspA* expression may be required for the

binding of Aar to a transcription factor, or maybe a transporter protein, which would direct Aar to or from the nucleus.

To gain a greater insight into what each of the regions of the protein that are now deemed important for Aar function, localisation studies were pursued.

6.4 What does the subcellular localisation of Aar reveal about Aar protein function?

In order to examine the subcellular localisation of Aar, a C-terminal GFP fusion was added to the protein, before expression in both the *aar* mutant and wild type cells. This work led to the observation that Aar may contain a destabilisation motif within its Arm domain.

Following transformation of cells with pDXA-aar-gfp, no fluorescence could be detected. This suggested that either the gene or the protein were absent. Northern analysis confirmed both the presence of the DNA construct and expression of the gene, leaving four possible explanations as to the lack of fluorescence:

- Incorrect synthesis of the polypeptide.
- Failure to translate the mRNA sequence.
- Incorrect folding of the fusion protein.
- Degradation of the fusion protein.

Sequence data showed that there was no reason to believe that the Aar-GFP polypeptide was being incorrectly synthesised. An over-expression phenotype was associated with the expression of pDXA-aar-gfp, Aar-V5-His could be detected by western blot and fluorescence of GFP alone could be detected. This shows that the cell is able to translate both the *aar* and *gfp* sequences and so there should be no reason why a fusion of the two can not be translated. The possibility of incorrect GFP folding cannot be ruled out from the

evidence presented in chapter 5, but successful GFP tagging of other Arm repeat-containing proteins has previously been reported, suggesting that Aar folding does not affect the fluorescence of GFP (Giannini et al., 2000; Miller and Moon, 1997; Mimori-Kiyosue et al., 2000; Oda and Tsukita, 1999).

The most probable explanation for the lack of fluorescence associated with Aar-GFP transformants is degradation. Either an insufficient level of Aar-GFP within the cell, or a turnover rate high enough to leave GFP with insufficient time to fold correctly, would prevent fluorescence. This would be analogous to β-catenin degradation in resting mammalian cells, where the F-box protein βTrcp binds following GSK-3 phosphorylation. In the case of Aar, however, there is no evidence for the involvement of a βTrcp protein or proteasome-mediated degradation as yet.

Treatment of cells with lithium chloride to inhibit GskA failed to induce fluorescence in Aar-GFP transformants. However, in a small number of transformants that showed fluorescence, the inhibition of GskA led to the redistribution of Aar-GFP within the cell. The localisation of the protein changed from a general cytoplasmic distribution to a high enrichment in the nucleus. All of the evidence to date suggests that the interaction between GskA and Aar is a positive one (Fraser et al., 2002; Grimson et al., 2000). If inhibition of GskA causes the accumulation of Aar in the nucleus, then how does GskA function to mediate *pspA* expression? A simple hypothesis would be that Aar functions to export a repressor of *pspA* expression from the nucleus. Nuclear export is also though to regulate the repressive function of the *C. elegans* TCF homologue POP-1 (see Korswagen, 2002). In *Dictyostelium*, GskA phosphorylation of Aar would be required for nuclear export. This is consistent with the previous observed role of GSK-3 phosphorylation in the nuclear export of cyclin D, NF-AT and DdStatA (Alt et al., 2000; Antos et al., 2002; Ginger et al., 2000). In addition, evidence for an Armadillo/Pangolin derepression mechanism required for the

expression of Wg target genes in *Drosophila* has emerged (Chan and Struhl, 2002). This is in contrast to the widely accepted belief that upon activation of Wnt signalling, Armadillo/β-catenin enters the nucleus and binds with Pan/TCF transcription factors to activate expression of target genes.

In conclusion, many, but not all, properties of Aar function and regulation are homologous to those of β-catenin in animal cells. Interestingly, upon initial analysis of Aar, its function appeared very different from β-catenin in the canonical pathway. However, it is becoming apparent that the current understanding of this pathway may be deficient. The observations described in this thesis offer an alternative means to study what could be a universal system.

Chapter 7

References

Adler, P.N. (1992) The genetic control of tissue polarity in Drosophila. *Bioessays*, **14**, 735-741.

Alt, J.R., Cleveland, J.L., Hannink, M. and Diehl, J.A. (2000) Phosphorylation-dependent regulation of cyclin D1 nuclear export and cyclin D1-dependent cellular transformation. *Genes Dev*, **14**, 3102-3114.

Amit, S., Hatzubai, A., Birman, Y., Andersen, J.S., Ben-Shushan, E., Mann, M., Ben-Neriah, Y. and Alkalay, I. (2002) Axin-mediated CKI phosphorylation of β-catenin at Ser 45: a molecular switch for the Wnt pathway. *Genes Dev*, **16**, 1066-1076.

Anjard, C., Chang, W.T., Gross, J. and Nellen, W. (1998) Production and activity of spore differentiation factors (SDFs) in *Dictyostelium*. *Development*, **125**, 4067-4075.

Anjard, C., van Bemmelen, M., Veron, M. and Reymond, C.D. (1997) A new spore differentiation factor (SDF) secreted by *Dictyostelium* cells is phosphorylated by the cAMP dependent protein kinase. *Differentiation*, **62**, 43-49.

Antos, C.L., McKinsey, T.A., Frey, N., Kutschke, W., McAnally, J., Shelton, J.M., Richardson, J.A., Hill, J.A. and Olson, E.N. (2002) Activated glycogen synthase-3β suppresses cardiac hypertrophy in vivo. *Proc Natl Acad Sci U S A*, **99**, 907-912.

Axelrod, J.D., Matsuno, K., Artavanis-Tsakonas, S. and Perrimon, N. (1996) Interaction between Wingless and Notch signaling pathways mediated by dishevelled. *Science*, **271**, 1826-1832.

Axelrod, J.D., Miller, J.R., Shulman, J.M., Moon, R.T. and Perrimon, N. (1998) Differential recruitment of Dishevelled provides signaling specificity in the planar cell polarity and Wingless signaling pathways. *Genes Dev*, **12**, 2610-2622.

Bafico, A., Liu, G., Yaniv, A., Gazit, A. and Aaronson, S.A. (2001) Novel mechanism of Wnt signalling inhibition mediated by Dickkopf-1 interaction with LRP6/Arrow. *Nat Cell Biol*, **3**, 683-686.

Behrens, J., Jerchow, B.A., Wurtele, M., Grimm, J., Asbrand, C., Wirtz, R., Kuhl, M., Wedlich, D. and Birchmeier, W. (1998) Functional interaction of an axin homolog, conductin, with β-catenin, APC, and GSK3β. *Science*, **280**, 596-599.

Belenkaya, T.Y., Han, C., Standley, H.J., Lin, X., Houston, D.W. and Heasman, J. (2002) pygopus Encodes a nuclear protein essential for wingless/Wnt signaling. *Development*, **129**, 4089-4101.

Berks, M. and Kay, R.R. (1988) Cyclic AMP is an inhibitor of stalk cell differentiation in *Dictyostelium discoideum*. *Dev Biol*, **126**, 108-114.

Bhanot, P., Brink, M., Samos, C.H., Hsieh, J.C., Wang, Y., Macke, J.P., Andrew, D., Nathans, J. and Nusse, R. (1996) A new member of the frizzled family from *Drosophila* functions as a Wingless receptor. *Nature*, **382**, 225-230.

Biben, C., Stanley, E., Fabri, L., Kotecha, S., Rhinn, M., Drinkwater, C., Lah, M., Wang, C.C., Nash, A., Hilton, D., Ang, S.L., Mohun, T. and Harvey, R.P. (1998) Murine cerberus homologue mCer-1: a candidate anterior patterning molecule. *Dev Biol*, **194**, 135-151.

Bienz, M. (1999) APC: the plot thickens. *Curr Opin Genet Dev*, **9**, 595-603.

Bierkamp, C., Schwarz, H., Huber, O. and Kemler, R. (1999) Desmosomal localization of β-catenin in the skin of plakoglobin null-mutant mice. *Development*, **126**, 371-381.

Birchmeier, W., Weidner, K.M. and Behrens, J. (1993) Molecular mechanisms leading to loss of differentiation and gain of invasiveness in epithelial cells. *J Cell Sci Suppl*, **17**, 159-164.

Boutros, M. and Mlodzik, M. (1999) Dishevelled: at the crossroads of divergent intracellular signaling pathways. *Mech Dev*, **83**, 27-37.

Boutros, M., Paricio, N., Strutt, D.I. and Mlodzik, M. (1998) Dishevelled activates JNK and discriminates between JNK pathways in planar polarity and wingless signaling. *Cell*, **94**, 109-118.

Bouwmeester, T., Kim, S., Sasai, Y., Lu, B. and De Robertis, E.M. (1996) Cerberus is a head-inducing secreted factor expressed in the anterior endoderm of Spemann's organizer. *Nature*, **382**, 595-601.

Brott, B.K. and Sokol, S.Y. (2002) Regulation of Wnt/LRP signaling by distinct domains of Dickkopf proteins. *Mol Cell Biol*, **22**, 6100-6110.

Brunner, E., Peter, O., Schweizer, L. and Basler, K. (1997) pangolin encodes a Lef-1 homologue that acts downstream of Armadillo to transduce the Wingless signal in *Drosophila*. *Nature*, **385**, 829-833.

Cadigan, K.M. and Nusse, R. (1997) Wnt signaling: a common theme in animal development. *Genes Dev*, **11**, 3286-3305.

Chan, S.K. and Struhl, G. (2002) Evidence that Armadillo Transduces Wingless by Mediating Nuclear Export or Cytosolic Activation of Pangolin. *Cell*, **111**, 265-280.

Coates, J.C. (1999) Armadillo homologues in *Dictyostelium discoideum*. *MRC Laboratory for Molecular Cell Biology & Dept. of Biology*. University of London Ph.D. Thesis.

Coates, J.C., Grimson, M.J., Williams, R.S., Bergman, W., Blanton, R.L. and Harwood, A.J. (2002) Loss of the β-catenin homologue aardvark causes ectopic stalk formation in *Dictyostelium*. *Mech Dev*, **116**, 117-127.

Coates, J.C. and Harwood, A.J. (2001) Cell-cell adhesion and signal transduction during *Dictyostelium* development. *J Cell Sci*, **114**, 4349-4358.

Cody, C.W., Prasher, D.C., Westler, W.M., Prendergast, F.G. and Ward, W.W. (1993) Chemical structure of the hexapeptide chromophore of the Aequorea green-fluorescent protein. *Biochemistry*, **32**, 1212-1218.

Cook, D., Fry, M.J., Hughes, K., Sumathipala, R., Woodgett, J.R. and Dale, T.C. (1996) Wingless inactivates glycogen synthase kinase-3 via an intracellular signalling pathway which involves a protein kinase C. *Embo J*, **15**, 4526-4536.

Cox, R.T., Kirkpatrick, C. and Peifer, M. (1996) Armadillo is required for adherens junction assembly, cell polarity, and morphogenesis during *Drosophila* embryogenesis. *J Cell Biol*, **134**, 133-148.

Cross, D.A., Alessi, D.R., Cohen, P., Andjelkovich, M. and Hemmings, B.A. (1995) Inhibition of glycogen synthase kinase-3 by insulin mediated by protein kinase B. *Nature*, **378**, 785-789.

Dajani, R., Fraser, E., Roe, S.M., Young, N., Good, V., Dale, T.C. and Pearl, L.H. (2001) Crystal structure of glycogen synthase kinase 3β: structural basis for phosphate-primed substrate specificity and autoinhibition. *Cell*, **105**, 721-732.

De Ferrari, G.V. and Inestrosa, N.C. (2000) Wnt signaling function in Alzheimer's disease. *Brain Res Brain Res Rev*, **33**, 1-12.

Ding, V.W., Chen, R.H. and McCormick, F. (2000) Differential regulation of glycogen synthase kinase 3β by insulin and Wnt signaling. *J Biol Chem*, **275**, 32475-32481.

Dormann, D., Siegert, F. and Weijer, C.J. (1996) Analysis of cell movement during the culmination phase of *Dictyostelium* development. *Development*, **122**, 761-769.

Early, A.E. and Williams, J.G. (1988) A *Dictyostelium* prespore-specific gene is transcriptionally repressed by DIF *in vitro*. *Development*, **103**, 519-524.

Eldar-Finkelman, H., Seger, R., Vandenheede, J.R. and Krebs, E.G. (1995) Inactivation of glycogen synthase kinase-3 by epidermal growth factor is mediated by mitogen-activated protein kinase/p90 ribosomal protein S6 kinase signaling pathway in NIH/3T3 cells. *J Biol Chem*, **270**, 987-990.

Fagotto, F., Jho, E., Zeng, L., Kurth, T., Joos, T., Kaufmann, C. and Costantini, F. (1999) Domains of axin involved in protein-protein interactions, Wnt pathway inhibition, and intracellular localization. *J Cell Biol*, **145**, 741-756.

Fang, X., Yu, S.X., Lu, Y., Bast, R.C., Jr., Woodgett, J.R. and Mills, G.B. (2000) Phosphorylation and inactivation of glycogen synthase kinase 3 by protein kinase A. *Proc Natl Acad Sci U S A*, **97**, 11960-11965.

Finch, P.W., He, X., Kelley, M.J., Uren, A., Schaudies, R.P., Popescu, N.C., Rudikoff, S., Aaronson, S.A., Varmus, H.E. and Rubin, J.S. (1997) Purification and molecular cloning of a secreted, Frizzled-related antagonist of Wnt action. *Proc Natl Acad Sci U S A*, **94**, 6770-6775.

Frame, S. and Cohen, P. (2001) GSK3 takes centre stage more than 20 years after its discovery. *Biochem J*, **359**, 1-16.

Franca-Koh, J., Yeo, M., Fraser, *E.*, Young, N. and Dale, T.C. (2002) The regulation of glycogen synthase Kinse-3 nuclear export by Frat/GBP. *J Biol Chem*, **277**, 43844-8.

Fraser, E., Young, N., Dajani, R., Franca-Koh, J., Ryves, J., Williams, R.S., Yeo, M., Webster, M.T., Richardson, C., Smalley, M.J., Pearl, L.H., Harwood, A. and Dale, T.C. (2002) Identification of the Axin and Frat binding region of glycogen synthase kinase-3. *J Biol Chem*, **277**, 2176-2185.

Giannini, A.L., Vivanco, M.M. and Kypta, R.M. (2000) Analysis of beta-catenin aggregation and localization using GFP fusion proteins: nuclear import of α-catenin by the β-catenin/Tcf complex. *Exp Cell Res*, **255**, 207-220.

Ginger, R.S., Dalton, E.C., Ryves, W.J., Fukuzawa, M., Williams, J.G. and Harwood, A.J. (2000) Glycogen synthase kinase-3 enhances nuclear export of a *Dictyostelium* STAT protein. *Embo J*, **19**, 5483-5491.

Ginsburg, G.T. and Kimmel, A.R. (1997) Autonomous and nonautonomous regulation of axis formation by antagonistic signaling via 7-span cAMP receptors and GSK3 in *Dictyostelium*. *Genes Dev*, **11**, 2112-2123.

Glinka, A., Wu, W., Delius, H., Monaghan, A.P., Blumenstock, C. and Niehrs, C. (1998) Dickkopf-1 is a member of a new family of secreted proteins and functions in head induction. *Nature*, **391**, 357-362.

Gomer, R.H., Yuen, I.S. and Firtel, R.A. (1991) A secreted 80 x 10(3) Mr protein mediates sensing of cell density and the onset of development in *Dictyostelium*. *Development*, **112**, 269-278.

Goode, N., Hughes, K., Woodgett, J.R. and Parker, P.J. (1992) Differential regulation of glycogen synthase kinase-3β by protein kinase C isotypes. *J Biol Chem*, **267**, 16878-16882.

Grimes, C.A. and Jope, R.S. (2001) The multifaceted roles of glycogen synthase kinase 3β in cellular signaling. *Prog Neurobiol*, **65**, 391-426.

Grimson, M.J., Coates, J.C., Reynolds, J.P., Shipman, M., Blanton, R.L. and Harwood, A.J. (2000) Adherens junctions and β-catenin-mediated cell signalling in a non-metazoan organism. *Nature*, **408**, 727-731.

Grimson, M.J., Haigler, C.H. and Blanton, R.L. (1996) Cellulose microfibrils, cell motility, and plasma membrane protein organization change in parallel during culmination in *Dictyostelium discoideum*. *J Cell Sci*, **109**, 3079-3087.

Haegel, H., Larue, L., Ohsugi, M., Fedorov, L., Herrenknecht, K. and Kemler, R. (1995) Lack of β-catenin affects mouse development at gastrulation. *Development*, **121**, 3529-3537.

Hagen, T. and Vidal-Puig, A. (2002) Characterisation of the phosphorylation of β-catenin at the GSK-3 priming site Ser45. *Biochem Biophys Res Commun*, **294**, 324-328.

Hart, M.J., de los Santos, R., Albert, I.N., Rubinfeld, B. and Polakis, P. (1998) Downregulation of β-catenin by human Axin and its association with the APC tumor suppressor, β-catenin and GSK3β. *Curr Biol*, **8**, 573-581.

Harwood, A.J. (1996) The rapid boiling method for small-scale preparation of plasmid DNA. *Methods Mol Biol*, **58**, 265-267.

Harwood, A.J. (2001) Regulation of GSK-3: a cellular multiprocessor. *Cell*, **105**, 821-824.

Harwood, A.J., Plyte, S.E., Woodgett, J., Strutt, H. and Kay, R.R. (1995) Glycogen synthase kinase 3 regulates cell fate in *Dictyostelium*. *Cell*, **80**, 139-148.

Herman, M.A. and Horvitz, H.R. (1994) The *Caenorhabditis elegans* gene lin-44 controls the polarity of asymmetric cell divisions. *Development*, **120**, 1035-1047.

Herman, M.A., Vassilieva, L.L., Horvitz, H.R., Shaw, J.E. and Herman, R.K. (1995) The *C. elegans* gene lin-44, which controls the polarity of certain asymmetric cell divisions, encodes a Wnt protein and acts cell nonautonomously. *Cell*, **83**, 101-110.

Hoang, B., Moos, M., Jr., Vukicevic, S. and Luyten, F.P. (1996) Primary structure and tissue distribution of FRZB, a novel protein related to *Drosophila* frizzled, suggest a role in skeletal morphogenesis. *J Biol Chem*, **271**, 26131-26137.

Hobmayer, B., Rentzsch, F., Kuhn, K., Happel, C.M., von Laue, C.C., Snyder, P., Rothbacher, U. and Holstein, T.W. (2000) WNT signalling molecules act in axis formation in the diploblastic metazoan Hydra. *Nature*, **407**, 186-189.

Hoeflich, K.P., Luo, J., Rubie, E.A., Tsao, M.S., Jin, O. and Woodgett, J.R. (2000) Requirement for glycogen synthase kinase-3β in cell survival and NF-kappaB activation. *Nature*, **406**, 86-90.

Hsieh, J.C., Kodjabachian, L., Rebbert, M.L., Rattner, A., Smallwood, P.M., Samos, C.H., Nusse, R., Dawid, I.B. and Nathans, J. (1999) A new secreted protein that binds to Wnt proteins and inhibits their activities. *Nature*, **398**, 431-436.

Hsu, W., Zeng, L. and Costantini, F. (1999) Identification of a domain of Axin that binds to the serine/threonine protein phosphatase 2A and a self-binding domain. *J Biol Chem*, **274**, 3439-3445.

Hu, G. and Fearon, E.R. (1999) Siah-1 N-terminal RING domain is required for proteolysis function, and C-terminal sequences regulate oligomerization and binding to target proteins. *Mol Cell Biol*, **19**, 724-732.

Huber, A.H. and Weis, W.I. (2001) The structure of the β-catenin/E-cadherin complex and the molecular basis of diverse ligand recognition by β-catenin. *Cell*, **105**, 391-402.

Huber, O., Bierkamp, C. and Kemler, R. (1996a) Cadherins and catenins in development. *Curr Opin Cell Biol*, **8**, 685-691.

Huber, O., Korn, R., McLaughlin, J., Ohsugi, M., Herrmann, B.G. and Kemler, R. (1996b) Nuclear localization of β-catenin by interaction with transcription factor LEF-1. *Mech Dev*, **59**, 3-10.

Huelsken, J. and Birchmeier, W. (2001) New aspects of Wnt signaling pathways in higher vertebrates. *Curr Opin Genet Dev*, **11**, 547-553.

Ikeda, S., Kishida, S., Yamamoto, H., Murai, H., Koyama, S. and Kikuchi, A. (1998) Axin, a negative regulator of the Wnt signaling pathway, forms a complex with GSK-3β and β-catenin and promotes GSK-3β-dependent phosphorylation of β-catenin. *Embo J*, **17**, 1371-1384.

Imamura, Y., Itoh, M., Maeno, Y., Tsukita, S. and Nagafuchi, A. (1999) Functional domains of α-catenin required for the strong state of cadherin-based cell adhesion. *J Cell Biol*, **144**, 1311-1322.

Jiang, J. and Struhl, G. (1998) Regulation of the Hedgehog and Wingless signalling pathways by the F-box/WD40-repeat protein Slimb. *Nature*, **391**, 493-496.

Julius, M.A., Schelbert, B., Hsu, W., Fitzpatrick, E., Jho, E., Fagotto, F., Costantini, F. and Kitajewski, J. (2000) Domains of axin and disheveled required for interaction and function in wnt signaling. *Biochem Biophys Res Commun*, **276**, 1162-1169.

Kaletta, T., Schnabel, H. and Schnabel, R. (1997) Binary specification of the embryonic lineage in *Caenorhabditis elegans*. *Nature*, **390**, 294-298.

Kanner, S.B., Reynolds, A.B. and Parsons, J.T. (1991) Tyrosine phosphorylation of a 120-kilodalton pp60src substrate upon epidermal growth factor and platelet-derived growth factor receptor stimulation and in polyomavirus middle-T-antigen-transformed cells. *Mol Cell Biol*, **11**, 713-720.

Karnovsky, A. and Klymkowsky, M.W. (1995) Anterior axis duplication in Xenopus induced by the over-expression of the cadherin-binding protein plakoglobin. *Proc Natl Acad Sci U S A*, **92**, 4522-4526.

Kawanishi, J., Kato, J., Sasaki, K., Fujii, S., Watanabe, N. and Niitsu, Y. (1995) Loss of E-cadherin-dependent cell-cell adhesion due to mutation of the β-catenin gene in a human cancer cell line, HSC-39. *Mol Cell Biol*, **15**, 1175-1181.

Kim, L., Harwood, A. and Kimmel, A.R. (2002) Receptor-Dependent and Tyrosine Phosphatase-Mediated Inhibition of GSK3 Regulates Cell Fate Choice. *Dev Cell*, **3**, 523-532.

Kim, L., Liu, J. and Kimmel, A.R. (1999) The novel tyrosine kinase ZAK1 activates GSK3 to direct cell fate specification. *Cell*, **99**, 399-408.

Kimmel, A.R. and Firtel, R.A. (1991) cAMP signal transduction pathways regulating development of *Dictyostelium discoideum*. *Curr Opin Genet Dev*, **1**, 383-390.

Kinch, M.S. and Burridge, K. (1995) Altered adhesions in ras-transformed breast epithelial cells. *Biochem Soc Trans*, **23**, 446-450.

Kipreos, E.T. and Pagano, M. (2000) The F-box protein family. *Genome Biol*, **1**, 3002.1-3002.7.

Kopachik, W., Oohata, A., Dhokia, B., Brookman, J.J. and Kay, R.R. (1983) *Dictyostelium* mutants lacking DIF, a putative morphogen. *Cell*, **33**, 397-403.

Korinek, V., Barker, N., Morin, P.J., van Wichen, D., de Weger, R., Kinzler, K.W., Vogelstein, B. and Clevers, H. (1997) Constitutive transcriptional activation by a β-catenin-Tcf complex in APC-/- colon carcinoma. *Science*, **275**, 1784-1787.

Korswagen, H.C. (2002) Canonical and non-canonical Wnt signaling pathways in *Caenorhabditis elegans*: variations on a common signaling theme. *Bioessays*, **24**, 801-810.

Korswagen, H.C., Coudreuse, D.Y., Betist, M.C., van de Water, S., Zivkovic, D. and Clevers, H.C. (2002) The Axin-like protein PRY-1 is a negative regulator of a canonical Wnt pathway in *C. elegans*. *Genes Dev*, **16**, 1291-1302.

Korswagen, H.C., Herman, M.A. and Clevers, H.C. (2000) Distinct β-catenins mediate adhesion and signalling functions in *C. elegans*. *Nature*, **406**, 527-532.

Kramps, T., Peter, O., Brunner, E., Nellen, D., Froesch, B., Chatterjee, S., Murone, M., Zullig, S. and Basler, K. (2002) Wnt/wingless signaling requires BCL9/legless-mediated recruitment of pygopus to the nuclear β-catenin-TCF complex. *Cell*, **109**, 47-60.

Krupnik, V.E., Sharp, J.D., Jiang, C., Robison, K., Chickering, T.W., Amaravadi, L., Brown, D.E., Guyot, D., Mays, G., Leiby, K., Chang, B., Duong, T., Goodearl, A.D., Gearing, D.P., Sokol, S.Y. and McCarthy, S.A. (1999) Functional and structural diversity of the human Dickkopf gene family. *Gene*, **238**, 301-313.

Kuhl, M., Sheldahl, L.C., Park, M., Miller, J.R. and Moon, R.T. (2000) The Wnt/Ca2+ pathway: a new vertebrate Wnt signaling pathway takes shape. *Trends Genet*, **16**, 279-283.

Lander, E.S., Linton, L. M., Birren, B., Nusbaum, C., Zody, M. C., Baldwin, J., Devon, K., Dewar, K., Doyle, M., FitzHugh, W., Funke, R., Gage, D., Harris, K., Heaford, A., Howland, J., Kann, L., Lehoczky, J., LeVine, R., McEwan, P., McKernan, K., Meldrim, J., Mesirov, J.P., Miranda, C., Morris, W., Naylor, J., Raymond, C., Rosetti, M., Santos, R., Sheridan, A., Sougnez, C., Stange-Thomann, N., Stojanovic, N., Subramanian, A., Rogers, D.W., Sulston, J., Ainscough, R., Beck, S., Bentley, D., Burton, J., Clee, C., Carter, N., Coulson, A., Deadman, R.,

Deloukas, P., Dunham, A., Dunham, I., Durbin, R., French, L., Grafham, D., Gregory, S., Hubbard, T., Humphray, S., Hunt, A., Jones, M., Lloyd, C., McMurray, A., Matthews, L., Mercer, S., Milne, S., Mullikin, J.C., Mungall, A., Plumb, R., Ross, M., Shownkeen, R., SimsRobert., S., Waterston, H., Wilson, R.K., Hillier, L. W., McPherson, J.D., Marra,. M.A., Mardis, E.R., Fulton, L.A., Chinwalla, A.T., Pepin, K.H., Gish, W.R., Chissoe, S.L., Wendl, M.C., Delehaunty, K.D., Miner, T.L., Delehaunty, A., Kramer, J.B., Cook, L.L., Fulton, R.S., Johnson, D.L., Minx, P.J., CliftonTrevor, S.W., Hawkins, E.B., Predki, P., Richardson, P., Wenning, S., Slezak, T., Doggett, N., Cheng, J.F., Olsen, A., Lucas, S., Elkin, C., Uberbacher, E., FrazierRichard, M. (2001) Initial sequencing and analysis of the human genome. *Nature*, **409**, 860-921.

Li, L., Mao, J., Sun, L., Liu, W. and Wu, D. (2002) Second cysteine-rich domain of Dickkopf-2 activates canonical Wnt signaling pathway via LRP-6 independently of dishevelled. *J Biol Chem*, **277**, 5977-5981.

Li, L., Yuan, H., Weaver, C.D., Mao, J., Farr, G.H., 3rd, Sussman, D.J., Jonkers, J., Kimelman, D. and Wu, D. (1999) Axin and Frat1 interact with dvl and GSK, bridging Dvl to GSK in Wnt-mediated regulation of LEF-1. *Embo J*, **18**, 4233-4240.

Lijam, N., Paylor, R., McDonald, M.P., Crawley, J.N., Deng, C.X., Herrup, K., Stevens, K.E., Maccaferri, G., McBain, C.J., Sussman, D.J. and Wynshaw-Boris, A. (1997) Social interaction and sensorimotor gating abnormalities in mice lacking Dvl1. *Cell*, **90**, 895-905.

Lin, R., Thompson, S. and Priess, J.R. (1995) pop-1 encodes an HMG box protein required for the specification of a mesoderm precursor in early *C. elegans* embryos. *Cell*, **83**, 599-609.

Liu, C., Kato, Y., Zhang, Z., Do, V.M., Yankner, B.A. and He, X. (1999) β-Trcp couples β-catenin phosphorylation-degradation and regulates *Xenopus* axis formation. *Proc Natl Acad Sci U S A*, **96**, 6273-6278.

Liu, C., Li, Y., Semenov, M., Han, C., Baeg, G.H., Tan, Y., Zhang, Z., Lin, X. and He, X. (2002) Control of β-catenin phosphorylation/degradation by a dual-kinase mechanism. *Cell*, **108**, 837-847.

Liu, J., Stevens, J., Rote, C.A., Yost, H.J., Hu, Y., Neufeld, K.L., White, R.L. and Matsunami, N. (2001a) Siah-1 mediates a novel β-catenin degradation pathway linking p53 to the adenomatous polyposis coli protein. *Mol Cell*, **7**, 927-936.

Liu, T., DeCostanzo, A.J., Liu, X., Wang, H., Hallagan, S., Moon, R.T. and Malbon, C.C. (2001b) G protein signaling from activated rat frizzled-1 to the β-catenin-Lef-Tcf pathway. *Science*, **292**, 1718-1722.

Lustig, B., Jerchow, B., Sachs, M., Weiler, S., Pietsch, T., Karsten, U., van de Wetering, M., Clevers, H., Schlag, P.M., Birchmeier, W. and Behrens, J. (2002) Negative feedback loop of Wnt signaling through upregulation of conductin/axin2 in colorectal and liver tumors. *Mol Cell Biol*, **22**, 1184-1193.

MacWilliams, H.K. and Bonner, J.T. (1979) The prestalk-prespore pattern in cellular slime molds. *Differentiation*, **14**, 1-22.

Manstein, D.J., Schuster, H.P., Morandini, P. and Hunt, D.M. (1995) Cloning vectors for the production of proteins in *Dictyostelium discoideum*. *Gene*, **162**, 129-134.

Mao, J., Wang, J., Liu, B., Pan, W., Farr, G.H., 3rd, Flynn, C., Yuan, H., Takada, S., Kimelman, D., Li, L. and Wu, D. (2001) Low-density lipoprotein receptor-related protein-5 binds to Axin and regulates the canonical Wnt signaling pathway. *Mol Cell*, **7**, 801-809.

Matsuzawa, S.I. and Reed, J.C. (2001) Siah-1, SIP, and Ebi collaborate in a novel pathway for β-catenin degradation linked to p53 responses. *Mol Cell*, **7**, 915-926.

Mehdy, M.C. and Firtel, R.A. (1985) A secreted factor and cyclic AMP jointly regulate cell-type-specific gene expression in *Dictyostelium discoideum*. *Mol Cell Biol*, **5**, 705-713.

Meneghini, M.D., Ishitani, T., Carter, J.C., Hisamoto, N., Ninomiya-Tsuji, J., Thorpe, C.J., Hamill, D.R., Matsumoto, K. and Bowerman, B. (1999) MAP kinase and Wnt pathways converge to downregulate an HMG-domain repressor in *Caenorhabditis elegans*. *Nature*, **399**, 793-797.

Miller, J.R. and Moon, R.T. (1997) Analysis of the signaling activities of localization mutants of β-catenin during axis specification in Xenopus. *J Cell Biol*, **139**, 229-243.

Mimori-Kiyosue, Y., Shiina, N. and Tsukita, S. (2000) Adenomatous polyposis coli (APC) protein moves along microtubules and concentrates at their growing ends in epithelial cells. *J Cell Biol*, **148**, 505-518.

Miyoshi, Y., Nagase, H., Ando, H., Horii, A., Ichii, S., Nakatsuru, S., Aoki, T., Miki, Y., Mori, T. and Nakamura, Y. (1992) Somatic mutations of the APC gene in colorectal tumors: mutation cluster region in the APC gene. *Hum Mol Genet*, **1**, 229-233.

Molenaar, M., van de Wetering, M., Oosterwegel, M., Peterson-Maduro, J., Godsave, S., Korinek, V., Roose, J., Destree, O. and Clevers, H. (1996) XTcf-3 transcription factor mediates β-catenin-induced axis formation in *Xenopus* embryos. *Cell*, **86**, 391-399.

Moon, R.T., Brown, J.D. and Torres, M. (1997) WNTs modulate cell fate and behavior during vertebrate development. *Trends Genet*, **13**, 157-162.

Moreno-Bueno, G., Cales, C., Behrens, M.M. and Fernandez-Renart, M. (2000) Isolation and characterization of casein kinase I from *Dictyostelium discoideum*. *Biochem J*, **349**, 527-537.

Morin, P.J., Sparks, A.B., Korinek, V., Barker, N., Clevers, H., Vogelstein, B. and Kinzler, K.W. (1997) Activation of β-catenin-Tcf signaling in colon cancer by mutations in β-catenin or APC. *Science*, **275**, 1787-1790.

Morris, H.R., Taylor, G.W., Masento, M.S., Jermyn, K.A. and Kay, R.R. (1987) Chemical structure of the morphogen differentiation inducing factor *from Dictyostelium discoideum*. *Nature*, **328**, 811-814.

Mudher, A., Chapman, S., Richardson, J., Asuni, A., Gibb, G., Pollard, C., Killick, R., Iqbal, T., Raymond, L., Varndell, I., Sheppard, P., Makoff, A., Gower, E., Soden, P.E., Lewis, P., Murphy, M., Golde, T.E., Rupniak, H.T., Anderton, B.H. and Lovestone, S. (2001) Dishevelled regulates the metabolism of amyloid precursor protein via protein kinase C/mitogen-activated protein kinase and c-Jun terminal kinase. *J Neurosci*, **21**, 4987-4995.

Nagafuchi, A. (2001) Molecular architecture of adherens junctions. *Curr Opin Cell Biol*, **13**, 600-603.

Nagar, B., Overduin, M., Ikura, M. and Rini, J.M. (1996) Structural basis of calcium-induced E-cadherin rigidification and dimerization. *Nature*, **380**, 360-364.

Newell, P.C. (1982) Cell surface binding of adenosine to *Dictyostelium* and inhibition of pulsatile signalling. *FEMS Microbiol. Lett.*, **13**, 417-421.

Nusse, R. and Varmus, H.E. (1982) Many tumors induced by the mouse mammary tumor virus contain a provirus integrated in the same region of the host genome. *Cell*, **31**, 99-109.

Oda, H. and Tsukita, S. (1999) Dynamic features of adherens junctions during *Drosophila* embryonic *epithelial* morphogenesis revealed by a Dα-catenin-GFP fusion protein. *Dev Genes Evol*, **209**, 218-225.

Orford, K., Crockett, C., Jensen, J.P., Weissman, A.M. and Byers, S.W. (1997) Serine phosphorylation-regulated ubiquitination and degradation of β-catenin. *J Biol Chem*, **272**, 24735-24738.

Ozawa, M., Baribault, H. and Kemler, R. (1989) The cytoplasmic domain of the cell adhesion molecule uvomorulin associates with three independent proteins structurally related in different species. *Embo J*, **8**, 1711-1717.

Parker, D.S., Jemison, J. and Cadigan, K.M. (2002) Pygopus, a nuclear PHD-finger protein required for Wingless signaling in *Drosophila*. *Development*, **129**, 2565-2576.

Peifer, M., Orsulic, S., Sweeton, D. and Wieschaus, E. (1993) A role for the *Drosophila* segment polarity gene armadillo in cell adhesion and cytoskeletal integrity during oogenesis. *Development*, **118**, 1191-1207.

Plyte, S.E., O'Donovan, E., Woodgett, J.R. and Harwood, A.J. (1999) Glycogen synthase kinase-3 (GSK-3) is regulated during *Dictyostelium* development via the serpentine receptor cAR3. *Development*, **126**, 325-333.

Polakis, P. (1997) The adenomatous polyposis coli (APC) tumor suppressor. *Biochim Biophys Acta*, **1332**, F127-147.

Polakis, P. (1999) The oncogenic activation of β-catenin. *Curr Opin Genet Dev*, **9**, 15-21.

Polakis, P. (2000) Wnt signaling and cancer. *Genes Dev*, **14**, 1837-1851.

Polakis, P. (2001) More than one way to skin a catenin. *Cell*, **105**, 563-566.

Pukatzki, S., Ennis, H.L. and Kessin, R.H. (2000) A genetic interaction between a ubiquitin-like protein and ubiquitin-mediated proteolysis in *Dictyostelium discoideum*. *Biochim Biophys Acta*, **1499**, 154-163.

Raper, K.B. (1935) *Dictyostelium discoideum*, a new species ofslime mould from decaying forest leaves. *J. Agr. Res*, **50**, 135-147.

Rathi, A. and Clarke, M. (1992) Expression of early developmental genes in *Dictyostelium discoideum* is initiated during exponential growth by an autocrine-dependent mechanism. *Mech Dev*, **36**, 173-182.

Rattner, A., Hsieh, J.C., Smallwood, P.M., Gilbert, D.J., Copeland, N.G., Jenkins, N.A. and Nathans, J. (1997) A family of secreted proteins contains homology to the cysteine-rich ligand-binding domain of frizzled receptors. *Proc Natl Acad Sci U S A*, **94**, 2859-2863.

Rocheleau, C.E., Downs, W.D., Lin, R., Wittmann, C., Bei, Y., Cha, Y.H., Ali, M., Priess, J.R. and Mello, C.C. (1997) Wnt signaling and an APC-related gene specify endoderm in early *C. elegans* embryos. *Cell*, **90**, 707-716.

Rocheleau, C.E., Yasuda, J., Shin, T.H., Lin, R., Sawa, H., Okano, H., Priess, J.R., Davis, R.J. and Mello, C.C. (1999) WRM-1 activates the LIT-1 protein kinase to transduce anterior/posterior polarity signals in *C. elegans*. *Cell*, **97**, 717-726.

Rosato, R., Veltmaat, J.M., Groffen, J. and Heisterkamp, N. (1998) Involvement of the tyrosine kinase fer in cell adhesion. *Mol Cell Biol*, **18**, 5762-5770.

Rosin-Arbesfeld, R., Townsley, F. and Bienz, M. (2000) The APC tumour suppressor has a nuclear export function. *Nature*, **406**, 1009-1012.

Rothbacher, U., Laurent, M.N., Blitz, I.L., Watabe, T., Marsh, J.L. and Cho, K.W. (1995) Functional conservation of the Wnt signaling pathway revealed by ectopic expression of *Drosophila* dishevelled in *Xenopus*. *Dev Biol*, **170**, 717-721.

Roura, S., Miravet, S., Piedra, J., Garcia de Herreros, A. and Dunach, M. (1999) Regulation of E-cadherin/Catenin association by tyrosine phosphorylation. *J Biol Chem*, **274**, 36734-36740.

Rubinfeld, B., Albert, I., Porfiri, E., Fiol, C., Munemitsu, S. and Polakis, P. (1996) Binding of GSK3β to the APC-β-catenin complex and regulation of complex assembly. *Science*, **272**, 1023-1026.

Rubinfeld, B., Robbins, P., El-Gamil, M., Albert, I., Porfiri, E. and Polakis, P. (1997) Stabilization of β-catenin by genetic defects in melanoma cell lines. *Science*, **275**, 1790-1792.

Ruel, L., Bourouis, M., Heitzler, P., Pantesco, V. and Simpson, P. (1993) *Drosophila* shaggy kinase and rat glycogen synthase kinase-3 have conserved activities and act downstream of Notch. *Nature*, **362**, 557-560.

Ryves, W.J., Fryer, L., Dale, T. and Harwood, A.J. (1998) An assay for glycogen synthase kinase 3 (GSK-3) for use in crude cell extracts. *Anal Biochem*, **264**, 124-127.

Sadot, E., Geiger, B., Oren, M. and Ben-Ze'ev, A. (2001) Down-regulation of β-catenin by activated p53. *Mol Cell Biol*, **21**, 6768-6781.

Sakanaka, C., Leong, P., Xu, L., Harrison, S.D. and Williams, L.T. (1999) Casein kinase Iε in the wnt pathway: regulation of β-catenin function. *Proc Natl Acad Sci U S A*, **96**, 12548-12552.

Salic, A., Lee, E., Mayer, L. and Kirschner, M.W. (2000) Control of β-catenin stability: reconstitution of the cytoplasmic steps of the wnt pathway in *Xenopus* egg extracts. *Mol Cell*, **5**, 523-532.

Sambrook, J., Fritsch, E. F., Maniatis, T. (1989) *Molecular cloning: A Laboratory Manual*. Cold Spring Harbor Laboratory Press.

Schaap, P. and Wang, M. (1986) Interactions between adenosine and oscillatory cAMP signaling regulate size and pattern in *Dictyostelium*. *Cell*, **45**, 137-144.

Schulkes, C. and Schaap, P. (1995) cAMP-dependent protein kinase activity is essential for preaggregative gene expression in *Dictyostelium*. *FEBS Lett*, **368**, 381-384.

Schwarz-Romond, T., Asbrand, C., Bakkers, J., Kuhl, M., Schaeffer, H.J., Huelsken, J., Behrens, J., Hammerschmidt, M. and Birchmeier, W. (2002) The ankyrin repeat protein Diversin recruits Casein kinase Iε to the β-catenin degradation complex and acts in both canonical Wnt and Wnt/JNK signaling. *Genes Dev*, **16**, 2073-2084.

Shibamoto, S., Hayakawa, M., Takeuchi, K., Hori, T., Oku, N., Miyazawa, K., Kitamura, N., Takeichi, M. and Ito, F. (1994) Tyrosine phosphorylation of β-catenin and plakoglobin enhanced by hepatocyte growth factor and epidermal growth factor in human carcinoma cells. *Cell Adhes Commun*, **1**, 295-305.

Sokol, S. (2000) A role for Wnts in morpho-genesis and tissue polarity. *Nat Cell Biol*, **2**, E124-125.

Song, D.H., Sussman, D.J. and Seldin, D.C. (2000) Endogenous protein kinase CK2 participates in Wnt signaling in mammary epithelial cells. *J Biol Chem*, **275**, 23790-23797.

Sutherland, C., Leighton, I.A. and Cohen, P. (1993) Inactivation of glycogen synthase kinase-3β by phosphorylation: new kinase connections in insulin and growth-factor signalling. *Biochem J*, **296 (Pt 1)**, 15-19.

Takeichi, M. (1991) Cadherin cell adhesion receptors as a morphogenetic regulator. *Science*, **251**, 1451-1455.

Tamai, K., Semenov, M., Kato, Y., Spokony, R., Liu, C., Katsuyama, Y., Hess, F., Saint-Jeannet, J.P. and He, X. (2000) LDL-receptor-related proteins in Wnt signal transduction. *Nature*, **407**, 530-535.

Theibert, A. and Devreotes, P.N. (1984) Adenosine and its derivatives inhibit the cAMP signaling response in *Dictyostelium discoideum*. *Dev Biol*, **106**, 166-173.

Theisen, H., Purcell, J., Bennett, M., Kansagara, D., Syed, A. and Marsh, J.L. (1994) dishevelled is required during wingless signaling to establish both cell polarity and cell identity. *Development*, **120**, 347-360.

Thompson, B., Townsley, F., Rosin-Arbesfeld, R., Musisi, H. and Bienz, M. (2002) A new nuclear component of the Wnt signalling pathway. *Nat Cell Biol*, **4**, 367-373.

Thorpe, C.J., Schlesinger, A. and Bowerman, B. (2000) Wnt signalling in *Caenorhabditis elegans*: regulating repressors and polarizing the cytoskeleton. *Trends Cell Biol*, **10**, 10-17.

Thorpe, C.J., Schlesinger, A., Carter, J.C. and Bowerman, B. (1997) Wnt signaling polarizes an early *C. elegans* blastomere to distinguish endoderm from mesoderm. *Cell*, **90**, 695-705.

Town, C.D., Gross, J.D. and Kay, R.R. (1976) Cell differentiation without morphogenesis in *Dictyostelium discoideum*. *Nature*, **262**, 717-719.

Tsubuki, S., Saito, Y., Tomioka, M., Ito, H. and Kawashima, S. (1996) Differential inhibition of calpain and proteasome activities by peptidyl aldehydes of di-leucine and tri-leucine. *J Biochem (Tokyo)*, **119**, 572-576.

Uemura, T., Oda, H., Kraut, R., Hayashi, S., Kotaoka, Y. and Takeichi, M. (1996) Zygotic *Drosophila* E-cadherin expression is required for processes of dynamic epithelial cell rearrangement in the *Drosophila* embryo. *Genes Dev*, **10**, 659-671.

Uren, A., Reichsman, F., Anest, V., Taylor, W.G., Muraiso, K., Bottaro, D.P., Cumberledge, S. and Rubin, J.S. (2000) Secreted frizzled-related protein-1 binds directly to Wingless and is a biphasic modulator of Wnt signaling. *J Biol Chem*, **275**, 4374-4382.

Urushihara, H. (2002) Functional genomics of the social amoebae, *Dictyostelium discoideum*. *Mol Cells*, **13**, 1-4.

van de Wetering, M., Cavallo, R., Dooijes, D., van Beest, M., van Es, J., Loureiro, J., Ypma, A., Hursh, D., Jones, T., Bejsovec, A., Peifer, M., Mortin, M. and Clevers, H. (1997) Armadillo coactivates transcription driven by the product of the *Drosophila* segment polarity gene dTCF. *Cell*, **88**, 789-799.

Van Haastert, P.J. (1995) Transduction of the chemotactic cAMP signal across the plasma membrane of *Dictyostelium* cells. *Experientia*, **51**, 1144-1154.

van Noort, M., Meeldijk, J., van der Zee, R., Destree, O. and Clevers, H. (2002) Wnt signaling controls the phosphorylation status of β-catenin. *J Biol Chem*, **277**, 17901-17905.

Vinson, C.R. and Adler, P.N. (1987) Directional non-cell autonomy and the transmission of polarity information by the frizzled gene of *Drosophila*. *Nature*, **329**, 549-551.

Wang, Q.M., Roach, P.J. and Fiol, C.J. (1994) Use of a synthetic peptide as a selective substrate for glycogen synthase kinase 3. *Anal Biochem*, **220**, 397-402.

Wang, S., Krinks, M., Lin, K., Luyten, F.P. and Moos, M., Jr. (1997) Frzb, a secreted protein expressed in the Spemann organizer, binds and inhibits Wnt-8. *Cell*, **88**, 757-766.

Wang, Y., Macke, J.P., Abella, B.S., Andreasson, K., Worley, P., Gilbert, D.J., Copeland, N.G., Jenkins, N.A. and Nathans, J. (1996) A large family of putative transmembrane receptors homologous to the product of the *Drosophila* tissue polarity gene frizzled. *J Biol Chem*, **271**, 4468-4476.

Wehrli, M., Dougan, S.T., Caldwell, K., O'Keefe, L., Schwartz, S., Vaizel-Ohayon, D., Schejter, E., Tomlinson, A. and DiNardo, S. (2000) Arrow encodes an LDL-receptor-related protein essential for Wingless signalling. *Nature*, **407**, 527-530.

Willert, K., Brink, M., Wodarz, A., Varmus, H. and Nusse, R. (1997) Casein kinase 2 associates with and phosphorylates dishevelled. *Embo J*, **16**, 3089-3096.

Woodgett, J.R. (1990) Molecular cloning and expression of glycogen synthase kinase-3/factor A. *Embo J*, **9**, 2431-2438.

Xu, Q., D'Amore, P.A. and Sokol, S.Y. (1998) Functional and biochemical interactions of Wnts with FrzA, a secreted Wnt antagonist. *Development*, **125**, 4767-4776.

Yamamoto, H., Hinoi, T., Michiue, T., Fukui, A., Usui, H., Janssens, V., Van Hoof, C., Goris, J., Asashima, M. and Kikuchi, A. (2001) Inhibition of the Wnt signaling pathway by the PR61 subunit of protein phosphatase 2A. *J Biol Chem*, **276**, 26875-26882.

Yamamoto, H., Kishida, S., Kishida, M., Ikeda, S., Takada, S. and Kikuchi, A. (1999) Phosphorylation of axin, a Wnt signal negative regulator, by glycogen synthase kinase-3β regulates its stability. *J Biol Chem*, **274**, 10681-10684.

Yanagawa, S., van Leeuwen, F., Wodarz, A., Klingensmith, J. and Nusse, R. (1995) The dishevelled protein is modified by wingless signaling in *Drosophila*. *Genes Dev*, **9**, 1087-1097.

Yost, C., Torres, M., Miller, J.R., Huang, E., Kimelman, D. and Moon, R.T. (1996) The axis-inducing activity, stability, and subcellular distribution of β-catenin is regulated in *Xenopus* embryos by glycogen synthase kinase 3. *Genes Dev*, **10**, 1443-1454.

Zeng, L., Fagotto, F., Zhang, T., Hsu, W., Vasicek, T.J., Perry, W.L., 3rd, Lee, J.J., Tilghman, S.M., Gumbiner, B.M. and Costantini, F. (1997) The mouse Fused locus encodes Axin, an inhibitor of the Wnt signaling pathway that regulates embryonic axis formation. *Cell*, **90**, 181-192.

Zhang, Y., Neo, S.Y., Wang, X., Han, J. and Lin, S.C. (1999) Axin forms a complex with MEKK1 and activates c-Jun NH(2)-terminal kinase/stress-activated protein kinase through domains distinct from Wnt signaling. *J Biol Chem*, **274**, 35247-35254.

Zheng, L., Zhang, J. and Carthew, R.W. (1995) frizzled regulates mirror-symmetric pattern formation in the *Drosophila* eye. *Development*, **121**, 3045-3055.

Appendix